

Aus dem Institut für Medizinische Mikrobiologie und Krankenhaushygiene

Direktor: Prof. Dr. Michael Lohoff

des Fachbereichs Medizin der Philipps-Universität Marburg

Dimethyl fumarate suppresses Tc17 cell fate
in autoimmunity via ROS accumulation

Inaugural-Dissertation

zur Erlangung des Doktorgrades der Naturwissenschaften

dem Fachbereich Medizin der Philipps-Universität Marburg

vorgelegt von

Christina Lückel

aus Winterberg

Marburg, 2018

Angenommen vom Fachbereich Medizin der Philipps-Universität Marburg
am: 15.08.2018

Gedruckt mit Genehmigung des Fachbereichs.

Dekan:	Prof. Helmut Schäfer
Referent:	Prof. Dr. Magdalena Huber
1. Korreferent:	Prof. Dr. Thomas Worzfeld

Originaldokument gespeichert auf dem Publikationsserver der
Philipps-Universität Marburg
<http://archiv.ub.uni-marburg.de>



Dieses Werk bzw. Inhalt steht unter einer
Creative Commons
Namensnennung
Keine kommerzielle Nutzung
Weitergabe unter gleichen Bedingungen
3.0 Deutschland Lizenz.

Die vollständige Lizenz finden Sie unter:
<http://creativecommons.org/licenses/by-nc-sa/3.0/de/>

Contents

List of Figures	v
Abbreviations	vi
1. Abstract	1
1. Zusammenfassung.....	2
2. Introduction.....	3
2.1 Pivotal role of T cells during immune responses	3
2.2 T cells in health and disease.....	4
2.2.1 Protective and pathogenic functions of CD4 ⁺ T cells	4
2.2.2 Protective and pathogenic functions of CD8 ⁺ T cells	5
2.3 Multiple sclerosis.....	6
2.3.1 Pathogenesis of multiple sclerosis	7
2.3.2 Contribution of Tc17 and Th17 cells to MS pathogenesis.....	9
2.3.3 Dimethyl fumarate in MS therapy and beyond.....	11
2.4 Signal transduction.....	13
2.4.1 Signalling networks in T cell differentiation	13
2.4.1.1 Transcriptional regulation of type 17 cell differentiation	14
2.4.1.2 ROS signalling in T cells	15
2.4.1.3 IL-2 signalling in T cells	16
2.5 Epigenetic regulation of gene expression	17
2.5.1 Chromatin remodelling	18
2.5.1.1 Histone tail modifications	18
2.5.1.2 DNA methylation.....	19
2.5.1.3 Nucleosome compaction and chromatin conformation	19
3. Material	20
3.1 Equipment	20
3.2 Chemicals and consumables	20
3.3 Kits and dyes.....	22
3.4 Buffers and Media	22
3.4.1 Buffers and media for cell biology	22
3.4.2 Buffers and media for molecular biology.....	23
3.5 Antibodies	23
3.5.1 Antibodies for CD8 ⁺ T cell isolation	23

3.5.2 Antibodies for cell culture	24
3.5.3 Antibodies for flow cytometry	24
3.5.4 Antibodies for ChIP.....	25
3.6 Cytokines	25
3.7 Primers	25
3.8 Plasmids.....	26
3.9 Mice.....	26
3.10 Cell lines	26
3.11 Software	27
4. Methods	28
4.1 Cell culture	28
4.2 Murine T cell isolation and <i>in vitro</i> differentiation	28
4.2.1 Preparation of lymph nodes and spleen	28
4.2.2 Magnetic cell purification of CD8 ⁺ T cells.....	28
4.2.3 Activation and differentiation of CD8 ⁺ T cells <i>in vitro</i>	29
4.3 Human T cell preparation and <i>in vitro</i> differentiation	30
4.3.1 Isolation of human PBMC from whole blood.....	30
4.3.2 Differentiation of human CD8 ⁺ T cells.....	30
4.3.3 Freezing and thawing of human PBMCs	30
4.3.4 Restimulation of human PBMCs.....	31
4.4 Flow cytometry.....	31
4.4.1 Cell sorting.....	31
4.4.2 Surface staining	32
4.4.3 Intracellular staining.....	32
4.4.4 Intranuclear staining	32
4.4.5 Phosflow	33
4.4.6 ROS staining.....	33
4.4.7 Proliferation and apoptosis staining	33
4.5 Retroviral overexpression	34
4.5.1 Transfection of HEK 293 cells	34
4.5.2 Generation of virus-containing supernatant.....	35
4.5.3 Spin-based transduction of T cells	35
4.6 Protein-biochemical methods	35
4.6.1 Enzyme-linked immunosorbent assay	35
4.7 Molecular biological methods.....	36

4.7.1 Quantitative real-time PCR	36
4.7.2 RNA sequencing	36
4.7.3 Chromatin immunoprecipitation	37
4.7.3.1 Cell lysis, fixation and shearing	37
4.7.3.2 Precipitation and elution.....	38
4.7.3.3 DNA purification and quantitative detection.....	39
4.7.4 Glutathione assay.....	39
4.8 Experimental autoimmune encephalomyelitis mouse model	40
4.8.1 Oral DMF application and EAE induction	40
4.8.2 T cell adoptive transfer and induction of EAE.....	41
4.8.3 T cell isolation from CNS	41
4.9 Bioinformatical analysis of RNA	42
4.9.1 Alignment, mapping and annotation	42
4.9.2 Differential gene expression analysis.....	42
4.9.3 Gene set enrichment analysis	42
4.9.4 Principal component analysis.....	43
4.10 Statistics	43
5. Results	44
5.1 DMF-mediated ROS accumulation leads to a robust IL-17 suppression in Tc17 cells	44
5.2 IL-17 is diminished by DMF-mediated transient ROS upregulation at early stages of Tc17 differentiation	46
5.3 DMF signalling suppresses IL-17 production independent of apoptosis or proliferation.	48
5.4 DMF-ROS axis modifies Tc17 cell gene signature	49
5.5 DMF via ROS suppresses permissive histone modifications at the <i>Il17</i> locus	51
5.6 DMF suppresses pathogenicity of Tc17 cells in EAE	52
5.6.1 Oral DMF treatment diminishes EAE severity.....	52
5.6.2 DMF limits pathogenicity of Tc17 cells <i>in vivo</i>	53
5.7 DMF treatment shifts Tc17 cells towards a CTL-like signature	56
5.8 DMF/ROS axis enhances IL-2 signalling in Tc17 cells	57
5.8.1 DMF limits IL-17 production of Tc17 cells via STAT-5 induction	59
5.8.2 DMF/ROS axis suppresses IL-17 production of Tc17 cells by elevated AKT/FOXO1/Tbet pathway	61
5.9 IL-17 production is differentially regulated in Tc17 and Th17 cells	63
5.10 DMF suppresses IL-17 production of human Tc17 cells in a ROS-dependent manner... ..	65
5.11 DMF treatment reduces frequencies of IL-17-producing CD8 ⁺ T cells in MS patients....	66

6. Discussion.....	68
Immune modulatory impact of DMF.....	68
6.1 ROS modifies Tc17 cell fate.....	68
6.1.1 DMF suppresses IL-17 in Tc17 cells via early GSH-depletion and subsequent ROS accumulation.....	68
6.1.2 Involvement of DMF/ROS axis on T cell proliferation and apoptosis.....	70
6.1.3 ROS shifts the Tc17 profile towards a CTL-like signature.....	70
6.1.4 DMF alters histone modifications of Tc17 cells in a ROS-dependent manner.....	71
6.2 ROS alter Tc17 network by enhancing IL-2 signalling.....	72
6.2.1 Elevated ROS increase STAT5 and PI3K/AKT signalling, thereby limiting IL-17 inhibition.....	73
6.2.2 Model of differential IL-17 regulation in Th17 and Tc17 cells.....	74
6.3 Impact of DMF treatment on EAE pathogenesis.....	75
6.3.1 The course of EAE is attenuated by oral DMF application.....	75
6.3.2 DMF treatment limits co-pathogenic function of Tc17 cells in EAE.....	75
6.4 DMF treatment suppresses human IL-17-producing CD8 ⁺ T cells.....	77
6.5 Potential implications of DMF/ROS-mediated Tc17 suppression.....	78
6.6 Final discussion and outlook.....	79
7. References.....	81
8. Appendix.....	95
8.1 List of academic teachers.....	95
8.2 Danksagung.....	96

List of Figures

Figure 1: Plasticity of CD8 ⁺ T cell subsets and their specific cytokine production	6
Figure 2: Typical course of the four major MS types	8
Figure 3: Hypothetical view of Tc17 and Th17 cell contribution to immune responses in acute MS lesions	10
Figure 4: DMF-GSH-ROS axis stably suppresses IL-17 production by Tc17 cells.....	45
Figure 5: DMF upregulates ROS transiently and suppresses IL-17 production at early stages of Tc17 differentiation.....	47
Figure 6: DMF does not influence apoptosis or proliferation of Tc17 cells at immune modulatory concentrations.....	48
Figure 7: Tc17 fate is suppressed by DMF treatment	50
Figure 8: DMF alters histone modifications at the Il17 locus of Tc17 cells in a ROS-dependent manner	51
Figure 9: Oral DMF treatment limits EAE severity	53
Figure 10: DMF limits CNS autoimmunity by suppressing the co-pathogenic function of Tc17 cells.....	55
Figure 11: DMF- induced ROS favours a CTL-like gene signature	57
Figure 12: IL-2 signalling is elevated by ROS and required for suppression of IL-17 in Tc17 cells	58
Figure 13: Elevated P-STAT5 contributes to the DMF-mediated IL-17 inhibition of Tc17 cells ..	60
Figure 14: ROS suppress IL-17 production in Tc17 cells via increased AKT/FOXO1/T-bet signalling.....	62
Figure 15: Differential impact of AKT- and mTORC1-signalling on IL-17 production of Tc17 and Th17 cells.....	64
Figure 16: DMF treatment limits IL-17 production in human Tc17 cells	65
Figure 17: DMF treatment limits IL-17 production of CD8 ⁺ T cells in MS patients	66
Figure 18: DMF disturbs the cooperation between Tc17 and Th17 cells during the onset of EAE	77
Figure 19: Influence of DMF on Tc17 cells	80

Abbreviations

Ac	Acetylation	LN	Lymph nodes
AKT/PKB	Protein kinase B	me	Methylated
APC	Antigen-presenting cell	MOG	Myelin oligodendrocyte protein
BBB	Blood-brain barrier	MS	Multiple sclerosis
CD	Cluster of differentiation	mTOR	Mammalian target of rapamycin
ChIP	Chromatin immunoprecipitation	NGS	Next generation sequencing
CNS	Central nervous system	NF-κB	Nuclear factor of kappa B
CSF	Cerebrospinal fluid	PB	Peripheral blood
CTL	Cytotoxic T cell	PI3K	phosphoinositide-3-kinase
DC	Dendritic cell	PML	Progressive multifocal leukoencephalopathy
DMF	Dimethyl fumarate	RORγt	RAR-related orphan receptor gamma
DMSO	Dimethyl sulfoxide	ROS	Reactive oxygen species
EAE	Experimental autoimmune encephalomyelitis	RRMS	Relapsing-remitting multiple sclerosis
FACS	Fluorescence-activated cell sorting	seq	Sequencing
FCS	Fetal calf serum	STAT	Signal transducer and activator of transcription
FOXO1	Forkhead box protein O1	T-bet	T-box transcription factor TBX21
Foxp3	Forkhead box protein 3	Tc	T cytotoxic
GSEA	Gene set enrichment analysis	TF	Transcription factor
HAT	Histone acetyltransferase	TGF-β	Transforming growth factor β
HDAC	Histone deacetylases	Th	T helper
ICS	Intracellular staining	TNF	Tumour necrosis factor
IFN	Interferon	Treg	Regulatory T cell
IL	Interleukin	TSA	Trichostatin A
IRF	Interferon regulatory factor	rpm	Rounds per minute

1. Abstract

Dimethyl fumarate (DMF) is approved for treatment of relapsing remitting multiple sclerosis (RRMS), a chronic inflammatory disease of the central nervous system (CNS) that is caused by autoreactive T cells. The effect mechanism of DMF is not fully elucidated so far; however, a preferential impact on CD8⁺ T cells was described. In the cerebrospinal fluid (CSF) of MS patients IL-17-producing CD8⁺ T (Tc17) cells are enriched. In addition, during experimental autoimmune encephalomyelitis (EAE), the mouse model for multiple sclerosis (MS), a co-pathogenic function of Tc17 was described. Hence, Tc17 cells crucially contribute to autoimmune processes in the CNS of men and mice.

This study shows that DMF elevated reactive oxygen species (ROS) in CD4⁺ T (Th17) cells and Tc17 cells by glutathione depletion, resulting in IL-17 suppression particularly in Tc17 cells. Accordingly, IL-17 production by CD8⁺ but not by CD4⁺ T cells was reduced in DMF-treated MS patients and DMF application diminished Tc17 cell pathogenicity in EAE. Accumulated ROS shifts the Tc17 transcriptome towards a cytotoxic T lymphocyte (CTL)-like signature by enhancing IL-2 signalling including phosphoinositide-3-kinase (PI3K)/ protein kinase B (AKT) and signal transducer and activator of transcription (STAT)5 pathways. AKT deactivated forkhead-box-Protein O (FOXO)1 leading to the upregulation of the transcription factor T-box transcription factor TBX21 (T-bet), which in turn suppressed IL-17. The modified transcriptional network was accompanied by altered histone modifications at the *IL17* locus. In line, T-bet-deficiency, inhibition of histone deacetylases (HDAC), PI3K/AKT or STAT5 partially prevented DMF-mediated suppression of Tc17 cells.

Thus, this work provides mechanistic insights into the selective modulation of Tc17 cell differentiation by DMF-mediated upregulation of ROS and IL-2 signalling with relevance for Tc17-driven pathologies including MS and psoriasis.

1. Zusammenfassung

Dimethylfumarat (DMF) wird zur Behandlung von schubförmig remittierender multipler Sklerose (RRMS) eingesetzt, einer chronisch-entzündlichen Erkrankung des zentralen Nervensystems (ZNS), die von autoreaktiven T-Zellen verursacht wird. Der Wirkmechanismus von DMF ist nicht vollständig aufgeklärt; es ist jedoch bekannt, dass insbesondere CD8⁺ T-Zellen beeinflusst werden. IL-17-produzierende CD8⁺ T-Zellen (Tc17) sind in der Zerebrospinalflüssigkeit (CSF) von MS-Patienten angereichert. Zusätzlich wurde die kopathogene Wirkung von Tc17-Zellen in der experimentellen autoimmunen Enzephalomyelitis (EAE), dem Mausmodell für MS, beschrieben. Diese Beobachtungen legen nahe, dass Tc17-Zellen zu autoimmunen Prozessen im ZNS bei Mensch und Maus beitragen.

Die vorliegende Studie zeigt, dass DMF durch Glutathiondepletion in IL-17-produzierenden CD4⁺ T-Zellen (Th17) und Tc17-Zellen Sauerstoffradikale anreicherte und dies besonders in Tc17-Zellen zu einer IL-17 Suppression führte. Dementsprechend konnte eine reduzierte IL-17-Produktion in CD8⁺ T-Zellen, nicht jedoch in CD4⁺ T-Zellen von DMF-behandelten MS-Patienten nachgewiesen werden. Ebenso verminderte die Verabreichung von DMF die Pathogenität von Tc17-Zellen in der EAE. Die Akkumulation von Sauerstoffradikalen trieb das Transkriptom von Tc17-Zellen in Richtung einer cytotoxischen T-Zell Signatur. Mechanistisch wurde dies durch die Verstärkung von IL-2-Signalwegen, wie Phosphoinositid 3-Kinase (PI3K)/ Proteinkinase B (AKT) und STAT5 realisiert. AKT deaktiviert FOXO1, einen Suppressor des Transkriptionsfaktors T-bet. Die daraus resultierende Induzierung von T-bet führte letztendlich zu einer IL-17 Hemmung. Die Modifizierung des transkriptionellen Netzwerks ging mit veränderten Histonmodifikationen am *IL17* Locus einher. Übereinstimmend konnten sowohl T-bet-Defizienz als auch die Inhibierung von Histon-Deacetylasen (HDAC), PI3K/AKT oder STAT5 die DMF-vermittelte Tc17-Suppression teilweise verhindern.

Zusammenfassend liefert diese Arbeit mechanistische Einblicke in die selektive Modulation der Tc17-Zelldifferenzierung durch eine DMF-vermittelte Induzierung von Sauerstoffradikalen und IL-2 Signalwegen und ist daher relevant für Tc17-vermittelte Krankheitsbilder wie MS und Psoriasis.

2. Introduction

2.1 Pivotal role of T cells during immune responses

The immune system is a complex network consisting of various cellular and soluble components that cooperate in order to protect the human body against pathogens and the development of cancer. However, misguided immune responses can evoke allergy or autoimmunity that represent important pathologies in industrialised nations.

Immune cells are derived from pluripotent hematopoietic stem cells and are categorised into the myeloid lineage, including dendritic cells (DC), macrophages, granulocytes, mast cells and erythrocytes or to the lymphoid lineage such as NK cells, innate lymphoid cells (ILC), T and B cells. T lymphocytes are further classified into cluster of differentiation (CD) 4^+ T helper (Th) and CD 8^+ cytotoxic T (Tc) cells, which differ in their reactivity to the major histocompatibility complex (MHC). Whereas the T cell receptor (TCR) of CD 4^+ Th cells binds peptide-loaded MHC class II molecules located on professional antigen-presenting cells (APC), all nucleated cells contain MHC class I that is recognised by the TCR of CD 8^+ T cells. During thymic selection, TCR/MHC interaction ensures that only T cells survive which bind to MHC molecules (positive selection) without reacting to self-antigens (negative selection). The naïve T cells that remain after this selection are largely non-responsive to self but capable of responding to foreign peptides and egress into the blood and lymphatic circulation. The activation of naïve T cells into effector T cells by APCs in lymphoid organs is realised by the interaction of TCR/MHC together with costimulatory stimuli and cytokine signalling, however recent data also imply the contribution of reactive oxygen species (ROS) in this process (Franchina, Dostert, & Brenner, 2018). At the end of a primary immune response, the majority of responding T cells dies by apoptosis. However, a small percentage survives and gives rise to immunological memory, a characteristic of the adaptive immunity. It is acquired by the development of memory T cells that ensure a fast and effective immune response in case of re-exposure to the cognate antigen (Murphy & Weaver, 2017). Human memory cells are further specified into central memory (TCM), effector memory (TEM) and effector memory T cells (TEMRA), depending on the expression of CC-chemokine receptor (CCR)7 and CD45RA (Geginat, Lanzavecchia, & Sallusto, 2003).

During immune responses, CD 4^+ and CD 8^+ T cells have distinct roles: Th cells coordinate specific immune responses by their cytokine production, whereas CD 8^+ T cells are able to kill target cells directly by inducing apoptosis through cytotoxic molecules like perforins or granzymes, in addition to cytokine production. However, in order to guarantee an efficient

immune response tailored to tumour cells and the variety of pathogens, the generation of distinct subsets of CD4⁺ and CD8⁺ T cells is required. The differentiation into subpopulations with specific defence mechanisms is driven by the surrounding cytokine milieu during T cell activation (Murphy & Weaver, 2017). The subsets differ particularly in their specific transcription factors (TF), cytokine profiles as well as their characteristic effector functions. In 1986, Mosman *et al.* first described the existence of interferon (IFN- γ)-producing Th1 and IL-4-producing Th2 cells (Mosmann, Cherwinski, Bond, Giedlin, & Coffman, 1986) since then a great number of CD4⁺ T cell subsets has been discovered, demonstrating the complexity of immunological responses. Beside Th1 and Th2 cells, IL-9-producing Th9 cells, regulatory T (Treg) cells, follicular T helper cells and Th17 cells with their signature cytokine IL-17 are known and orchestrate immune responses against specific pathogens (J Zhu, Yamane, & Paul, 2010). Recent data show that also CD8⁺ T cells can be subdivided into different subtypes, comparable to their CD4⁺ counterparts. Besides classical cytotoxic T lymphocytes (CTL or Tc1) also Tc2, Tc9, CD8⁺ Treg and Tc17 cells have been described (Mittrücker, Visekruna, & Huber, 2014).

2.2 T cells in health and disease

Both, CD4⁺ and CD8⁺ T cells play central roles in the function of the immune system by clearing diverse pathogens and eliminating of tumorigenic cells. However, due to their central function in immune responses, dysregulation of T cells can have tremendous consequences and lead to pathological immune reactions as allergy or autoimmunity (J Zhu *et al.*, 2010). Therefore, the variety of T cell subsets and their functional diversity have the potential to initiate a multitude of pathologies.

2.2.1 Protective and pathogenic functions of CD4⁺ T cells

On the one hand, Th1 cells contribute to the clearance of intracellular pathogens by activating macrophages via their IFN- γ production (Jinfang Zhu & Paul, 2008) but on the other they can also contribute to delayed-type hypersensitivity responses and autoimmunity (Damsker, Hansen, & Caspi, 2010). Combating extracellular pathogens, such as worms, is mediated by IL-4, IL-5 and IL-13-producing Th2 cells and subsequent activation of B cells, however dysregulation can induce allergic responses (Damsker *et al.*, 2010). Similar to Th2, also Th9 cells combat against parasites and in addition possess anti-tumour immunity by producing IL-9. On the other side, they can also contribute to the induction of allergy and asthma (Carrascosa *et al.*, 2017; Kaplan, Hufford, & Olson, 2015; J Zhu *et al.*, 2010). The clearance of intracellular pathogens is mediated by Th17 cells, which produce pro-inflammatory IL-17, IL-21 and IL-22

and thereby trigger neutrophil recruitment to the infection site (Jinfang Zhu & Paul, 2008). However, the ability to induce inflammation predetermines Th17 cells to contribute to the development of autoimmune disorders such as multiple sclerosis (MS), rheumatoid arthritis, Crohn's disease and many others (Tabarkiewicz, Pogoda, Karczmarczyk, Pozarowski, & Giannopoulos, 2015). In order to prevent autoimmunity and maintain immune homeostasis, Treg cells secrete anti-inflammatory cytokines as TGF- β and IL-10 (Jinfang Zhu & Paul, 2008), but the suppression of immune responses makes them to key-players in tumour progression (Chaudhary & Elkord, 2016), impressively demonstrating the requirement of fine-tuned immune responses.

2.2.2 Protective and pathogenic functions of CD8⁺ T cells

CD8⁺ T cells fulfil crucial functions in immune responses against intracellular pathogens and tumours (Klenerman & Hill, 2005; Y. Lu et al., 2014; Su, Lee, & Kung, 2010; Sukumar et al., 2013), but also contribute to allergic and autoimmune disorders (Huber et al., 2009; Loser et al., 2010; Tang et al., 2012; Visekruna et al., 2013). The best-characterized subset of CD8⁺ T cells are CTLs, which can kill infected or cancerous cells directly by releasing cytotoxic molecules and production of cytokines as IFN- γ and tumour necrosis factor (TNF)- α (Kaech & Cui, 2012), but they are also implicated in autoimmune processes (Blanco, Viallard, Pellegrin, & Moreau, 2005). Similar to Th2 cells, Tc2 cells secrete IL-4, IL-5 as well as IL-13 and can show high or low cytotoxicity, dependent on the type of immune response (Mittrücker et al., 2014). Functionally, they contribute to rheumatoid arthritis (Cho et al., 2012) and Th2-mediated allergy (Tang et al., 2012). Th2/Tc2-dependent airway inflammation is further promoted by IL-9- and IL-10-producing Tc9 cells (Visekruna et al., 2013), however, this subset is also implicated in the provision of a strong anti-tumour response via IL-9 (Y. Lu et al., 2014). CD8⁺ Tregs reflect to large extend the properties of CD4⁺ Treg by secreting anti-inflammatory IL-10 and TGF- β , determining them to important regulators of T cell-mediated responses (Mittrücker et al., 2014). However, comparable to their CD4⁺ counterparts, also CD8⁺ Treg cells at least partially promote tumour progression (Zhang et al., 2015) and contribute to autoimmune diseases such as lupus (Dinesh, Skaggs, La Cava, Hahn, & Singh, 2010).

Similar to Th17 cells, also murine Tc17 cells produce the pro-inflammatory marker cytokine IL-17A and can co-secrete further cytokines including IL-17F, IFN- γ , granulocyte monocyte-colony stimulating factor (GM-CSF), IL-21, IL-22 or TNF- α (Srenathan, Steel, & Taams, 2016). A high plasticity towards IFN- γ production as well as variability in cytotoxicity have been reported and represent characteristic features of Tc17 cells (Srenathan et al., 2016). Due to the production of pro-inflammatory IL-17, they provide immunity against bacterial, viral and fungal

infections (Hamada et al., 2009; Naik et al., 2015; Nanjappa et al., 2017; Yeh et al., 2010) on the one hand, but there is strong evidence for a pathogenic function of Tc17 cells in autoimmunity on the other. Amongst others, their contribution to MS (Huber et al., 2013), psoriasis (Kryczek et al., 2008) and autoimmune colitis (Tajima et al., 2008) has been reported. The function of Tc17 cells in anti-tumour responses is contradictory and ranges from clearance of cancer to promoting of tumour growth (Hinrichs et al., 2009; Kuang et al., 2010).

It was demonstrated that CD8⁺ T cell subtypes can acquire the characteristic cytokine production of other subpopulations, while retaining the initial cytokine production, a phenomenon called T cell plasticity (Zhou, Chong, & Littman, 2009). Thus, Tc17 cells positive for IL-17 and IFN- γ or Tc2 cells that co-express IFN- γ together with IL-4 and IL-10 were detected (Mittrücker et al., 2014).

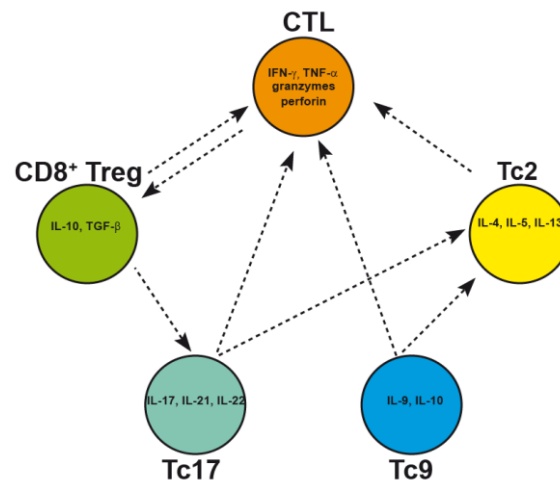


Figure 1: Plasticity of CD8⁺ T cell subsets and their specific cytokine production

Similar to CD4⁺ T cells, CD8⁺ T cells also show lineage plasticity and acquire different subset phenotypes described as CTL, Tc2, Tc9, Tc17 and CD8⁺ Treg. These subsets produce specific cytokines and cytotoxic molecules to combat pathogens and tumour development. Arrows show the ability of cells to acquire characteristics of the other Tc subsets. Modified from (Mittrücker et al., 2014).

2.3 Multiple sclerosis

Worldwide, approximately 2.5 million people suffer from MS, a disease of the central nervous system (CNS) that mainly affects young adults between 20 and 40 years of age, especially women. During the course of the disease, autoreactive immune responses cause the development of lesions in the CNS, leading to disturbed neuronal signalling. Dependent on the location of lesions, clinical manifestation is heterogenous and can include motor impairments up to fatigue or visual disturbances (Dendrou, Fugger, & Friese, 2015). Intense research over the past years led to a better understanding of the mechanisms involved in MS pathogenesis and the development of new therapeutics however, until now there is no effective cure for the disease (Comabella & Houry, 2012).

2.3.1 Pathogenesis of multiple sclerosis

MS is an inflammatory disease of the CNS, which is considered to be caused by autoreactive T cells that initiate immune responses against myelin antigens such as myelin basic protein (MBP) or oligodendrocyte glycoprotein (MOG) (Dendrou et al., 2015; Nylander & Hafler, 2012). Usually, autoreactive T cells are killed during the selection process in the thymus; however, this process is imperfect, leading to the release of some autoreactive T cells in the periphery. During functional immune regulation, these cells are controlled by peripheral tolerance mechanisms. If this tolerance is dysregulated, autoreactive CD4⁺ and CD8⁺ T cells can be activated by self-antigen presenting cells and infiltrate the CNS, leading to inflammation and tissue damage by re-activation and specific effector functions (Dendrou et al., 2015). Both, genetic and environmental factors, including infectious agents, can contribute to this process and thereby lead to manifestation and progression of the disease (Dendrou et al., 2015). The development of inflammatory lesions is a hallmark of MS pathology and caused by immune cell infiltration across the blood-brain barrier (BBB) that initiates inflammation. This process leads to focal demyelination, neuroaxonal injury and in the end loss of neurological function (Dendrou et al., 2015).

In order to understand the pathogenesis of MS, the animal model experimental autoimmune encephalomyelitis (EAE) was established 70 years ago (Rivers, 1933). EAE is induced by immunisation of mice with myelin peptides or by transfer of myelin-reactive T cells (Holmøy & Hestvik, 2008). Despite the fact that EAE provided important pathogenic mechanisms for the development of MS therapies, one has to keep in mind that this model cannot cover the entire spectrum of the immunological and pathological features of the disease ('t Hart, Gran, & Weissert, 2011; Lassmann, 2017).

The pathology of MS is subdivided into four major types, based on the course of disease. The most common form is the *relapsing-remitting MS* (RRMS), affecting 80-90% of MS patients (Goldenberg, 2012). This type is characterised by relapses followed by remission phases, when symptoms improve or disappear. Over time this course often converts into the *secondary progressive MS* with or without periods of remission and progressive neurological deficits. The *primary progressive MS* affects 10 % of the patients and is marked by symptoms worsened from the beginning without relapses or remission. The fourth type, *progressive-relapsing MS*, is a rare form with progressive course from the start and intermittent flare-ups, without periods of remission (Goldenberg, 2012; Loma, 2011).

The aforementioned MS types are used to predict the course of the disease, but besides prognosis purpose they are also important for treatment decisions. Nowadays many drugs

against MS exist that reduce relapses; however, they cannot substantially cure the disease or reverse axonal damage (Dendrou et al., 2015).

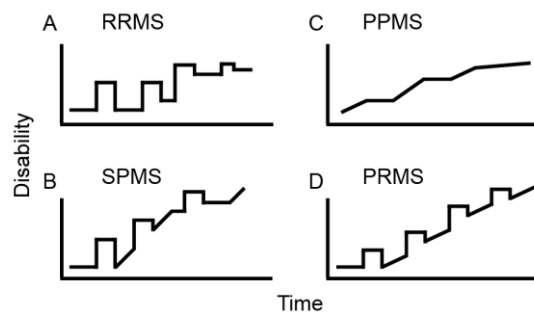


Figure 2: Typical course of the four major MS types

(A) Relapsing-remitting MS (RRMS) is the most common type that is characterised by times of relapses and recovery. (B) Secondary-progressive MS (SPMS) is marked by initial relapses, followed by gradual increase of disability that is not associated with acute attacks. (C) Primary-progressive (PPMS) patients show a steady functional decline from the onset of disease without relapses or remission phases. (D) Progressive-relapsing MS (PRMS) is characterised by steady functional decline from onset of disease with acute relapses.

B cells have been shown to contribute to the pathogenesis of MS by mediating aberrant T cell activation in the periphery and by producing myelin-specific auto-antibodies that are found in the serum and cerebrospinal fluid (CSF) of some patients (Pröbstel, Sanderson, & Derfuss, 2015). The treatment with B cell-depleting anti-CD20 monoclonal antibodies (mAb) ameliorated the disease, underlining the important role of B cells in MS pathogenesis (Hauser et al., 2008; Michel et al., 2015). In addition, some studies suggest the involvement of innate immune cells such as macrophages, microglial cells and DCs to the pathogenesis of MS by influencing the effector functions of B and T cells (Gandhi, Laroni, & Weiner, 2010; Mishra & Yong, 2016).

For a long time, autoreactive IFN- γ -producing Th1 cells were considered to be the key-mediators of MS pathogenesis (Compston & Coles, 2008). Further studies demonstrated the contribution of various cell types and T cell subsets, with a central role of Th17 cells (McFarland & Martin, 2007). In addition, it was shown that MS patients show reduced Treg function, although similar numbers in MS patients and controls have been found (Haas et al., 2005). Besides the involvement of CD4⁺ T cells, growing evidence supports the pathogenic role of CD8⁺ T cells in the pathogenesis of MS (Denic, Wootla, & Rodriguez, 2013). It was found that CD8⁺ T cells even outnumber the numbers of CD4⁺ T cells in CNS parenchyma and active lesions of MS patients (Babbe et al., 2000; Booss, Esiri, Tourtellotte, & Mason, 1983), suggesting a critical contribution to the disease. As IL-17-producing T cells contribute to the pathogenicity of MS, they will be discussed in more detail in the following chapter.

2.3.2 Contribution of Tc17 and Th17 cells to MS pathogenesis

A number of studies highlight the important role of IL-17-producing CD4⁺ and CD8⁺ T cells in the development and pathogenesis of MS and EAE (Huber et al., 2013; Komiyama et al., 2006; Tzartos et al., 2008). Both, Th17 and Tc17 cells have been detected in acute and chronic MS lesions (Tzartos et al., 2008). In RRMS patients, high frequencies of Th17 cells are found in the CSF during relapses, whereas patients in remission show lower numbers (Brucklacher-Waldert, Stuermer, Kolster, Wolthausen, & Tolosa, 2009). In addition, MS severity was shown to correlate with a high expression of IL-17 (Matusevicius et al., 1999), further suggesting key functions in the pathogenesis.

Previously it was thought that Th1 cells drive MS inflammation, but it was shown that Th17 cells were able to induce EAE following adoptive transfer, whereas Th1 cells failed to induce EAE. Moreover, antibody-mediated neutralisation of IL-17 reduced the severity of EAE, while blocking IFN- γ exacerbated the disease (Langrish et al., 2005). However, in another study simultaneous neutralisation of IL-17A and IL-17F had only marginal effects on disease outcome (Haak et al., 2009), demonstrating some difficulties in defining the role of Th17 cells. A possible explanation might be the instability and plasticity of the type 17 phenotype, as they can switch to IFN- γ production (Abromson-Leeman, Bronson, & Dorf, 2009; G. Shi et al., 2008; Srenathan et al., 2016). The pathogenic role of IL-17 family cytokines is linked to many autoimmune diseases (Jin & Dong, 2013) as it induces the generation of pro-inflammatory cytokines and chemokines such as IL-1 β , IL-6, TNF- α or GM-CSF that promote the infiltration of neutrophils and macrophages to inflammation site (Jadidi-Niaragh & Mirshafiey, 2011; Jin & Dong, 2013).

To cause inflammation in the CNS, autoreactive T cells need to cross the BBB after activation in the periphery. By using EAE, the C-C chemokine receptor (CCR) 6-dependent entry of Th17 cells through the choroid plexus at the beginning of the disease was revealed (Reboldi et al., 2009). After invasion into the CNS, they increase BBB permeability via IL-17 and IL-22 production and initiate a pathological immune cell infiltration including Th1, CD8⁺ T cells, B cells and plasma cells (Kebir et al., 2007).

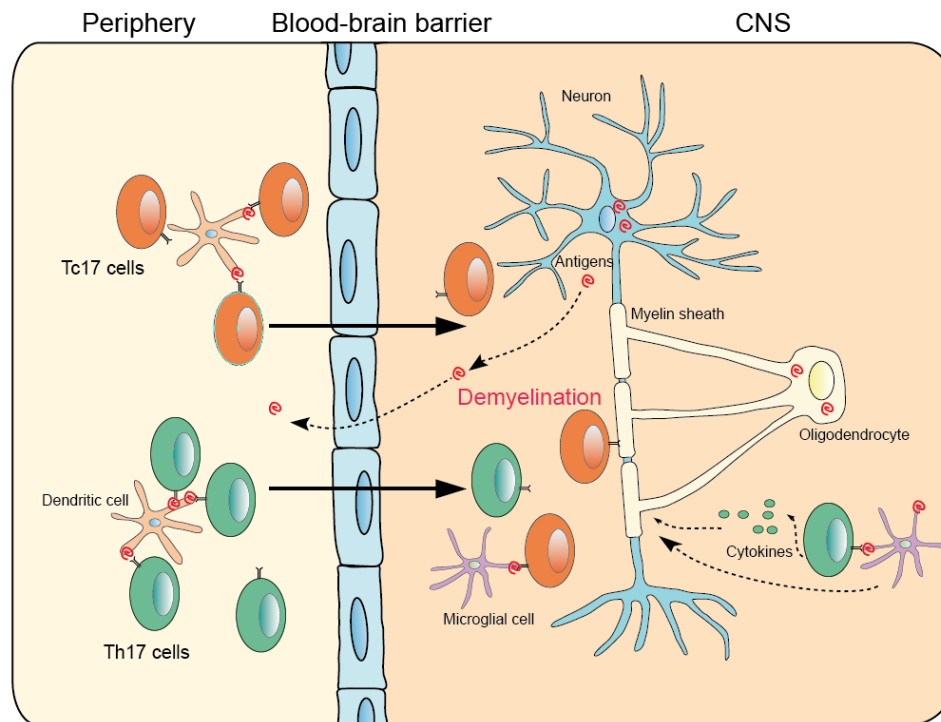


Figure 3: Hypothetical view of Tc17 and Th17 cell contribution to immune responses in acute MS lesions

Tc17 and Th17 cells are primed in the periphery by APCs presenting antigens that are released from the CNS or by cross-reactive foreign antigens. After clonal expansion they invade the CNS where re-activation of Th17 cells leads to an increased production of inflammatory cytokines. These cytokines attract other immune cells, which contribute to the immune response by direct phagocytic attack on the myelin layer. Tc17 cells are re-activated by MHC class I-presenting glial or neuronal cells and cause damage by secretion of cytokines and cytotoxic molecules. Modified from (Hemmer, Cepok, Nessler, & Sommer, 2002).

Besides Th17 cells, also IL-17-producing CD8⁺ T cells contribute to MS pathogenesis. It was shown that CD8⁺ and CD4⁺ T cells produce similar amounts of IL-17 in active MS lesions (Tzartos et al., 2008) and a selective enrichment of Tc17 numbers in CSF of MS patients at early stages were detected (Huber et al., 2013). Interestingly, transferred Tc17 cells alone were not able to infiltrate the CNS of EAE-resistant interferon regulatory factor (IRF)4-deficient mice after immunization and could not induce EAE on their own. However, transfer of CD8⁺ T cells and a subpathogenic number of CD4⁺ T cells together caused the onset of EAE in *Irf4*^{-/-} mice, indicating a cooperation between both cell types (Huber et al., 2013). In addition, it was demonstrated that the cooperation during early stages of EAE required both, CCR6 expression of CD4⁺ T cells and the IL-17A production by CD8⁺ T cells. In a first step, Tc17 cells via their IL-17A secretion increased the pathogenicity of Th17 cells, including IL-17 production. Subsequently, Th17 cells were able to infiltrate the CNS CCR6-dependently in a first step and recruit Tc17 cells to the CNS in a second step, which was CCR6-independent (Huber et al., 2013). This data point to the importance of Tc17 cells during the onset of EAE, as they enable

the infiltration of Th17 cells into the CNS in early phases of the disease by their IL-17 production (Huber et al., 2013).

2.3.3 Dimethyl fumarate in MS therapy and beyond

Due to intense research during the last decades several drugs have been introduced for MS therapy (Comi, Radaelli, & Soelberg Sørensen, 2017). One of them is dimethyl fumarate (DMF), a fumaric acid ester that was approved by the Food and Drug Administration (FDA) and the European Medicines Agency (EMA) as first-line treatment of RRMS in 2013. It is marketed under the name Tecfidera® and approved for patients suffering from RRMS with oral application of 240 mg twice a day (Bomprezzi, 2015). Already since the 1990s a combination of DMF and ethyl hydrogen fumarates (Fumaderm®) is used for treatment of psoriasis, an inflammatory skin disease to which Tc17 cells are contributing (Res et al., 2010), providing DMF with a long record of efficacy and safety.

A phase II clinical study in RRMS patients with a modified fumaric acid ester, BG-12, demonstrated a significant reduction by 69% in the number of gadolinium enhancing lesions after 12-24 weeks of treatment as compared to placebo (Kappos et al., 2008). A decrease of relapse rate and reduced progression of disability was found in a phase III clinical study (Gold et al., 2012). In EAE, DMF has been shown to exert neuroprotective and immunomodulatory effects and to improve the clinical score (Ghoreschi et al., 2011; Linker et al., 2011; Schilling, Goelz, Linker, Luehder, & Gold, 2006).

MS is considered to be a T cell-mediated disease; thus, the effect of DMF therapy on circulating T lymphocytes is of major interest. Studies revealed that DMF decreased the numbers of peripheral blood lymphocyte (Fox et al., 2012; Gold et al., 2012) with disproportionate CD8⁺ T cell reduction in stable patients, who showed no radiological or clinical evidence of disease activity after six months of treatment (Fleischer et al., 2017; Spencer, Crabtree-Hartman, Lehmann-Horn, Cree, & Zamvil, 2015). In rare cases treatment with DMF-containing drugs Tecfidera® or Fumaderm® led to progressive multifocal leukoencephalopathy (PML) in patients (Ermis, Weis, & Schulz, 2013; Longbrake & Cross, 2015; Rosenkranz, Novas, & Terborg, 2015).

During the last years, several studies aimed to clarify the exact mode of action of DMF in MS treatment, but it is still not fully elucidated. Similar to other immunomodulatory therapies, it became clear that DMF rather exerts a plethora of mechanisms on various cell types (Linker & Haghikia, 2016). Fumarates are α , β -unsaturated electrophilic metabolites that covalently bind to cysteine residues of proteins, leading to their succination that can result in inactivation (Blatnik, Thorpe, & Baynes, 2008). It was demonstrated that DMF exerts protective effects

against oxidative stress in DCs, astrocytes and neurons by induction of a nuclear factor erythroid 2-related factor 2 (Nrf2)-dependent antioxidant response (Ghoreschi et al., 2011; Linker et al., 2011; Scannevin et al., 2012). Succination and inactivation of kelch-like ECH-associated protein 1 (Keap1) by DMF, results in the release of Nrf2 from Keap1-binding, its translocation in the nucleus and induction of antioxidant gene transcription. However, the use of an EAE model in wildtype (WT) and Nrf2-deficient mice revealed an almost similar protection following DMF treatment, indicating that the anti-inflammatory effects of DMF may occur Nrf2-independent (Schulze-Toppfhoff et al., 2016).

Furthermore, DMF was shown to bind and succinate the ROS scavenger glutathione (GSH), resulting in a reduced antioxidant capacity and a subsequent increase of ROS in DCs, tumour cells, monocytes and macrophages (Ghoreschi et al., 2011; Hoetzenecker et al., 2012; Sullivan et al., 2013; Zheng et al., 2015). Another study reported a significant increase in cytosolic ROS in T cells of in MS patients after 3 months of DMF treatment (Diebold et al., 2017). Of note, GSH depletion and ROS accumulation induce DCs that rather produce IL-10 instead of proinflammatory IL-12 and IL-23, thereby indirectly rather promoting Th2 than Th1/Th17 differentiation (Ghoreschi et al., 2011).

As DMF is a derivative of fumarate, a metabolic intermediate of the tricarboxylic acid (TCA) cycle, it is not surprising that DMF can influence the metabolism of cells: beyond succination of KEAP1 and glutathione, DMF succinates the glycolytic enzyme glyceraldehyde-3-phosphat-dehydrogenase (GAPDH) *in vivo* and *in vitro*. This results in GAPDH inactivation, followed by the downregulation of aerobic glycolysis in macrophages and Th1 as well as Th17 cells (Sui et al., 2018). Activated macrophages and T cells require glycolysis for their survival, differentiation and effector functions (Gerriets & Kishton, 2014; Macintyre et al., 2014; Tannahill et al., 2013; Wang et al., 2011). In line, Kornberg et al. found suppressed IFN- γ and IL-17 production in Th1 and Th17 respectively upon DMF treatment (Sui et al., 2018). A study of Diebold et al confirmed the suppression of glycolysis in T cells during DMF treatment in MS patients (Diebold et al., 2017).

Besides succination, DMF and its metabolite monomethyl fumarate (MMF) are reported agonists of the G protein-coupled membrane receptor hydroxycarboxylic acid receptor 2 (HCA2). It was shown that DMF decreased neutrophil infiltration and demyelination of spinal cords in WT but not in HCA2-deficient mice, indicating that DMF mediates its therapeutic effects by HCA2 (H. Chen et al., 2014).

DMF treatment also impacts B cell subsets *in vivo* and *in vitro* (Li et al., 2017). Li et al revealed that DMF modulates MS disease activity by reducing the phosphorylation of nuclear factor 'kappa-light-chain-enhancer' of activated B-cells (NF- κ B) as well as reducing GM-CSF, IL-6 and

TNF- α production, thereby shifting the balance between pro-and anti-inflammatory B cell responses (Li et al., 2017; M. D. Smith, Martin, Calabresi, & Bhargava, 2017) A reduced NF- κ B translocation into the nucleus is reported by several studies and for different cell types (Diebold et al., 2017; Kastrati et al., 2016; Seidel et al., 2009).

DMF is further known to influence the hypoxia-sensitive TF hypoxia-inducible factor-1 α (HIF-1 α) (Laukka et al., 2016; Zhao et al., 2014), alter histone modifications (Sullivan et al., 2013) and increase DNA hypermethylation by inhibition of TET enzymes that catalyse demethylation by converting 5-methylcytosine to 5-hydroxymethylcytosine (5-hmC) (Laukka et al., 2016; Xiao et al., 2012).

Collectively, the aforementioned studies reveal the wide range of immune modulatory and neuroprotective effects by DMF, which affect a variety of cell types. It shows a broad efficiency; however, rare cases of PML require therapy control, especially during the first year of treatment.

2.4 Signal transduction

In order to respond to the environment, cells of the immune system have to sense extracellular stimuli. These signals are transmitted via surface receptors that trigger intracellular signalling cascades, which regulate cellular processes including transcription, translation and posttranslational modifications (Murphy & Weaver, 2017). The differentiation into distinct T cells subsets is based on signal transduction initiated by cytokine signalling, followed by ligand-induced activation of serine/threonine or tyrosine kinases (Kishimoto, Taga, & Akira, 1994). Finally, this cytokine-induced cascade regulates the cellular fate by forming a network of TFs (J Zhu et al., 2010).

2.4.1 Signalling networks in T cell differentiation

The differentiation in specific T cell subsets is mediated by extracellular cytokine signals that induce a complex network of TFs, ultimately leading to the characteristic signature of the respective subpopulation. For inducing and maintaining CD4⁺ and CD8⁺ T cell subsets the expression of lineage-specific master regulators is a central mechanism. Th1 cells are induced by IFN- γ signalling and subsequent activation of signal transducers and activators of transcription (STAT)4, which results in the induction of the master regulator T-box expressed in T cells (T-bet). T-bet maintains Th1 differentiation by several mechanisms: by inducing endogenous IFN- γ production in a positive feedback loop (Szabo et al., 2000), increasing sensitivity to IL-12 signalling (Mullen et al., 2001) and repressing Gata binding protein (GATA)3

functions and thereby suppressing Th2 differentiation (Hwang, Szabo, Schwartzberg, & Glimcher, 2005). The differentiation of naïve CD8⁺ T cells into effector CTLs is mediated by IL-2 and IL-12 and the combined activities of the TF B lymphocyte-induced maturation protein-1 (Blimp-1), T-bet (Joshi et al., 2007; Kalia et al., 2010; Pipkin et al., 2010; Xin et al., 2016) Id2 (Cannarile et al., 2006) and IRF4 (Man et al., 2013; Raczkowski et al., 2013; Yao et al., 2013). Th2 and Tc2 cells differentiate in the presence of IL-4-mediated STAT6 activation ultimately leading to GATA3 expression, which promotes Th2 proliferation and prevents Th1 differentiation (Jin角度 Zhu, Yamane, Cote-Sierra, Guo, & Paul, 2006). For Th2 cells it is known that IL-2-induced STAT5 is required for an optimal differentiation (Cote-Sierra et al., 2004). The combination of IL-4 and TGF- β drives Th9/Tc9 cell fate and the TF PU.1 and IRF4 regulate the expression of type 9 specific genes (Chang et al., 2010; Staudt et al., 2010). The master regulator retinoic acid-related orphan receptor (ROR γ t) initiates the differentiation into Th17 and Tc17 cells (Mittrücker et al., 2014; J Zhu et al., 2010). The transcriptional regulation of type 17 differentiation is described more in detail in the following chapter.

Despite the aforementioned classification into CD4⁺ and CD8⁺ subsets with specific master regulators, differentiated T cells still have the ability to de- or redifferentiate, a phenomenon called 'T cell plasticity' (Mittrücker et al., 2014; Zhou et al., 2009).

2.4.1.1 Transcriptional regulation of type 17 cell differentiation

Only a few years ago, the presence of IL-17-producing CD8⁺ T cells has been described in human and mouse (Hamada et al., 2009; Huber et al., 2009; Intlekofer et al., 2008; Kondo, Takata, Matsuki, & Takiguchi, 2009). Similar to Th17 cells, also Tc17 cells differentiate in response to IL-6 or IL-21 along with TGF- β (Hamada et al., 2009; Huber et al., 2009; Yen et al., 2009), resulting in the expression of ROR γ t that is crucial for production of the marker cytokines IL-17A and IL-17F (Ivanov et al., 2006). The presence of IL-23 stabilises the pathogenic phenotype (Langrish et al., 2005). IL-6- and IL-21-mediated intracellular signal transduction induces the activation and phosphorylation of the TF STAT3 (Ivanov, Zhou, & Littman, 2007), which induces expression of type 17 regulators ROR γ t, ROR α and the cytokine IL-17A by binding to the respective promoters (Arra et al., 2017; Laurence et al., 2007; X. O. Yang et al., 2008; Yen et al., 2009). In line, STAT3-deficient T cells do not produce IL-17 nor ROR γ t (Laurence et al., 2007; X. O. Yang et al., 2008; Zhou et al., 2007). Furthermore, STAT3 mediates the transcription of *IL-21* and *IL-23R* that contribute to the stabilisation of the type 17 phenotype (Arra et al., 2017; Huber et al., 2009; Zhou et al., 2007). It was shown that IL-6 induces the expression of IL-21, thereby supporting type 17 phenotype by a positive feedback mechanism (Korn et al., 2007; Nurieva et al., 2007). In addition, IL-21 induces the expression of

IL-23R, thus further stabilising the type 17 phenotype (Ciric, El-behi, Cabrera, Zhang, & Rostami, 2009).

In addition, the TCR-induced TF IRF4 is critical for Tc17 differentiation by inducing ROR γ t and ROR α on the one side and restricting Eomes and Foxp3 expression on the other (Huber et al., 2013). The absence of IRF4 results in disturbed Tc17 differentiation, demonstrating its importance (Huber et al., 2013). In contrast to classical CTLs, Tc17 cells are low-cytotoxic and express diminished levels of Eomes and T-bet (Huber et al., 2009; Intlekofer et al., 2008; Srenathan et al., 2016). Recently, it was shown that costimulatory cytotoxic T-lymphocyte-associated protein 4 (CTLA-4) regulated Tc17 differentiation and stability by enhancing STAT3 binding to the IL-17 promoter (Arra et al., 2017).

IFN- γ and IL-27 signalling restricts type 17 differentiation by inducing STAT1 expression (Hu & Ivashkiv, 2009; Stumhofer et al., 2006). The ratio of STAT1 /STAT3 has been shown to regulate the type 17 fate (Peters et al., 2015). In addition, IL-2 has been shown to suppress Th17 differentiation by STAT5 (Gilmour, Pine, & Reich, 1995) as STAT5 and STAT3 are known to compete at the *IL17* locus of Th17 cells, leading to activation or suppression respectively (X. P. Yang et al., 2011).

2.4.1.2 ROS signalling in T cells

ROS are small, highly reactive oxygen-containing molecules. For long time, they have been seen as exclusively harmful, causing cell damage. However, recent data demonstrate that ROS are essential second messengers in a multitude of immune functions, including antiviral, antibacterial and anti-tumour responses (Belikov, Schraven, & Simeoni, 2015; Franchina et al., 2018; Sena & Chandel, 2012). Most intracellular ROS are generated in mitochondria in the electron transport chain (ETC) during the reduction of O₂ to H₂O (Belikov et al., 2015). Enzymatic or non-enzymatic antioxidant mechanisms dynamically balance ROS levels within the cell and protect against oxidative damage (Meister, 1983). The most abundant antioxidant GSH scavenges ROS by formation of oxidised glutathione disulfide (GSSG), which can be reversed to GSH by glutathione reductase (S. C. Lu, 2013).

ROS produced by macrophages have been reported to exert immunosuppressive functions and being functional for Treg induction (Kraaij, 2010). In addition, cancer cells and tumour-infiltrating immune cells including macrophages produce high levels of ROS in the tumour microenvironment, thereby suppressing T cell responses and contributing to tumour growth (X. Chen, Song, Zhang, & Zhang, 2016).

TCR signalling during activation of T cells leads to a release of Ca²⁺ from the endoplasmatic reticulum. Ca²⁺ is taken up by mitochondria and results in elevated ETC, leading to increased

oxygen consumption and ROS production (Murphy & Weaver, 2017). Depending on their levels and localisation, ROS can influence T cell responses by altering signalling transduction and metabolism (Franchina et al., 2018; Sena & Chandel, 2012). It revealed that high ROS levels suppress T cell activity (Gelderman, Hultqvist, Holmberg, Olofsson, & Holmdahl, 2006) and initiate DNA damage and cell death (Sena & Chandel, 2012), whereas low ROS concentrations promote T cell activation, expansion and effector functions (Devadas, Zaritskaya, Rhee, Oberley, & Williams, 2002; Jackson, Devadas, Kwon, Pinto, & Williams, 2004). Sena et al showed that an ROS-dependent signalling is required for activation of nuclear factor of activated T-cells (NFAT) and IL-2 expression (Sena et al., 2013), thus, confirming ROS as an essential component for T cell activation. Furthermore, there is evidence for the ability of ROS to affect T cell differentiation: T cells lacking the ROS-producing enzyme NADPH oxidase showed diminished expression of STAT1, STAT4 and T-bet, resulting in reduced production of IL-2, IL-4, IFN- γ and TNF- α , whereas STAT3, IL-17 and TGF- β were elevated (Tse et al., 2010). These results underline the capacity of ROS to modify immune responses.

2.4.1.3 IL-2 signalling in T cells

The cytokine IL-2 belongs to the common γ -chain family and plays a central role in the regulation of tolerance and immunity (Malek & Castro, 2010). It mediates its functional activity by binding to the cell surface receptor complex consisting of IL-2R α (CD25), IL-2R β (CD122) and IL-2R γ (CD132). Interestingly, IL-2R α is not expressed on resting, naïve T cells, thereby preventing a response to physiologic doses of IL-2 (Malek & Castro, 2010). Upon T cell activation IL-2R α is induced and the cells become sensitive to IL-2 signalling (Boyman & Sprent, 2012). Binding of IL-2 to its receptor leads to a conformational change that initiates the activation of associated cytoplasmic kinases Janus kinase 1 (JAK)1 and JAK3, which subsequently phosphorylate several tyrosine residues on the IL-2R β chain. In the following steps, several IL-2 downstream pathways are induced: STAT5 is recruited and phosphorylated by the two tyrosine residues Tyr³⁹² and Tyr⁵¹⁰, leading to transcription of IL-2-dependent genes (Lin et al., 2012). In addition, phosphoinositide 3-kinase (PI3K) and mitogen-activated protein kinase (MAPK) are activated by Tyr³³⁸ and the adapter protein Shc (G. A. Smith, Taunton, & Weiss, 2017). Depending on the physiologic context, these three signals ultimately trigger proliferation, differentiation into specific T cell subpopulations and production of effector molecules (G. A. Smith et al., 2017).

Functionally, IL-2 induces the expression of IL-2R α on activated CD4⁺ and CD8⁺ T cells and stimulates their proliferation (G. A. Smith et al., 2017). Furthermore, IL-2 is essential for the development of Treg cells during thymic development (Cheng, Yu, Dee, & Malek, 2013;

Shevach et al., 2006), contributes to T memory formation (Bachmann & Oxenius, 2007; Williams, Tyznik, & Bevan, 2006) and terminal differentiation into T effector cells (Kalia et al., 2010; Pipkin et al., 2010). Interestingly, strong or extended IL-2 signalling drives CTL effector cell differentiation, whereas weak or limited IL-2 signals enhance CTL memory cell formation (Kalia et al., 2010; Pipkin et al., 2010). IL-2 induces Blimp-1 that supports terminal differentiation of effector T cells (Cretney et al., 2011; Kallies et al., 2006; Kallies, Xin, Belz, & Nutt, 2009; Kallies & Nutt, 2007; Rutishauser et al., 2009), but also contributes to programming of memory CTLs (Feau, Arens, Togher, & Schoenberger, 2011; Williams et al., 2006). Therefore, IL-2 signalling in CTL differentiation is complex and still incompletely understood (Xin et al., 2016). The other CTL-skewing cytokine, IL-12, enhances the expression of T-bet and Id2 (Joshi et al., 2007; X. P. Yang et al., 2011) and via phosphoinositide 3-kinase (PI3K)-AKT also drives the serine/threonine protein kinase mammalian target of rapamycin (mTOR) activity (Araki et al., 2009). Of note, the loss of both CTL-driving TF T-bet and Blimp-1 was shown to induce a substantial IL-17 production in CD8⁺ T cells (Xin et al., 2016), demonstrating the plasticity of T cells as well as the importance of T-bet and Blimp-1 for CTL fate.

Whereas CTL and Treg differentiation is supported by IL-2 signalling (Kalia et al., 2010; Pipkin et al., 2010; Shevach et al., 2006), IL-2 opposes Th17 cells by inducing STAT5, leading to elevated binding of the negative regulator to the *IL17* promoter (Laurence et al., 2007).

Despite similarities in IL-2-dependent signal transduction in CD4⁺ and CD8⁺ T cells, there are also differences: whereas IL-2 signalling in CD4⁺ T cells initiates a biphasic STAT5 phosphorylation (P-STAT5), CD8⁺ T cells show a single, sustained peak of P-STAT5, indicating functional differences in downstream-signalling cascades in both T cell classes (G. A. Smith et al., 2017). Furthermore, the phosphorylation of S6, a downstream target of the PI3K/AKT and mTOR kinase pathway is higher in CD8⁺ T cells compared to CD4⁺ T cells (Yu, Zhu, Altman, & Malek, 2009).

2.5 Epigenetic regulation of gene expression

In a multicellular organism all cells contain homogeneous genetic information. However, these cells with the same underlying DNA sequence are extremely heterogeneous in their phenotype and function due to differential gene expression, which is preserved through cell division (Kanno, Vahedi, Hirahara, Singleton, & O'Shea, 2012). Gene expression is not exclusively regulated by the presence/ absence or activation of specific TFs; additionally, other factors contribute to the transcription of a genomic sequence. The term 'epigenetics' is used to

describe heritable changes in gene expression that do not involve changes of the DNA sequence (Dupont, Armant, & Brenner, 2009).

2.5.1 Chromatin remodelling

Eukaryotic DNA has to be densely packed in order to fit in the nucleus. Therefore, it is tightly wrapped around octamers of histones, forming structures called nucleosomes, in this way a 10,000 to 20,000-fold compaction is achieved (Zentner & Henikoff, 2013). The close binding of DNA to the nucleosomes is ensured by the negatively charged backbone of the DNA and the positively charged histones. The properties of nucleosomes can be modified in several ways, a process called chromatin remodelling, thereby allowing or preventing access to the DNA. Several elements contribute to remodelling of chromatin, including histone tail modifications, DNA methylation and chromosome conformation (Kanno et al., 2012).

2.5.1.1 Histone tail modifications

More than 50 years ago, it was discovered that active gene transcription correlates with hyperacetylation of histones (Allfrey, Faulkner, & Mirsky, 1964). Since then a plethora of posttranslational histone modifications has been described, such as acetylation (Ac), methylation (me), phosphorylation, ubiquitination and further more (Kanno et al., 2012). Two opposing enzymes, histone acetyltransferases (HATs) and histone deacetylases (HDACs), are associated with sites of active transcription, suggesting their contribution to chromatin remodelling (Kanno et al., 2012; Zentner & Henikoff, 2013). Acetylation of N-terminal histone tails is mediated by HATs. By neutralisation of positive charges of lysine residues of the histones, the interaction between negatively charged DNA and nucleosomes is disturbed, leading to elevated accessibility of the chromatin to the transcription machinery (Zentner & Henikoff, 2013). On the other side, HDACs mediate the removal of acetyl groups, causing tight binding of nucleosomal DNA to the histones. Thus, classically HDACs are associated with histone deacetylation and therefore reduced transcription, whereas HATs are related to acetylated chromatin and active transcription (Kanno et al., 2012).

Further regulatory elements are histone methylations. In contrast to acetylation, methylations do not alter the charges of the amino acid lysine. Thus, the impact of histone methylation on nucleosome compaction is less direct and can activate or repress gene transcription (Zentner & Henikoff, 2013). Whether a gene is activated or silenced is depending on the number of methyl groups as well as the lysine position on the histone. Methylation is known to occur on histone H3 (K4, K9, K27, K36) and H4 (K20) (Dimitrova, Turberfield, & Klose, 2015; Kouzarides, 2002).

For example, H3K4me is linked with active gene transcription, whereas H3K27me is seen as a repressing histone methylation (Kouzarides, 2002).

2.5.1.2 DNA methylation

DNA methylation occurs on cytosines in CG-rich regions of the DNA and is widely associated with gene silencing (Kanno et al., 2012). CG-rich regions, so called CpG islands, are short DNA sequences with a high frequency of 5'-CpG-3' sequences. They often occur at transcription start sites (TSS) and are mostly unmethylated, leading to active transcription (Chatterjee & Vinson, 2012). The methylation of CpG islands by DNA methyltransferases was considered to be the most stable epigenetic mark that transfers heritable epigenetic memory (Kanno et al., 2012). However, 10 years ago ten eleven translocation (TET) proteins were discovered, which are able to modify methyl cytosine and thereby probably remove DNA methylations (Tahiliani et al., 2009), implying that DNA methylation patterns are not as stable as previously assumed (Rasmussen 2016).

2.5.1.3 Nucleosome compaction and chromatin conformation

Accessible DNA is required to allow binding of the transcription machinery in order to achieve gene transcription. It was shown that nucleosomes can alter their position with respect to a specific DNA sequence, thereby reducing their occupancy at a promoter and allowing active transcription. This process is called nucleosome compaction and is mediated by ATP-dependent nucleosome remodelers, multiprotein complexes that are able to slide or disassemble histone octamers (Kanno et al., 2012).

In addition to histone modifications, DNA methylation and nucleosome compaction also three-dimensional chromatin conformation has been recognised to affect regional gene transcription (Deng & Blobel, 2010). Chromatin looping allow close contact between distal regulatory elements and their respective promoter region. These interactions realised by formation of three-dimensional structures can take place on the same (cis) or even between regions of different chromosomes (trans)(Kanno et al., 2012).

3. Material

3.1 Equipment

Device	Model	Company
Bioruptor	Bioruptor® Plus	Diagenode, Liège, Belgium
Flow cytometers	<i>BD FACSCalibur</i> <i>BD FACSAriaIII</i>	BD, Franklin Lakes, USA
Incubator	HERAcell240i	Heraeus, Hanau
pH meter	inoLab pH Level 2	WTW, Weilheim
Plate photometer	FLUOstar Omega	BMG Labtech, Ortenberg
qPCR machine	StepOnePlus™	Applied Biosystems, Darmstadt

3.2 Chemicals and consumables

Chemical	Company
AB serum	Sigma-Aldrich, St. Louis, USA
Aqua dest.	Braun, Melsungen
Akt1/2 kinase inhibitor	Merck, Darmstadt
Biotinylated microBeads	Institute for Med. Microbiology, Marburg
Bovine serum albumin	Biomol, Hamburg
Brefeldin A	Sigma-Aldrich, St. Louis, USA
β-Mercaptoethanol	Sigma-Aldrich, St. Louis, USA
2-DG	Merck, Darmstadt
Dimethyl fumarate	Sigma-Aldrich, St. Louis, USA
Dimethyl sulfoxide (DMSO)	Sigma-Aldrich, St. Louis, USA
DNase I	Sigma-Aldrich, St. Louis, USA
Dulbecco's Modified Eagle's Medium	Sigma-Aldrich, St. Louis, USA
EDTA	Thermo Fisher Scientific, Waltham, USA
Fetal calf serum	Sigma-Aldrich, St. Louis, USA
Glutathione, reduced form ethyl ester	Sigma-Aldrich, St. Louis, USA
Glycine	Riedel-de Haën, Seelze
Halt Protease Inhibitor Single Use Cocktail	Thermo Fisher Scientific, Waltham, USA

HEPES	Roth, Karlsruhe
Incomplete Freund's adjuvans (IFA)	Sigma-Aldrich, St. Louis, USA
Ionomycin	Sigma-Aldrich, St. Louis, USA
L-glutamine	Biochrom, Berlin
Lithium chloride	Merck, Darmstadt
Ly294002	Cell Signaling Technology, Danvers, USA
MOG ₃₇₋₅₀ peptide	synthesised by R. Volkmer, Charite Berlin, Germany
<i>Mycobacteria tuberculosis</i> H37 RA	Difco, Michigan, USA
Non-essential amino acids (NEAS) 100x	PAA, Pasching, Österreich
NP-40 (Igepal-CA6309)	Sigma-Aldrich, St. Louis, USA
Pancoll (ficoll solution)	Pan Biotech, Aidenbach
para-formaldehyde 4 %	Sigma-Aldrich, St. Louis, USA
Penicillin G	Biochrom, Berlin
Pertussis toxin from <i>Bordetella pertussis</i>	Sigma-Aldrich, St. Louis, USA
Phorbol 12-Myristate 13-Acetate (PMA)	Sigma-Aldrich, St. Louis, USA
Phosphate buffered saline (PBS) 10x	Biochrom, Berlin
PIPES	Roth, Karlsruhe
Protein A Sepharose Beads 4 FastFlow	GE Healthcare, Chalfont St. Giles, UK
RPMI 1640	Sigma-Aldrich, St. Louis, USA
Saponin	Sigma-Aldrich, St. Louis, USA
Streptavidin-Biotin α -FITC	Institute for Med. Microbiology, Marburg
Sodium bicarbonate (NaHCO ₃)	Biochrom, Berlin
Sodium chloride (NaCl)	Sigma-Aldrich, St. Louis, USA
Sodium dodecyl sulphate (DOC)	Sigma-Aldrich, St. Louis, USA
Sodium pyruvate	Sigma-Aldrich, St. Louis, USA
STAT5-Inhibitor	Cayman Chemicals, Ann Arbor, USA
Streptomycin sulphate	Biochrom, Berlin
TEMED	Sigma-Aldrich, St. Louis, USA
Tris-Base	Roth, Karlsruhe
Tris-HCl	Roth, Karlsruhe
Triton-X 100	Sigma-Aldrich, St. Louis, USA

3.3 Kits and dyes

Kit	Company
Annexin V APC	Biolegend, San Diego, USA
BD Phosflow Lyse/ Fix Buffer	BD, Franklin Lakes, USA
BD Phosflow Perm Buffer III	BD, Franklin Lakes, USA
5(6)-Carboxyfluorescein diacetate N-succinimidyl ester (CFSE)	Thermo Fisher Scientific, Waltham, USA
CM-H2DCFDA	Thermo Fisher Scientific, Waltham, USA
Fast SYBR™ Green Master Mix	Thermo Fisher Scientific, Waltham, USA
FoxP3 Transcription Factor Fixation/Permeabilization Concentrate and Diluent	Thermo Fisher Scientific, Waltham, USA
GSH/GSSG Glo™ Assay	Promega, Madison, USA
High Pure RNA Isolation Kit	Roche, Basel, Switzerland
IL17 DuoSet ELISA, murine	R&D systems, Wiesbaden
LIVE/DEAD Fixable Near-IR Dead Cell Stain Kit	Thermo Fisher Scientific, Waltham, USA
Propidium iodide	Sigma-Aldrich, St. Louis, USA
RevertAid First Strand cDNA synthesis Kit	Thermo Fisher Scientific, Waltham, USA

3.4 Buffers and Media

3.4.1 Buffers and media for cell biology

Buffer / media	Composition
Balanced Salt Solution	9.9 g/l Hank's Balanced Salt, 1.425 g/l NaHCO ₃ , 10 mM HEPES in Aqua dest. (pH 7.2)
Coating buffer for cell culture	50 mM Tris-Base (pH 9.5) in Aqua dest.
DMEM (complete media for cell culture)	50 µM ME, 60 mg/ml Penicillin G, 100 mg/ml Streptomycin, 2.4 g/l HEPES, 1.4g/l NaHCO ₃ , 10 % FCS, 2 mM Glutamine
Fetal calf serum	Heat inactivated (30 min, 56°C)
MACS buffer	0.5 % BSA [w/v], 2 mM EDTA (pH 8.0) in PBS
PBS	PBS powder concentrate in Aqua dest. (pH 7.2)
PBS/ 1% FCS	1 % FCS [v/v] in PBS

RPMI (complete media)	10 % FCS, 2 mM Glutamine, 1% NEAS [v/v], 50 μ M β -Mercaptoethanol, 60 mg/ml Penicillin G, 100 mg/ml Streptomycin in RPMI 1640
Saponin buffer	0.3 % Saponin [w/v], 2% FCS [v/v] in PBS

3.4.2 Buffers and media for molecular biology

Application	Buffer	Composition
ChIP	Lysis buffer I	5 mM PIPES (pH 8.0), 85 mM KCl, 0.5 % NP-40
	Lysis buffer II	10 mM Tris-HCl (pH 7.5), 150 mM NaCl, 1% NP-40, 1 % DOC, 1 mM EDTA
	Wash buffer I	20 mM Tris-HCl (pH 8.0), 150 mM NaCl, 2 mM EDTA, 0.1% SDS, 1 % Triton-X 100
	Wash buffer II	20 mM Tris-HCl (pH 8.0), 500 mM NaCl, 0.1 % SDS, 1 % Triton-X 100
	Wash buffer III	10 mM Tris-HCl (pH 8.0), 1% NP-40, 1 % DOC, 1 mM EDTA, 0.25 % LiCl
	TE buffer	10 mM Tris-HCl (pH 8.0), 1 mM EDTA
	Elution buffer	1 % SDS, 0.1 M NaHCO ₃
	Reversal crosslinking	0.2 M NaCl, 10 mM EDTA (pH8), 40 mM Tris (pH 7.2), 40 μ g/ml Proteinase K, 20 μ g/ml RNase A

3.5 Antibodies

3.5.1 Antibodies for CD8⁺ T cell isolation

Epitope	Conjugate	Clone	Company
α -m B220	FITC	RA3-6B2	Thermo Fisher Scientific, Waltham, USA
α -m CD11b	FITC	M1/70	Thermo Fisher Scientific, Waltham, USA
α -m CD11c	FITC	N418	Thermo Fisher Scientific, Waltham, USA
α -m CD49b	FITC	DX5	Thermo Fisher Scientific, Waltham, USA
α -m CD4	FITC	6K1.5	Thermo Fisher Scientific, Waltham, USA
α -m Ter119	FITC	TER-119	Thermo Fisher Scientific, Waltham, USA

3.5.2 Antibodies for cell culture

Epitope	Clone	Company
α -m CD28	Hamster IgG, 37-51	Hybridoma supernatant
α -m CD3 ϵ	Hamster IgG, 145-2c11	Hybridoma supernatant
α -m IFN- γ	Rat IgG, XMG 1.2	Hybridoma supernatant

3.5.3 Antibodies for flow cytometry

	Epitope	Conjugate	Clone	Dilution	Company
Murine	α -CD4	PE	RPA-T4	1:500	Thermo Fisher, Waltham, USA
	α -CD4	V450	RM4-5	1:500	BD, Franklin Lakes, USA
	α -CD8a	APC	53-6.7	1:500	Thermo Fisher, Waltham, USA
	α -CD8a	V500	53-6.7	1:500	BD, Franklin Lakes, USA
	α -CD44	PE	IM7	1:1000	BD, Franklin Lakes, USA
	α -CD62L	AFI 700	MEL-14	1:500	BD, Franklin Lakes, USA
	α -Eomes	APC	Dan11mag	1:500	Thermo Fisher, Waltham, USA
	α -IFN- γ	APC	XM61.2	1:500	Biolegend, San Diego, USA
	α -IL-17A	PE	eBio17B7	1:500	Thermo Fisher, Waltham, USA
	α -P-Akt Ser473	AFI488	D9E	1:100	Cell Signaling, Danvers, USA
	α -P-Akt Thr308	PE	D25E6	1:100	Cell Signaling, Danvers, USA
	α -P-S6 (Ser235/236)	AFI488	D57.2.2E	1:500	Cell Signaling, Danvers, USA
	α -P-STAT5 (Tyr694)	PE	SRBCZX	5 μ l/ test	Thermo Fisher, Waltham, USA
	α -ROR γ t	PE	B2D	1:500	Thermo Fisher, Waltham, USA
	α -T-bet	PE	eBio4B10	1:500	Thermo Fisher, Waltham, USA

Human	α -CD8a	BV510	SK1	3 μ l/test	Biolegend, San Diego, USA
	α -CD4	Pacific Blue	RPA-T4	4 μ l/test	Biolegend, San Diego, USA
	α -CD14	FITC	HCD14	3 μ l/test	Biolegend, San Diego, USA
	α -CD45RA	BV650	HI100	1 μ l/test	Biolegend, San Diego, USA
	α -IFN- γ	APC	4S.B3	3 μ l/test	Biolegend, San Diego, USA
	α -IL-17A	PE	BL168	3 μ l/test	Biolegend, San Diego, USA

3.5.4 Antibodies for ChIP

Epitope	Catalogue Nr	Amount for IP	Company
α -H3K4me3	39159	2.5 μ g	Active motif, La Hulpe, Belgium
α -H3K27ac	ab4729	2.5 μ g	Abcam, Cambridge, UK
α -H3K27me3	39155	2.5 μ g	Active motif, La Hulpe, Belgium
α -H4ac	06-866	5 μ l	Millipore, Darmstadt

3.6 Cytokines

Cytokine	Company
rh IL2	Novartis, Basel, Switzerland
rh TGF- β	PeproTech, Hamburg
rm IL-6	PeproTech, Hamburg
rm IL-1 β	PeproTech, Hamburg
rm IL-23	R&D systems, Wiesbaden

3.7 Primers

Application	Target	Sequence	Company
qRT-PCR	<i>Il17a</i>	5'-TTTAACTCCCTTGGCGCAAAA-3'	Metabion, Martinsried
		5'-CTTCCCTCCGCATTGACAC-3'	
	<i>Hprt</i>	5'-CTGGTGAAAAGGACCTCTCG-3'	Metabion, Martinsried
		5'-TGAAGTACTCATTATAGTCAAGGGCA-3'	
	<i>Ifng</i>	5'-TTCTTCAGCAACAGCAAGGC-3'	Metabion, Martinsried
		AGCTCATTGAATGCTTGGCG-3'	
	<i>Rorc</i>	5'-TTTGGAACTGGCTTCCATC-3'	Metabion, Martinsried
		5'-AAGATCTGCAGCTTTCCACA-3'	

ChIP	<i>Il17a promoter</i>	5'-GAACTTCTGCCCTTCCCATCT -3' 5'-AGCACAGAACCACCCCTTT-3'	Metabion, Martinsried
	<i>Il17a -5 enhancer</i>	5'-CGATACTTTTCAGTGACATCCGTTT-3' 5'-TGCTGACTTCATCTGATACCCTTAGA-3'	Metabion, Martinsried
	<i>RPL32 promoter</i>	5'-TCATTTCTCAGGCACATCTT-3' 5'-ACTCACCGTAAAACAGATGG-3'	Metabion, Martinsried
	<i>Il10 promoter</i>	5'-GCAGAAGTTCATTCCGACCA-3' 5'-GGCTCCTCCTCCCTCTTCTA-3'	Metabion, Martinsried

3.8 Plasmids

Plasmid	Company
pMIG-STAT3 (CSTAT3)	CSTAT3 was provided by Dr. M. Klein (University of Mainz)
pMIG-STAT5 (STAT5A1*6)	STAT5A1*6 was made by E. Bothur as described before (Dissertation E. Bothur, University Marburg)

3.9 Mice

Mouse strain	Description	Company/breeding
C57BL/6	Inbred wildtype mouse strain	Charles River Laboratories
<i>Irf4</i> ^{-/-}	IRF4-deficient, on C57BL/6 background	Own breeding (Animal facility Biomedical Research Center, Marburg)
2D2	transgenic MOG ₃₅₋₅₅ specific TCR, on C57BL/6 background	Own breeding (Animal facility Biomedical Research Center, Marburg)
<i>Tbx21</i> ^{-/-}	T-bet-deficient, on C57BL/6 background	<i>Tbx21</i> ^{-/-} mice were provided by Dr. H. Garn (University of Marburg)

3.10 Cell lines

Cell line	Origin	Modification
HEK 293	Human embryonic kidney cells	Transformed with adenovirus 5 DNA

3.11 Software

Name	Company
Adobe Illustrator C3S	Adobe Systems, San José, USA
Flow Jo	Treestar, San Carlos, USA
GraphPad Prism 5.0	GraphPad Software, La Jolla, USA
MS Office 2010 (Word, PowerPoint, Excel)	Microsoft, Redmond, USA
StepOne	Thermo Fisher Scientific, Waltham, USA
R Studio, Bioconductor	Free software

4. Methods

4.1 Cell culture

For this work primary murine lymphocytes from lymph nodes, spleen or central nervous system, human PBMCs and human embryonic kidney (HEK) 293 cells were used as indicated below. Primary murine lymphocytes were cultured in RPMI complete media with 10% FCS, while human primary cells were cultured in RPMI complete media with 5% AB serum. HEK293 cells were cultured in DMEM complete media with 10% FCS. All cells were handled and cultured under sterile conditions in sterile bench and incubators at 37°C with 5% CO₂. Cell numbers were determined by using a Neubauer counting chamber according to manufacturer's instructions.

4.2 Murine T cell isolation and *in vitro* differentiation

C57BL/6 WT mice were purchased from Charles River Laboratory. *Irf4*^{-/-}, *Tbx21*^{-/-} and transgenic 2D2 mice were bred at the animal facility of the Biomedical Research Center, University Marburg. All experiments were carried out in accordance to the German animal protection law and Regierungspräsidium Gießen.

4.2.1 Preparation of lymph nodes and spleen

To receive murine, naïve CD8⁺ T cells, mice were sacrificed by cervical dislocation. Thereafter lymph nodes and spleen were removed and stored in BSS on ice. To obtain a single cell suspension, the organs were crushed separately through 30 µm cell strainers and washed with BSS. All following washing steps were performed at 1500 rpm at 4°C for 5 min. In order to lyse remaining erythrocytes, the spleen pellet was treated with 5 ml NH₄Cl₂ for 4 min and then washed with MACS buffer to stop the lysis reaction. After centrifugation cells from spleen and lymph nodes were pooled and the total cell number was determined.

4.2.2 Magnetic cell purification of CD8⁺ T cells

To obtain CD8⁺ T cell fraction from homogenised lymph node and splenic cell suspension, magnetic negative cell separation was applied. During this method unwanted cell types like NK cells, macrophages or DC are labelled with antibodies binding to surface markers, followed by magnetic separation of labelled cells (non CD8⁺ T cells) from non-labelled CD8⁺ T cells.

Therefore, the mixed cell suspension was washed with MACS buffer and the pellet was resuspended with a primary FITC-conjugated antibody cocktail (2.5 $\mu\text{l}/100 \times 10^6$ cells) directed against surface markers of unwanted cell populations. After incubation for 10 min at 4°C the cells were washed again with MACS buffer, resuspended with secondary streptavidin- α -FITC antibodies (1 $\mu\text{l}/100 \times 10^6$ cells) and incubated for 15 min at 4°C. Thereafter the cells were washed twice with MACS buffer and biotinylated microbeads (30 $\mu\text{l}/100 \times 10^6$ cells) were added and incubated on a rotator at 4°C for 20 min. Finally, the suspension was placed on a magnet at room temperature (RT) to separate the magnetic beads-labelled non-CD8⁺ T cells from non-labelled CD8⁺ T cells and after 20 min the supernatant was removed carefully, washed with MACS buffer and resuspended in RPMI complete media. Cell purity was determined by FACS analysis using α -CD8 staining and was usually $\geq 90\%$. To obtain naïve CD8⁺CD62L⁺CD44⁻ T cells, purified CD8⁺ T cells were either sorted subsequently or directly cultured *in vitro* upon magnetic cell separation.

4.2.3 Activation and differentiation of CD8⁺ T cells *in vitro*

T cell activation and differentiation requires three signals, which are provided by APCs and other cells under physiological conditions. In addition to (i) antigen-specific TCR binding to MHC, (ii) non-specific costimulatory signals and (iii) cytokine-induced signaling pathways are necessary to fully activate T cells.

During *in vitro* cultivation these signals are provided by monoclonal antibodies directed against (i) the CD3 molecule of the TCR and (ii) the CD28 costimulatory receptor. To ensure differentiation into the desired subtype (iii) recombinant cytokines are added.

After purification the cells were plated under Tc17 conditions (indicated in Table 1) in 24, 48- or 96-well plates ($1.0/0.3/0.12 \times 10^6$) usually for 3 days and indicated in figure legends, if different. Resting periods were performed as indicated in figure legends.

Table 1: Culture conditions for murine Tc17 differentiation

	Murine Tc17 conditions
α -CD3, coated	5 $\mu\text{g}/\text{ml}$
α -CD28	0.5 $\mu\text{g}/\text{ml}$
α -m IFN- γ	5 $\mu\text{g}/\text{ml}$
rh IL-2	50 U/ml
rh TGF- β	0.5 ng/ml
rm IL-6	30 ng/ml

4.3 Human T cell preparation and *in vitro* differentiation

4.3.1 Isolation of human PBMC from whole blood

To obtain human peripheral blood mononuclear cells (PBMC) from healthy control persons, a ficoll gradient was performed with whole blood. 60 ml of whole blood contained app. 80×10^6 PBMCs. For separation, 15 ml of ficoll solution (at RT) was pipetted into a 50 ml tube, followed by careful addition of 35 ml whole blood on top. After centrifugation at 2000 rpm for 35 min at RT without brake, the PBMC ring was transferred into a fresh 50 ml tube and two washing steps with PBS were performed (1500 rpm, 5 min, 4°C). The cells were either stored at - 80°C overnight and transferred in liquid nitrogen for long-time storage or processed immediately.

4.3.2 Differentiation of human CD8⁺ T cells

Upon ficoll density gradient centrifugation, human PBMCs were incubated with antibodies and memory CD8⁺ T cells were sorted (CD8⁺CD45RA⁻) using a FACS AriaIII (see section 4.4.1). Like murine T cells, also human T cells require for full activation three signals (TCR and costimulatory signals as well as cytokines), indicated in Tab. 2. Cells were cultured in flat bottom 96-well culture plates for 4-5 days. Experiments were performed in collaboration with Dr. C. Zielinski from Technical University of Munich.

Table 2: Culture conditions for human Tc17 differentiation

	Human Tc17 conditions
α-CD3, coated	2 µg/ml
α-CD28	2 µg/ml
rh TGF-β	20 ng/ml
rh IL-1β	20 ng/ml
rh IL-6	10 ng/ml

4.3.3 Freezing and thawing of human PBMCs

For freezing of PBMCs, the cell pellet was resuspended in 250 µl ice-cold RPMI complete media containing 5% human albumin and transferred to a cryotube. Then another 250 µl of RPMI complete media with 5% human albumin and 20% DMSO was added dropwise while gently swivelling. The tube was placed immediately in 4°C cold EtOH and put overnight to - 80°C to ensure mild freezing. The next day cells were transferred into liquid nitrogen.

In order to analyse frozen PBMCs, cryotubes were thawed, transferred in a 15 ml tube and washed (1500 rpm, 5 min, 4°C) twice with RPMI complete media containing 5% AB serum to remove the DMSO. For recovery, cells were rested for 2 h at 37°C, before restimulation.

4.3.4 Restimulation of human PBMCs

For analysis of frozen PBMC samples from untreated RRMS patients and 12 months after start of DMF treatment (240 mg orally twice a day), we thawed the PBMCs and added cold RPMI/ 5% AB serum dropwise to a volume of 6 ml. Cells were washed twice with RPMI/ 5% AB serum (1500 rpm, 5 min, 4°C), followed by resting in 1 ml RPMI/ 5% AB serum at 37°C for 2h. Thereafter, cells were restimulated with 50 ng/ml PMA and 1 µg/ml ionomycin and incubated for 2.5 h at 37°C. After addition of brefeldin A for another 2.5 h, cells were washed with PBS and surface staining was performed as indicated in 4.4.2 for 30 min at 4°C. Upon fixation with 2% para-formaldehyde, cells were stained intracellularly as mentioned in 4.4.3 for 45-60 min at 4°C. Thereafter cells were analysed using *FACS AriaIII*.

4.4 Flow cytometry

Flow cytometry allows simultaneous multiparametric analysis of heterogenous cell suspensions as well as sorting of certain cell populations. Therefore, single cells suspended in a liquid stream are passed through a laser light beam and the interaction with the light is measured by an electronic detection apparatus as light scatter and fluorescence intensity. This gives information about cell size and granularity, cell viability and expression of fluorescence dye-labelled epitopes based on antibody binding or transfection. Cells were measured on *FACS Calibur* using CellQuest (version 0.3) or *FACS AriaIII* using Diva software (version 8.0.2.) and analysed with FlowJo Software.

4.4.1 Cell sorting

Fluorescence-activated cell sorting (FACS) enables sorting of desired cell populations based on respective parameters, like surface markers or intracellular amines in dead cells.

After labelling the cell suspension with antibodies directed against surface markers, primary naïve CD8⁺CD62L⁺CD44⁻ T cells were sorted by charge into separate vessels. Therefore, the cells were washed with PBS and incubated for 10 min at RT with *LIVE/DEAD Fixable Near-IR Dead Cell Stain Kit* to label dead cells. After washing the cells with PBS, they were incubated with appropriate surface antibodies for 15 min at 4°C, washed and resuspended in a suitable

volume of PBS/1% FCS for sorting procedure. Sorting was performed under sterile conditions at *FACS AriaIII*. Analysis usually confirmed a sorting purity of $\geq 98\%$.

4.4.2 Surface staining

Cells express distinct surface markers that give information about cell type, subsets and biological function. Additional staining of dead or dying cells with amine-reactive dyes was used to determine viability of the cells.

Surface molecules are stained prior to any fixation and can be analysed without fixation. Therefore, cells were washed with PBS and stained with *LIVE/DEAD Fixable Near-IR Dead Cell Stain Kit* according to manufacturer's information for 10 min at RT to determine dead or dying cells, then again washed with PBS. Murine cells were stained with respective antibodies in PBS for 15 min at 4°C in the dark, while human PBMCs were stained for 30 min. After an additional washing step with PBS/1%FCS cells were analysed or subjected to further staining procedures.

4.4.3 Intracellular staining

To analyse cytokine production, cells have to be restimulated. Therefore, cells were incubated with PMA and ionomycin to increase TCR signalling, whereas the addition of brefeldin A blocks the protein transport from endoplasmatic reticulum to golgi apparatus to enrich produced cytokines within the cell. Furthermore, cells were fixed with formaldehyde to crosslink proteins, followed by permeabilisation to access intracellular molecules.

Therefore, murine cells were washed with PBS, resuspended in 1 ml restimulation medium containing 50 ng/ml PMA, 1 µg/ml ionomycin and 50 µg/ml brefeldin A and incubated for 4 h at 37°C. Then, cells were washed with PBS and fixed with 0.5 ml 2% para-formaldehyde for 20 min at RT. After fixation, cells were washed with PBS/1% FCS and saponin buffer, followed by antibody incubation for 15 min for murine cells, whereas human PBMCs were stained for 45-60 min at 4°C. For this, fluorescence-labelled antibodies in saponin buffer were added to the cells in a final volume of app. 150 µl. Upon incubation were washed with saponin buffer and PBS/1% FCS, resuspended in PBS/1% FCS and subsequently analysed.

4.4.4 Intranuclear staining

To analyse the expression of nuclear proteins and TFs the nuclear membrane has to be permeabilised, which requires a harsher fixation method.

Therefore, the cells were washed in PBS and fixed with 0.5 ml 1x *FoxP3 Transcription Factor Fixation/Permeabilization Kit* for 20 min at 4°C.

If cells were additionally transduced with GFP-expressing vectors, cells were previously fixed with 0.2 ml 0.5% formaldehyde for 5 min to prevent leakage of cytoplasmic GFP and then washed with PBS, followed by fixation with FoxP3 Transcription Factor Fixation/Permeabilization Kit.

After fixation, cells were washed with PBS/1% FCS and saponin buffer, followed by antibody staining in a volume of app. 150 μ l for 20 min at 4°C. Finally, cells were washed with PBS/1% FCS and saponin buffer and analysed by flow cytometry.

4.4.5 Phosflow

The detection of phosphorylated proteins requires a harsh and highly optimized fixation and permeabilisation. Therefore, the cells were washed with PBS, fixed with 1x *BD Phosflow Lyse/Fix Buffer* and permeabilised with *BD Phosflow Perm Buffer III* according to the manufacturer's specifications.

4.4.6 ROS staining

Measuring ROS levels within a cell was performed by usage of CM-H₂DCFDA, an indicator of free ROS. After passive diffusion into the cell, acetate groups of CM-H₂DCFDA are cleaved by intracellular esterases. Subsequent oxidation by ROS results in DCF, a highly fluorescent compound, which allows measurement by flow cytometry.

Prior to staining, cells were washed with PBS and the cells incubated in 500 μ l of 1 μ M CM-H₂DCFDA loading solution in PBS for 10 min at 37°C. Thereafter cells were washed twice with PBS, after the last wash step the pellet was resuspended in 500 μ l RPMI and incubated for 15 min at 37°C for recovery. After a final wash step with PBS/1% FCS, cells were subsequently analysed.

4.4.7 Proliferation and apoptosis staining

For assessment of proliferation, CD8⁺ T cells were isolated (see section 4.2) and incubated for 8 min with 5 μ M 5(6)-Carboxyfluorescein diacetate N-succinimidyl ester (CFSE) staining solution at 37°C. Then, cells were washed and cultured under Tc17-driving conditions with DMSO, DMF or DMF in combination with GSH for 3 days. Proliferation was analysed by flow cytometry.

For assessment of apoptosis cells were stained with Annexin V and propidium iodide. Annexin V binds to phosphatidylserine (PS), which is located on the cytoplasmic surface of the cell membrane in viable cells. However, in intermediate stages of apoptosis, PS is translocated to the outer leaflet of the membrane and can be bound by Annexin V, leading to a fluorescence

signal that can be analysed by flow cytometry. Simultaneous staining with propidium iodide, a DNA intercalating dye that cannot cross the membrane of living cells, allows measurement of apoptotic and dead cells.

Tc17 cells were differentiated for 3 days, washed with PBS and stained with Annexin V dye and propidium iodide according to the manufacturer's instructions and analysed by flow cytometry.

4.5 Retroviral overexpression

Retroviral overexpression of CD8⁺ T cells allows the functional analysis of specific TFs. First, HEK 293 cells are transfected with a plasmid containing the coding sequence of the gene of interest, usually tagged with GFP to track the expression. The transfection process takes advantage of the ability of retroviruses to integrate into genomic DNA and be stably expressed. Upon calcium-phosphate-mediated transfection, HEK cells release virus-like particles (VLPs), expressing the protein of interest in a massive amount. In order to transfect murine primary T cells with VLP-containing supernatant coding for the gene of interest, a murine stem cell retroviral expression system was used.

4.5.1 Transfection of HEK 293 cells

Transfection is the process of introducing nucleic acids into eukaryotic cells. This can be realised with a calcium-phosphate transfection method, which is based on forming calcium-phosphate DNA precipitates. Positively charged calcium-phosphate facilitates the binding to the negatively charged backbone of DNA, allowing the DNA to enter the cell by endocytosis.

One day before transfection, $1.5\text{-}2 \times 10^6$ HEK 293 cells were plated in a 10 cm² petri dish. Transfection was performed by generating calcium-phosphate DNA precipitates by mixing 106 μl 2 M CaCl₂, respective amount of DNA (3 μg each of the packaging elements pECO and pCPG and 14 μg retroviral vector) and Aqua dest. to a total volume of 850 μl . In the end, 850 μl of HBS (pH 7.05) were added dropwise while reverse pipetting constantly to create air bubbles and thereby ensure fine precipitate. After incubation for 10 min at RT, DMEM media of HEK cells was exchanged and the transfection mix was added dropwise to the plate. The transfected cells were incubated for 8 h at 37°C to allow endocytosis of calcium-phosphate DNA precipitates. Thereafter, the transfection mix was removed by washing the cells twice with BSS and replaced by 5 ml prewarmed RPMI complete media.

4.5.2 Generation of virus-containing supernatant

After transfection of HEK 293 cells, they release virus-like particles (VLP) to the supernatant, which are able to transfect other cells with the gene of interest.

Therefore, transfected HEK 293 cells were washed and RPMI complete media was added, as described in 4.5.1. 24 h after transfection, the VLP-containing supernatant was transferred to a new tube, 5 ml of fresh RPMI complete media was pipetted to the cells and collected 48 h post-transfection. Both virus-containing supernatants (24 h and 48 h) were pooled, centrifuged, aliquoted and stored at - 80°C.

4.5.3 Spin-based transduction of T cells

In comparison to HEK 293 cells, the calcium-phosphate method is less appropriate to introduce the gene of interest in murine primary T cells as these cells are hard to transfect. Therefore, a murine stem cell retroviral expression system was used.

T cells were isolated as described in 4.2, plated in a 48-well plate with 0.3×10^6 cells per well and centrifugated to ensure sticking to the plate bottom. In the meantime, a transduction mix was prepared, containing 400 μ l viral supernatant containing the gene of interest, 7 μ g/ml polybrene to enhance transduction efficiency and 50U/ml rh IL-2 to ensure cell survival. Upon centrifugation, the media was removed completely and replaced by the transduction mix. Thereafter, the T cells were transduced by a centrifugation process at 2700 rpm at 37°C for 90 min. The viral supernatant was discarded afterwards and replaced by a Tc17 differentiation mix. To increase the efficiency of the spin-based transduction, the process was repeated for a second time after 2 h of incubation. Thereafter, cells were incubated under Tc17-driving conditions (see section 4.2.3) for 3 days. On day three, cells were washed and rested in RPMI complete media containing 50 U/ml rh IL-2 and 5 μ g/ml anti-mIFN- γ for 3 days. Thereafter, cells were re-cultured under Tc17 conditions for additional 72 h, then washed, restimulated and analysed by flow cytometer (see section 4.4).

4.6 Protein-biochemical methods

4.6.1 Enzyme-linked immunosorbent assay

Sandwich enzyme-linked immunosorbent assay (ELISA) was performed in collaboration with Dr. C. Zielinski from TU Munich.

ELISA is a plate-based assay technique designed for detecting and quantifying proteins, like cytokines. Briefly, a first antibody is coated to a 96-well plate, followed by incubation with the sample solution. Then, a second detection antibody is added, which is conjugated to an

enzyme that induces a horse radish peroxidase-mediated colour change. By comparing the colour intensity of the sample to a dilution series of a protein with known concentration, the protein concentration of the sample can be calculated.

Cell culture supernatant was collected and human IL17 *DuoSet ELISA* was performed as described in the manufacturer's specifications.

4.7 Molecular biological methods

4.7.1 Quantitative real-time PCR

Quantitative real-time polymerase chain reaction (qRT-PCR) allows the analysis of transcriptional efficiencies. Beforehand total RNA has to be isolated and reversely transcribed into cDNA, following qRT-PCR. Thereby, the amplification of the targeted gene can be monitored in real-time using SYBR Green intercalation. To evaluate the relative mRNA expression, the threshold cycle (Ct) of the target gene is normalized to a housekeeping gene (Δ Ct) and compared with a control condition ($\Delta\Delta$ Ct).

In a first step, $2\text{-}8 \times 10^5$ cells were washed twice with PBS and resuspended in 200 μ l PBS, followed by RNA extraction with *High Pure RNA Isolation Kit*, which was used accordingly to manufacturer's instructions.

Subsequently, cDNA synthesis was performed to reversely transcribe cDNA from the RNA template. Herefore, 11 μ l of RNA was transcribed using Oligo-dT primers on basis of the *RevertAid First Strand cDNA synthesis Kit*, according to manufacturer's specifications. The resulting cDNA was diluted with Aqua dest. and used for qRT-PCR with *Fast SYBR™ Green Master Mix* on a StepOnePlus Real-Time PCR system.

Thermocycler conditions consisted of an initial denaturation step at 95°C for 1 min, followed by 35 cycles of a two-step PCR program consisting of 95°C/ 3 sec and 60°C/ 30 sec. Melting curves were included to determine primer specificity. Ct values were analysed for gene expression by using the $\Delta\Delta$ Ct method.

4.7.2 RNA sequencing

RNA-Seq is an approach to transcriptome profiling that reveals the complete set of transcripts and their quantity in a cell. The sequencing process starts with the preparation of a library. For that RNA is isolated, transcribed to cDNA and sheared into short fragments. These fragments are size-selected and oligo-adaptors are ligated at both ends. In a second step, the adapter-ligated library is loaded onto a flow cell with adaptor-complementary oligos on its surface, leading to DNA fragment hybridisation to the flow cell. The library is then clonally amplified,

resulting in cluster generation around the initial copy of fragment. In a third step, clusters are sequenced similar to Sanger sequencing, with a reversible terminator-based detection of single nucleotides. In a final step, sequenced reads are aligned to the reference genome, allowing data analysis.

RNA-Seq was performed in cooperation with Dr. M. Klein and Dr. F. Marini from University of Mainz. Therefore, 5×10^5 naïve CD8⁺ T cells were differentiated to Tc17 cells (see Table 1) for 48 h, washed twice with PBS, resuspended in Trizol and RNA was isolated according to manufacturer's specifications. Determination of RNA quality was assessed on a Bioanalyzer 2100 using an RNA 6000 Nano chip, whereas RNA quantification was performed on a Qubit 2.0 fluorometer. In the next step, libraries were prepared with 300 ng RNA (RNA integrity number > 9) on the basis of *NEBnext® ultra™ RNA Library Prep Kit* for Illumina. The following sequencing was performed on a HiSeq2500.

4.7.3 Chromatin immunoprecipitation

Chromatin immunoprecipitation (ChIP) is used to analyse the interaction of proteins with DNA at specific genomic regions in primary T cells, as well as examination of histone modifications. Cells are first fixed to stabilise protein/DNA interactions reversibly (crosslinking) and lysed in a second step. Then, chromatin is subsequently sheared using sonication, followed by immunoprecipitation (IP) of cross-linked DNA fragments with appropriate specific antibodies. After removal of crosslinks, DNA is purified and qRT-PCR is performed to analyse the abundance of a particular DNA sequence. The enrichment of the DNA-Sequence is expressed as fold enrichment above background enrichment of a non-specific antibody control.

4.7.3.1 Cell lysis, fixation and shearing

For analysing histone modifications in primary T cells, $2-5 \times 10^6$ Tc17 cells were harvested, washed twice with PBS and transferred to a sonication tube. For crosslinking, cells were fixed with 1 ml of 1% formaldehyde at RT for 3 min. Fixation was stopped by adding 100 μ l 1.25 M glycine and subsequent rotation for 30 min at RT. Thereafter, cells were pelleted (8000 g, 7 min, RT) and washed twice with cold PBS. After resuspending the cells in 1 ml lysis buffer I complete to disrupt cell membranes, they were either stored at -80°C or processed immediately.

To obtain DNA fragments, cells were sheared by sonication. Herefore, 75 μ l of lysis buffer II complete with 4 % SDS was added for 5 min at RT to disrupt nuclear membranes and release chromatin. To dilute SDS content, 225 μ l of lysis buffer II complete 0% SDS were added to the

nuclei, followed by incubation on ice for 3 min. Then the tubes were inserted into a Bioruptor and 28 cycles of sonication were performed at high power intensity for 30 secs on/ off each to obtain 200-500 bp DNA fragments. Subsequently, samples were diluted by adding 1.2 ml lysis buffer II 0.1% SDS and pelleted (15000 g, 15 min, 4°C). 1.3 ml of the chromatin was stored at 4°C for immunoprecipitation, whereas the remaining 200 µl were used to determine shearing efficiency. Herefore, chromatin was incubated with reversal crosslinking solution for 3 h at 55°C, followed by incubation at 65°C overnight. By adding 750 µl 100 % of ice-cold EtOH and 30 µl 3 M sodium acetate and centrifugation at 15000 g for 15 min at 4°C chromatin was precipitated. Supernatant was removed and chromatin visualized with 1 ml 75 % EtOH and 2 µl glycogen. After further centrifugation, the chromatin pellet was first dried and then reconstituted in 20 µl Aqua dest. 4 µl of loading dye were added before running the DNA on a 1.5 % agarose gel at 80 V for 1.5 h. If sonication was successful, the stored chromatin was further processed.

4.7.3.2 Precipitation and elution

Protein A-coupled sepharose beads were used for immunoprecipitation, as they are able to bind heavy chains of antibodies, allowing a selective purification of target protein-bound DNA fragments. Therefore, they were washed twice with 5 ml of lysis buffer II 0.1 % SDS (3000 g, 3 min, 4°C) and blocked with 600 µl BSA and 1 % fish skin gelatine in 5 ml lysis buffer II 0.1 % SDS overnight to prevent unspecific protein binding. The next day, blocked beads were washed again with 5 ml lysis buffer II 0.1 % SDS (3000 g, 3 min, 4°C) and divided into three different tubes:

App. ½ of the blocked beads was stored at 4°C for the actual immunoprecipitation.

App. ¼ of beads were used for preclearing I. Therefore, 20 µl blocked beads per IP were incubated together with chromatin for 2 h on a rotator to get rid of DNA/protein complexes that unspecifically bind to the beads.

App. another ¼ was used for preclearing II by adding 1 µl of unspecific IgG antibody per IP for 1 h at 4°C on a rotator in order to prevent unspecific IgG binding.

After 1 h of preclearing II, the beads were washed thrice with 5 ml lysis buffer II 0.1% SDS (3000 g, 3 min, 4°C) and split into fresh tubes (20 µl per IP). Precleared chromatin (from 2) was centrifuged (8000 g/ 5 min/ 4°C) and transferred to the tubes with IgG-precleared beads and subsequently incubated on a rotator for another 2 h at 4°C.

After following centrifugation (8000 g, 5 min, 4°C), the chromatin was divided into fresh tubes for immunoprecipitation. Therefore, the total volume of 1.3 ml was split in accordance to the number of IPs, an IgG control and non-precipitated chromatin, called 'input'. The input made

up 10 % of the volume for IP samples and was stored at 4°C. 2.5-5 µg of specific antibody was added to the IP samples, whereas 0.4 µg unspecific IgG antibody was added to the control IP. The antibody binding was performed at 4°C on a rotator overnight. On the following day the antibody-bound chromatin was incubated together with 30 µl blocked beads (from 1) per IP on a rotator at 4°C for 2 h.

In order to remove non-specific bound chromatin, the immunoprecipitated complexes were washed by adding 1 ml of ice-cold buffers with increasing salt concentrations, including twice washing buffer I, twice washing buffer II, thrice washing buffer III and twice TE buffer (8000 rpm, RT, 2 min). Thereafter, samples were eluted by adding 500 µl of freshly prepared elution buffer, vortexing and incubation on a rotator at RT for 30 min. After centrifugation, the chromatin was transferred to a fresh tube and the protein-DNA crosslinking was reversed by adding proteinase K-containing crosslinking reversal buffer. Also, the 'input' samples were filled up to 500 µl with elution buffer before adding crosslinking reversal buffer. Then, all samples were incubated at 55°C for 3 h followed by a 65°C incubation overnight.

4.7.3.3 DNA purification and quantitative detection

In order to perform qRT-PCR, DNA had to be purified. Therefore, a silica membrane-based technique was used, as nucleic acids bind to silica membrane depending on salt concentrations and pH. By using *QIAquick PCR Purification Kit*, the precipitated DNA was diluted in 2.5 ml of PB buffer and 700 µl of the sample were successively transferred to the column and centrifuged (13000 rpm, 1 min, RT). After loading the sample completely, the column was washed by adding 500 µl of PE buffer and dried afterwards by centrifugation at 13000 rpm at RT for 2 min. To elute purified DNA, 50 µl of elution buffer were applied to the column, and after incubation for 10 min at 55°C, the sample was centrifuged (13000 rpm, 1 min, RT). The eluted DNA was stored at 4°C and used for qRT-PCR by using *Fast SYBR™ Green Master Mix* according to manufacturer's specifications. qRT-PCR was performed on the Thermocycler StepOnePlus with an initial denaturation step at 95°C for 10 min, followed by 35 cycles of a three-step PCR program consisting of 95°C/ 30 sec, 55°C/ 30 sec and 72°C/ 20 sec. Melting curves consisting of 95°C for 15 sec, 55°C at 1 min and 95°C for 15 sec were included to determine primer specificity.

4.7.4 Glutathione assay

Glutathione is the most important ROS scavenger within a cell. Most glutathione exists in the reduced form (GSH) to detoxify ROS and only a small percentage of glutathione is oxidised (GSSG) and present as a dimer of two of the peptide elements connected by a disulfide bond.

Changes in levels of GSH or GSSG can provide information about cell health, with low GSH/GSSG ratio indicating oxidative stress. To detect and quantify total glutathione (GSH and GSSG), GSSG levels and GSH/GSSG ratios the *GSH/GSSG-Glo™ Assay* was used. Briefly, cells are lysed and GSH and GSSG are determined, based on a GSH-dependent conversion of a GSH probe to luciferin. The luminescent signal is proportional to the amount of GSH. To measure total glutathione, all glutathione (GSH and GSSG) is converted to the reduced form, whereas the oxidised form is measured in a second configuration by adding a reagent that blocks all GSH while leaving GSSG intact. In a second reducing step, GSSG is converted to GSH for quantification in the luminescent reaction.

CD8⁺ T cells were isolated as described in section 4.2 and cultured in Tc17-driving conditions for the indicated time. Thereafter cells, were washed with PBS and seeded in a 96-well ELISA plate with 0.3×10^6 cells per well. Centrifugation at 1500 rpm for 5 min was performed to ensure sticking to the plate bottom, thereafter supernatant was removed and *GSH/GSSG-Glo™ Assay* was used according to the manufacturer's instructions.

4.8 Experimental autoimmune encephalomyelitis mouse model

Experimental autoimmune encephalomyelitis (EAE) is the most commonly used animal model to examine human inflammatory demyelinating diseases of the CNS, like MS. EAE induction is facilitated by the transfer of T cells, that are specific for myelin-associated autoantigens and simultaneous application of MOG-peptide, pertussis toxin and *Mycobacteria tuberculosis* together with incomplete Freund's adjuvans (IFA) to enhance the immune response and ensure activation and migration of disease-mediating T cells into the CNS.

4.8.1 Oral DMF application and EAE induction

Oral DMF application and EAE induction was performed in collaboration with Dr. F. Kurschus from University of Mainz.

For induction of EAE, C57BL/6 or SJL/L mice were immunized s.c. at the tail basis with 50 µg MOG₃₅₋₅₅ (C57BL/6) or 100 µg PLP₁₃₉₋₁₅₁ peptide (SJL/L) emulsified in complete Freund's adjuvant (CFA) supplemented with 10 mg/ml of heat-inactivated *M. tuberculosis* (strain H37RA). Along with immunisation and on day 2 post immunisation, 100 ng pertussis toxin in PBS was administered by i.p. injection. Oral DMF treatment was applied by supplying the drinking water with 0.5 mg/ml DMF starting 10 days before EAE induction during the entire course of the disease. Daily clinical scoring of EAE symptoms was conducted as follows: Score 0, no symptoms, normal behaviour; Score 1, tail paralysed; Score 2, impaired righting reflex

and gait; Score 3, partial hind limb paralysis; Score 4, hind legs completely paralysed; Score 5, tetraparesis; Score 6, dead. Draining lymph nodes (dLN), spinal cord and brain were analysed at peak of disease (day 14–17 after immunization).

4.8.2 T cell adoptive transfer and induction of EAE

For transfer experiments, CD8⁺ T cells were differentiated under Tc17 conditions for 4 days *in vitro* before 6×10^6 cells were injected i.p. together with 1×10^4 antigen-specific CD4⁺ 2D2 cells into EAE-resistant *Irf4*^{-/-} recipient mice (d-1). On the following day (d0) EAE was induced by s.c. injection of 200 μ l emulsion consisting of incomplete Freund's adjuvans (IFA), 200 μ g MOG₃₇₋₅₀ peptide and 500 μ g *M. tuberculosis* (strain H37RA) in the two flanks of the mice (injection of 100 μ l at each side). At the same day, 200 ng pertussis toxin in 100 μ l PBS was injected i.p. to promote opening of the blood-brain barrier and allowing reactive T cells to migrate into the CNS. Pertussis toxin injection was repeated similarly on d2 upon EAE induction. Thereafter, mice were inspected at least daily and EAE scoring was performed. The following classification was applied: Score 0: healthy, no symptoms; Score 1: flaccid tail; Score 2: paralysed tail; Score 3: hind limb weakness, ataxia; Score 4: partial hind limb paralysis. As soon as the mice were scored with 4 they were sacrificed, CNS and dLN were removed and infiltrating T cells were isolated and processed.

4.8.3 T cell isolation from CNS

Isolation of T cells from lymph nodes was performed as described in section 4.2, whereas the isolation of T cells from CNS required a more complex conduction. Therefore, the head and waist of the mouse had to be removed allowing removal of spinal cord. By means of a syringe filled with PBS, spinal cord was rinsed out of the spine into a petri dish. Brain and spinal cord were crushed by scalpel and transferred into RPMI complete media containing 0.5 mg/ml collagenase D and 10 μ g/ml DNase I. After digestion on a shaker at 37°C for 45 min, tissue was crushed through a 70 μ m cell strainer and washed with RPMI media. To enrich lymphocyte fraction, the cell solution was applied to ficoll gradient centrifugation. Therefore, cells were resuspended in 5 ml of 40 % ficoll solution and pipetted on 3 ml of 70 % ficoll solution. Upon centrifugation at 620 g, w/o brake at RT for 30 min lymphocyte fraction was transferred in a fresh tube and washed twice with RPMI media. Then, cell number was determined as described in 4.1 and cells were restimulated and stained as described in section 4.4.2 and 4.4.3.

4.9 Bioinformatical analysis of RNA sequencing

Bioinformatics is an interdisciplinary field that provides important practical software tools to interpret and analyse high-throughput RNA sequencing data and was performed in collaboration with Dr. F. Marini from University of Mainz.

To analyse differential gene expression, alignment of sequenced reads, mapping to a reference genome and annotation of genes was performed. By using FastQC and QoRTs (Quality of RNA-Seq Toolset) (Hartley & Mullikin, 2015), RNA quality was evaluated.

4.9.1 Alignment, mapping and annotation

Reads were aligned and mapped to mouse reference genome (*Mus musculus* GRCm38). Corresponding gene annotation referred to ENSEMBL v76 and STAR aligner (version 2.4.0b) was used to perform mapping to reference genome.

4.9.2 Differential gene expression analysis

Differential gene expression analysis was performed to estimate the magnitude of differential expression between the samples, especially calculating the fold change of read counts and furthermore to estimate the significance of the differences.

Differential expression analysis was performed with Bioconductor DESeq2 package (version 1.12.3) and the pheatmap package (version 1.0.8), setting the false discovery rate (FDR) to 0.05 or as indicated. To visualise the expression values of analysed samples, heatmaps were generated. Heatmaps show the colour-coded z-scores for the regularized logarithm (rlog) transformed and batch-corrected expression values of the most highly changed genes. Z-scores indicate the number of standard deviations away from the mean of expression in a reference sample. Differential gene expression analysis was performed with the R programming language.

4.9.3 Gene set enrichment analysis

Broad Institute's *Gene set enrichment analysis* (GSEA) was used to perform functional analysis of RNA-Seq data (Subramanian et al., 2005). The method derives its power by focusing on groups of genes that are involved in the same biological pathway or share common regulation or biological function. GSEA software was downloaded from the Broad institute. The hallmark gene set collection of the Molecular Signature Database (MSigDB) as well as published gene sets were used for GSEA. Genes were ranked and p value as well as FDR were calculated.

4.9.4 Principal component analysis

Principal component analysis (PCA) is a classical multidimensional scaling method and was applied to categorise gene expression profiles (Ringnér & Ringner, 2008). Thereby it extracts the most important information from the data table and expresses this information as a set of new orthogonal variables called *principal components*. Thereby, this algorithm reduces the dimensionality of the data, while retaining most of the variation of a data set. PCA was performed using the pcaExplorer package.

4.10 Statistics

Data are means \pm SD, unless indicated otherwise, and p values were determined by unpaired Students's t test or two-way ANOVA test with Bonferroni's post-hoc test with Prism 5.0 (GraphPad). *P* values ≤ 0.05 were considered significant (* $p < 0.05$; ** $p < 0.01$; *** $p < 0.001$), $p \geq 0.05$ not significant (ns).

5. Results

Autoreactive IL-17-producing CD4⁺ and CD8⁺ T cells have been implicated in MS pathology and were detected in active areas of acute and chronic MS lesions (Kebir et al., 2007; Tzartos et al., 2008). Hence, unravelling the mechanisms which control Tc17 cell differentiation is essential for future treatment options.

One approved drug for MS is DMF (Tecfidera®) which is used for treatment of RRMS as it reduces disease activity and progression (Kappos et al., 2008) by various mechanisms: besides inducing anti-inflammatory DCs (Ghoreschi et al., 2011) and B cells (Li et al., 2017), DMF increases the ratio of CD4⁺/CD8⁺ T cells, indicating a major impact on CD8⁺ T cells (Spencer et al., 2015). In DCs, monocytes and macrophages (Ghoreschi et al., 2011; Hoetzenecker et al., 2012; Sullivan et al., 2013; Zheng et al., 2015), DMF accumulates ROS by depletion of glutathione, the most important ROS scavenger. Not much is known on the impact of ROS on T cell activation and differentiation: Generally, elevated ROS levels on the one hand are able to support CD8⁺ T cell activation (Sena et al., 2013), whereas on the other hand can also dramatically impair T cell proliferation and function (Mak et al., 2017).

Taking into consideration the impact of DMF-mediated ROS accumulation on Tc17 cells, we analysed the role of DMF on the differentiation of murine as well as human Tc17 cells and evaluated its influence on the onset of EAE. Furthermore, we determined the influence of Tecfidera treatment on CD4⁺ and CD8⁺ T cells in peripheral blood (PB) of RRMS patients by analysing their cytokine production before and after the first year of treatment.

5.1 DMF-mediated ROS accumulation leads to a robust IL-17 suppression in Tc17 cells

DMF binds to glutathione, thereby abolishing its antioxidative capacity and causing increased ROS levels in a variety of cells including DCs, astrocytes and tumour cells (Ghoreschi et al., 2011; Scannevin et al., 2012; Sullivan et al., 2013). Considering the wide-ranging effects of elevated ROS levels together with the preferential impact on CD8⁺ T cells by DMF during RRMS treatment (Fleischer et al., 2017; Spencer et al., 2015), we evaluated whether DMF via elevated ROS influences Tc17 cells.

To examine if DMF has an impact on IL-17-producing CD8⁺ T cells, murine wildtype (WT) CD8⁺ T cells were differentiated under Tc17 conditions *in vitro* and reduced GSH as well as oxidised GSSG contents were measured. The analysis revealed that DMF depletes the intracellular pool of GSH, leading to a decrease in the GSH/GSSG ratio (**Fig. 1 A**). Reduced GSH

levels resulted in a significant upregulation of endogenous ROS as confirmed by staining with CM-H₂DCFDA, a general oxidative stress indicator, and flow cytometric analysis (Fig. 1 B). The addition of cell-permeable reduced GSH-ethyl ester (GSH-OEt, GSH) largely restored intracellular GSH concentration and reversed increased ROS levels comparable to control.

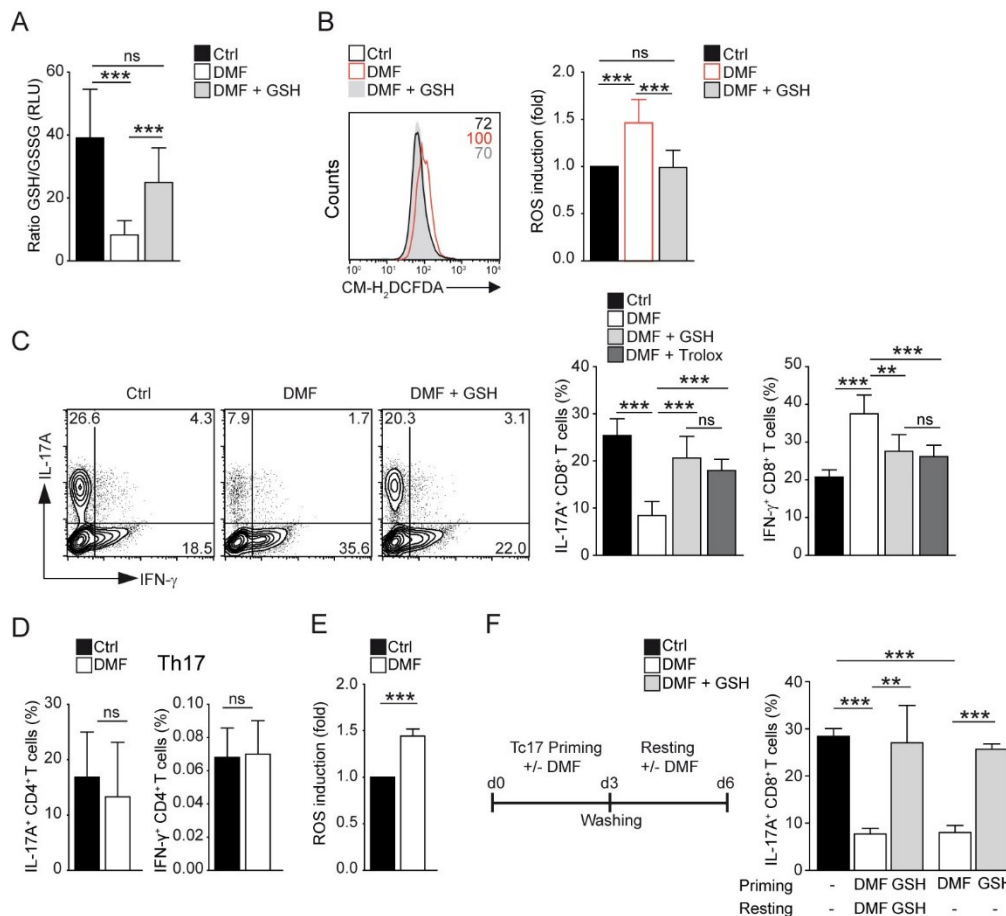


Figure 4: DMF-GSH-ROS axis stably suppresses IL-17 production by Tc17 cells

(A - F) Murine CD8⁺ or CD4⁺ T cells were isolated and cultured *in vitro* under type 17 conditions (TGF- β + IL-6 + IL-2) and treated with 0.2% DMSO (control, Ctrl) 20 μ M DMF alone or together with 50 μ M GSH or 400 μ M Trolox as indicated. **(A)** Ratio of reduced to oxidized glutathione contents was determined after 2 h of culture. **(B)** Flow cytometric analysis of ROS levels by CM-H₂DCFDA staining after 2 h of culture. Numbers in histogram represent MFI. Bars show fold ROS induction relative to control. **(C)** Flow cytometric analysis of IL-17A⁺ and IFN- γ ⁺ CD8⁺ T cells after three days. Numbers in plots represent % of gated cells. Bars show percentages of IL-17A⁺ and IFN- γ ⁺ CD8⁺ T cells. **(D)** Flow cytometric analysis of IL-17A⁺ and IFN- γ ⁺ CD4⁺ T cells after three days of culture. Bars show percentages of IL-17A⁺ and IFN- γ ⁺ CD4⁺ T cells. **(E)** Flow cytometric analysis of ROS levels by CM-H₂DCFDA staining of CD4⁺ T cells after 2 h of culture under type 17 conditions. **(F)** Outline of experimental strategy is depicted. To the right, flow cytometric analysis of IL-17A⁺ CD8⁺ T cells after six days of culture. CD8⁺ T cells were primed under Tc17 conditions and treated \pm DMF \pm GSH for three days. Then, the cells were washed, rested in the presence of IL-2 as well as anti-IFN- γ and left either untreated or treated again with DMF \pm GSH for the next three days. Histograms and contour plots are representative for seven (B, C) independent experiments. Bars show mean \pm SD from three (D, E, F), five (A) or seven (B, C) combined experiments. Statistical analysis was performed using unpaired two-tailed Student's t-test (ns $P > 0.05$, * $P < 0.05$, ** $P < 0.01$, *** $P < 0.001$).

DMF is able to suppress pro-inflammatory cytokine production in DCs (Ghoreschi et al., 2011), macrophages (McGuire et al., 2016) and B cells (M. D. Smith et al., 2017), demonstrating its immune modulatory mode of action.

To investigate the influence of DMF-mediated ROS upregulation on the production of pro-inflammatory IL-17, the effector cytokine of Tc17 cells, we performed intracellular staining for IL-17 and IFN- γ . DMF was able to suppress IL-17 significantly and simultaneously upregulated IFN- γ production in a ROS-dependent manner. Neutralisation of ROS with the anti-oxidants GSH or Trolox, a vitamin E derivative, restored cytokine levels comparable to control Tc17 cells (**Fig. 1 C**). Next, we differentiated Th17 cells *in vitro* and exposed them to DMF to examine whether DMF impacts Th17 cells, the CD4⁺ counterpart of Tc17 cells, by a similar mechanism. Surprisingly, DMF influenced neither IL-17 nor IFN- γ production of Th17 cells, although ROS were upregulated significantly (**Fig. 1 D, E**). To investigate the duration of the DMF-mediated IL-17 reduction in Tc17 cells that allows a prediction about the stability of IL-17 suppression during treatment, cells were primed under Tc17 conditions for three days with DMSO, DMF alone or in combination with GSH, followed by washing and resting in the absence or presence of DMF for further three days. Flow cytometric analysis revealed a stable IL-17 inhibition, as IL-17-producing cells remained significantly reduced after the resting phase, comparable to continuous DMF treatment over six days (**Fig 1 F**).

Hence, DMF-mediated GSH depletion resulted in an early ROS upregulation, leading to increased IFN- γ levels and a robust IL-17 suppression in Tc17 cells.

5.2 IL-17 is diminished by DMF-mediated transient ROS upregulation at early stages of Tc17 differentiation

DMF induces an anti-oxidant response in astrocytes (Scannevin et al., 2012), neurons (Linker et al., 2011) and DCs (Ghoreschi et al., 2011) by succination of Keap1 and thereby activation of the NRF2 pathway. After detecting elevated ROS levels in Tc17 cells upon DMF treatment, we thought to elucidate the compatibility between moderate accumulation of ROS on one side and an induction of anti-oxidative stress responses on the other.

Therefore, the ratio of GSH/GSSG as well as ROS levels were determined 24 h post Tc17 differentiation and DMF treatment. Surprisingly, GSH/GSSH ratio showed an upward trend and ROS levels were already significantly reduced after 24 h of DMF treatment as compared to control (**Fig. 2 A, B**). In line with this finding, anti-oxidative NRF2 targets were upregulated in DMF-treated Tc17 cells, indicating an activation of mechanisms counteracting the previous ROS accumulation (**Fig. 2 C**). To examine whether the early ROS increase by DMF-

mediated GSH-depletion was sufficient to restrict IL-17 production, DMF was added to the cells at later time points of differentiation. It revealed that only the early application of DMF after up to 17 h of differentiation was sufficient to suppress IL-17 production, whereas DMF hardly affected the already established Tc17 cells (**Fig. 2 D**).

In summary, the DMF-mediated increase of endogenous ROS at early stages of Tc17 differentiation is required for an efficient IL-17 inhibition, despite a rapid counter regulation by induction of oxidative stress response pathways. In contrast, DMF treatment at later time points of differentiation is not able to limit IL-17 production.

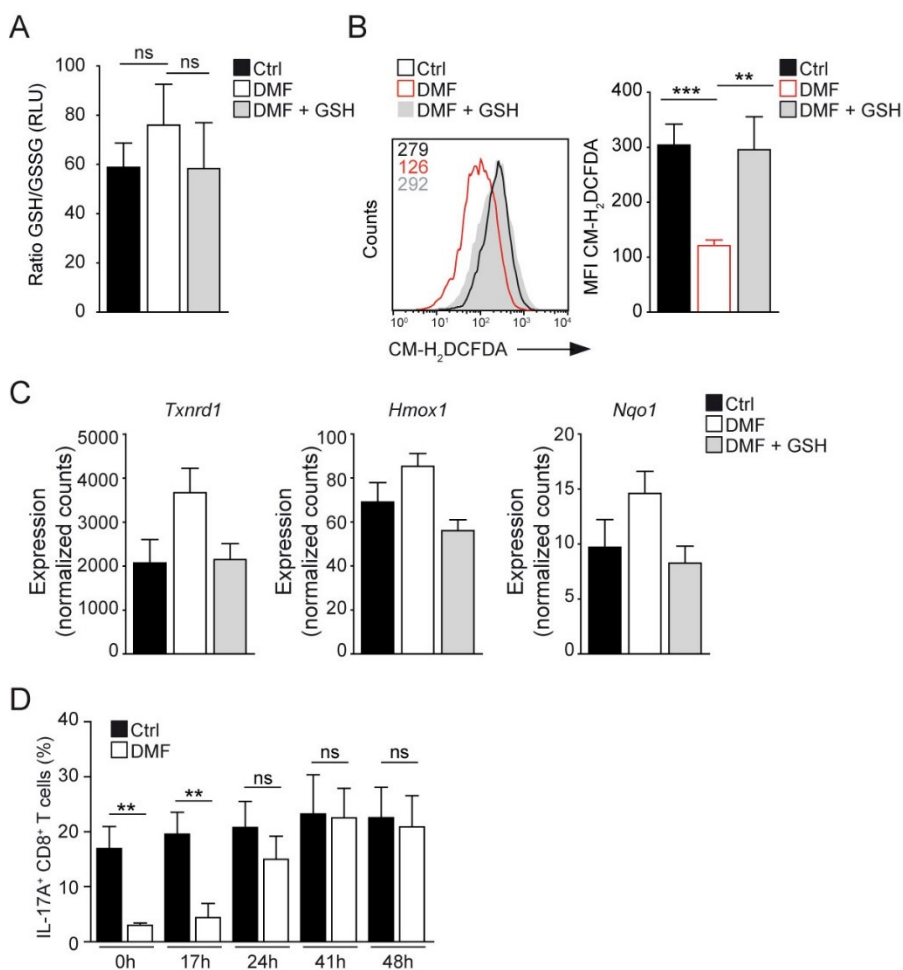


Figure 5: DMF upregulates ROS transiently and suppresses IL-17 production at early stages of Tc17 differentiation

(A-D) WT CD8⁺ T cells were isolated and cultured *in vitro* under type 17 conditions and treated with 0.2% DMSO (control, Ctrl) 20 μ M DMF alone or together with 50 μ M GSH as indicated. **(A)** Ratio of reduced to oxidized glutathione contents was determined after 24 h of culture. **(B)** Flow cytometric analysis of ROS levels by CM-H₂DCFDA staining after 24 h of culture. Numbers in histogram represent MFI. Bars show MFI of CM-H₂DCFDA staining. **(C)** Expression of normalised counts of NRF2 target genes as determined by RNA-Seq. CD8⁺ T cells were cultured *in vitro* under type 17 conditions with indicated treatment for two days. Total RNA was purified and RNA-Seq was performed (n=3). **(D)** Flow cytometric analysis of IL-17A⁺ CD8⁺ T cells after three days of Tc17 priming with addition of DMSO (Ctrl) or DMF at indicated time points after culture start. Bars show percentages of IL-17⁺ CD8⁺ T cells. Histogram in B is representative

for three independent experiments. (A - D) Bars show mean \pm SD from three combined experiments. Statistical analysis was performed using unpaired two-tailed Student's t-test (ns $P > 0.05$, * $P < 0.05$, ** $P < 0.01$, *** $p < 0.001$).

5.3 DMF signalling suppresses IL-17 production independent of apoptosis or proliferation

The positive safety record of DMF is compromised by the occurrence of lymphopenia, or in rare cases of PML in MS patients under Tecfidera treatment (Linker & Haghikia, 2016). To examine if the altered cytokine production is an effect of elevated apoptosis, Annexin V and propidium iodide staining was performed in Tc17 cells. 20 μ M DMF, the concentration that significantly reduced IL-17 production, did not induce apoptosis, whereas higher DMF concentrations were pro-apoptotic (**Fig. 3 A**). Interestingly, this effect was reversed by adding the antioxidant GSH, confirming that DMF via ROS upregulation leads to cell death at high concentrations, whereas moderate ROS levels rather alter Tc17 cells fate.

In addition, the influence of DMF-treatment on proliferation of Tc17 cells was assessed. It revealed that DMF-treated Tc17 cells showed a non-significant tendency towards reduced division as indicated by CFSE staining and flow cytometric analysis after three days (**Fig. 3 B**). However, this did not influence the IL-17 production, as the frequencies of IL-17-producing cells in DMF-treated samples were similarly reduced in each proliferation stage as compared to control (**Fig. 3 C**).

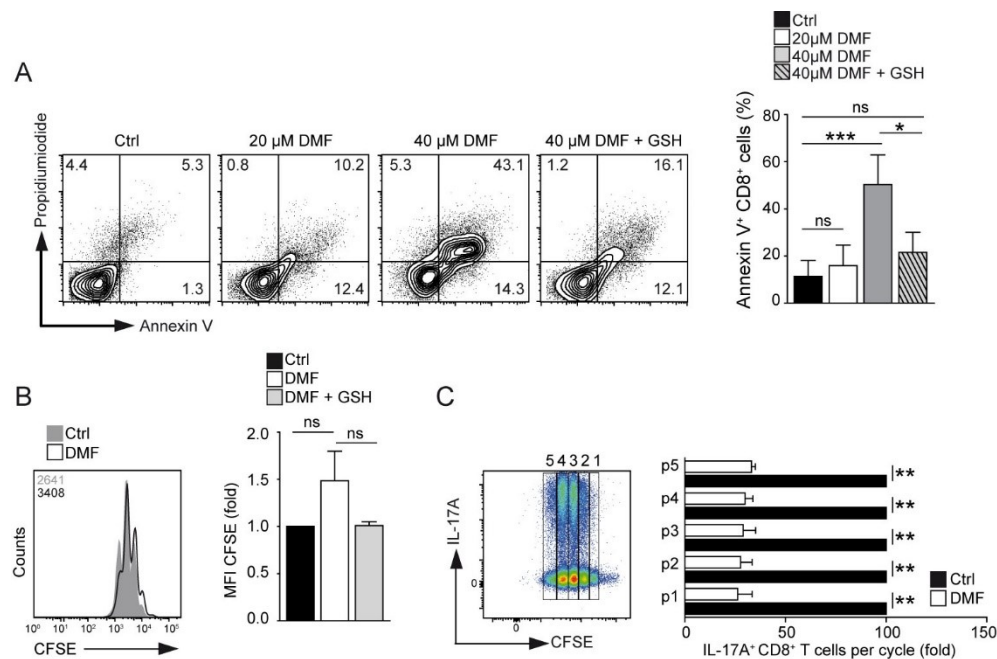


Figure 6: DMF does not influence apoptosis or proliferation of Tc17 cells at immune modulatory concentrations

(A) Flow cytometric analysis of apoptosis via Annexin V and propidium iodide staining. CD8⁺ T cells were primed *in vitro* under Tc17 conditions treated with DMSO, 20 or 40 μ M DMF alone or in combination with GSH as indicated for three days. Numbers represent % of gated cells. Bars show quantification of Annexin V⁺ Tc17 cells. **(B)** Flow cytometric assessment of proliferation by CFSE staining. CD8⁺ T cells were stained with CFSE, washed and primed under Tc17 conditions with indicated treatment for three days. Numbers in histogram represent MFI. Bars show fold changes of MFI of CFSE-stained cells. **(C)** Dot blot of CFSE-stained Tc17 cells with marking of each proliferation cycle. Bars show fold changes of IL-17A⁺ CD8⁺ T cells at each proliferation cycle after three days of differentiation relative to control. Histograms and dot plots are representative for three (A - C) independent experiments. Bars show mean \pm SD from three (A - C) combined experiments. Statistical analysis was performed using unpaired two-tailed Student's t-test (ns $P > 0.05$, * $P < 0.05$, ** $P < 0.01$, *** $P < 0.001$).

5.4 DMF-ROS axis modifies Tc17 cell gene signature

After having confirmed that DMF-mediated ROS suppressed IL-17 independent of apoptosis and proliferation, RNA-Sequencing (RNA-Seq) was performed to examine the impact of DMF on Tc17 cells on a genome-wide level. In addition, principal component analysis (PCA) was carried out to compare genetic profiles between differently treated Tc17 cells. Furthermore, gene set enrichment analysis (GSEA) was performed as previously described (Subramanian, 2005) to determine involved pathways in IL-17 suppression mediated by the DMF/ROS axis.

In DMF-treated Tc17 cells, 994 transcripts were significantly upregulated and 898 significantly downregulated (FDR < 0.01, as compared to control. Interestingly, most of the altered gene expression was restored by addition of GSH, indicating a major contribution of increased ROS levels to the modulation of Tc17 cells. To visualise and compare gene expression profiles, PCA was performed which showed a distinct gene expression between DMF-treated and control Tc17 cells. Interestingly, the profiles of Tc17 cells that received DMF in combination with GSH were similar to control cells (**Fig. 4 A, B**). By performing GSEA it was confirmed, that DMF treatment significantly downregulated Tc17-associated genes, whereas ROS neutralisation by GSH restored the transcriptional program comparable to control cells (**Fig. 4 C**). Amongst the 70 most significantly downregulated transcripts, several Tc17-associated genes were found, as *Il17a*, *Il17f*, *Il21*, *Rorc* and *Il21* (**Fig. 4 D**). In line, the main transcription factor of Tc17 cells, ROR γ t, was significantly reduced on protein level in cells treated with DMF as compared to control, an effect that was again dependent on ROS (**Fig. 4 E**).

Taken together, these results revealed that DMF treatment via ROS controls Tc17 differentiation by suppressing the Tc17 transcriptional program *in vitro*.

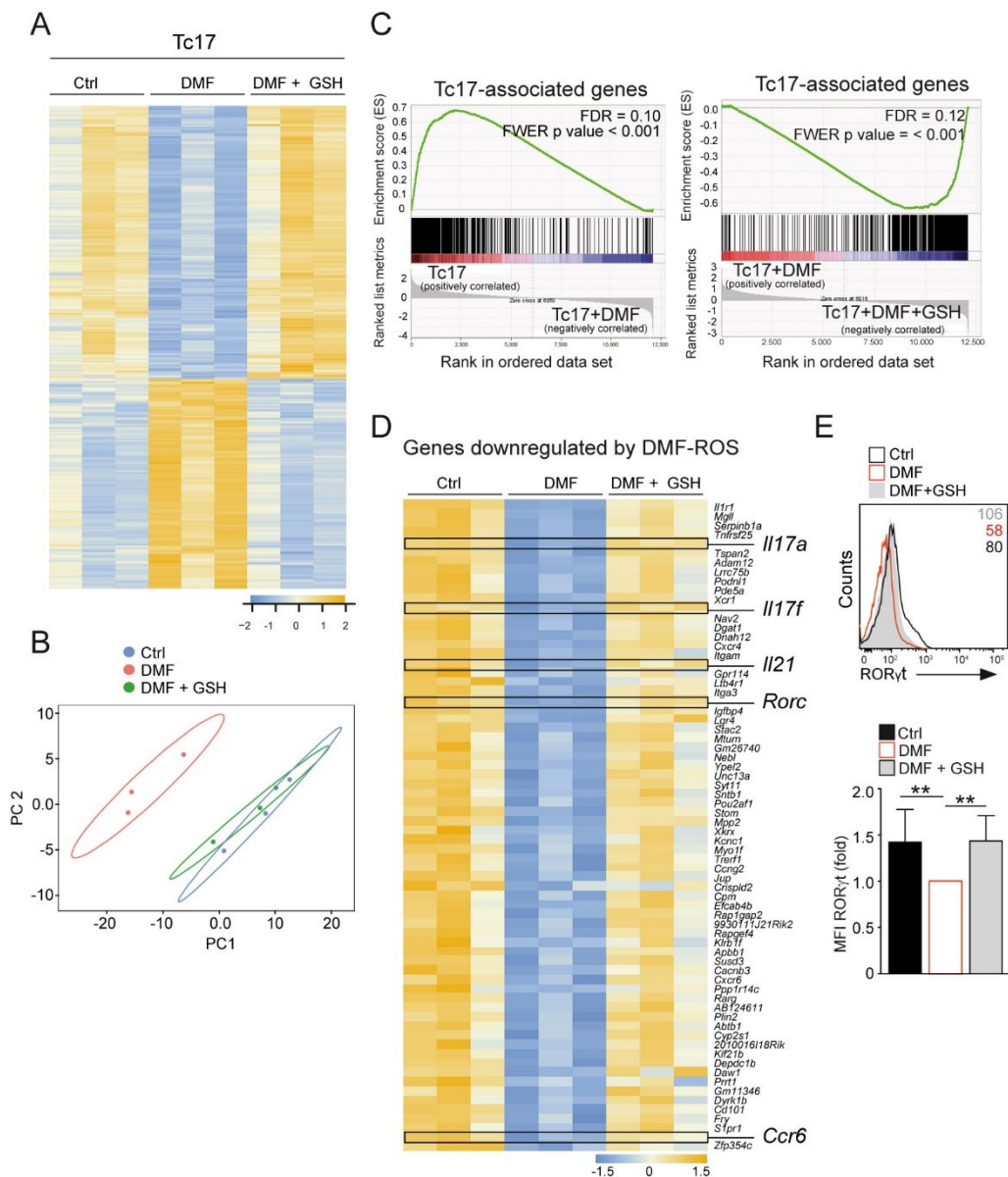


Figure 7: Tc17 fate is suppressed by DMF treatment

(A-D) CD8⁺ T cells were cultured under Tc17 conditions and treated with DMSO (Ctrl), DMF alone or in combination with GSH for two days. RNA was isolated and RNA-Seq was performed (n=3). **(A)** Heatmap shows color-coded z-scores for the regularized logarithm (rlog) transformed batch-corrected expression values. Displayed are 659 differentially expressed genes with an effect size of at least > 1.5-fold (log₂) and FDR < 0.01 in the expression between control vs DMF-treated Tc17 cells. **(B)** Principal component analysis (PCA) of Tc17 cells treated as indicated **(C)** GSEA comparing the relative expression of genes of Tc17 cells with indicated treatment, examining the distribution of genes associated with Tc17 phenotype as defined in GSE110346. **(D)** Heatmap shows color-coded z-scores for the rlog transformed batch-corrected expression values. Displayed are the top 70 core enriched hits of genes downregulated in DMF-treated Tc17 cells. **(E)** Flow cytometric analysis of ROR γ t levels in CD8⁺ T cells after three days of Tc17 priming and treatment with DMSO (Ctrl), DMF alone or in combination with GSH. Numbers in histogram represent MFI. Bars show fold MFI changes relative to DMF treatment. Histogram in E is representative for three independent experiments. Bars in E show mean \pm SD from three combined experiments. Statistical analysis was performed using unpaired two-tailed Student's t-test (ns $P > 0.05$, * $P < 0.05$, ** $P < 0.01$, *** $P < 0.001$).

5.5 DMF via ROS suppresses permissive histone modifications at the *IL17* locus

Elevated ROS levels can modulate the activity of intracellular signalling molecules and pathways, including epigenetic modifications such as histone methylation and acetylation (Kim, Ryan, & Archer, 2013; Kreuz & Fischle, 2016).

To evaluate whether the DMF/ROS axis suppresses IL-17 in Tc17 by affecting the epigenetic landscape, Tc17 cells were differentiated *in vitro* for three days and ChIP assays were performed.

First, we compared permissive total acetylation levels of H4 as well as for H3K27 in Tc17 cells treated with control, DMF alone or in combination with GSH. While DMF treatment reduced H4Ac as well as H3K27Ac levels at the *IL17* promoter and enhancer, the addition of GSH restored the occupancy of acetylation at both sides, indicating a ROS-dependent mechanism (Fig. 5 A). After having demonstrated that DMF via ROS modified histone acetylation, we evaluated whether ROS could impact the acetylation status of histones.

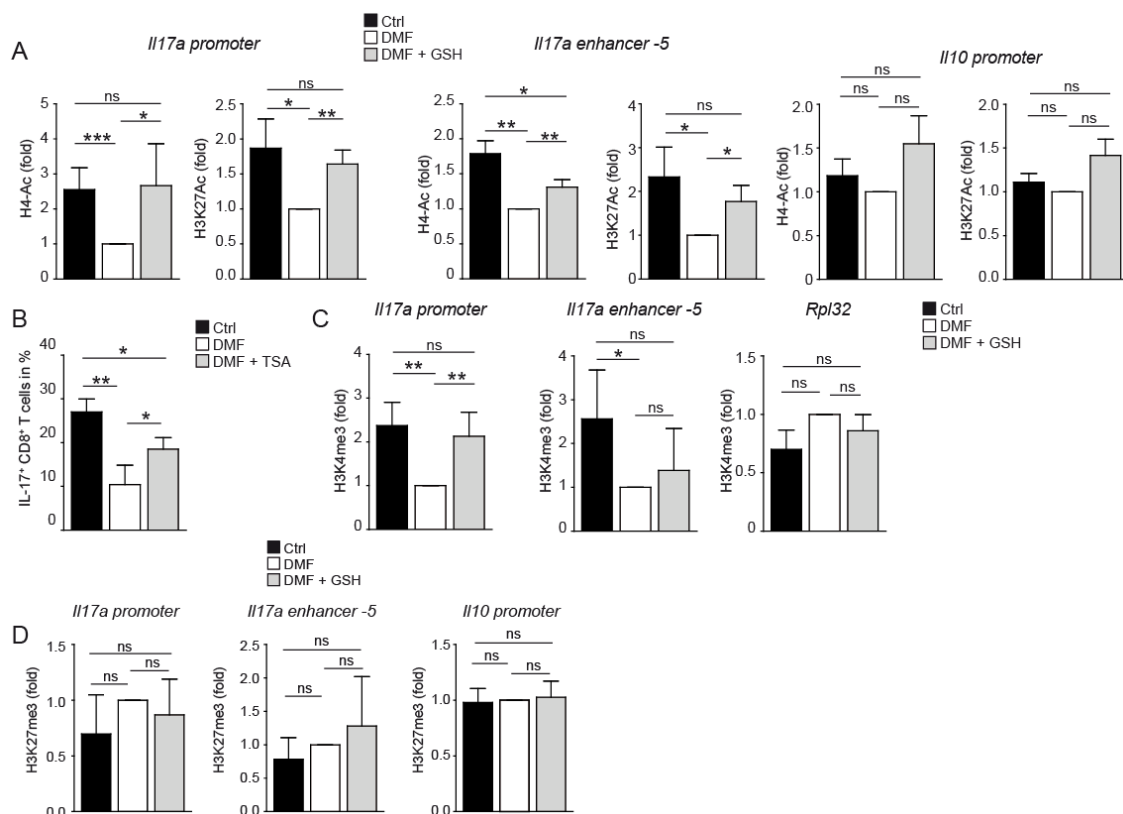


Figure 8: DMF alters histone modifications at the *IL17* locus of Tc17 cells in a ROS-dependent manner

(A, C, D) CD8⁺ T cells were differentiated for 3 days under Tc17 conditions with indicated treatment and ChIP analysis were performed. (A) ChIP analysis for H4Ac and H3K27Ac at the *IL17* promoter, *IL17* enhancer-5 and *IL10* promoter. (B) Flow cytometric determination of IL-17⁺ CD8⁺ T cells differentiated for 3 days under Tc17 conditions with indicated treatment. (C) ChIP analysis for H3K4me3 at the *IL17*

promoter, *Il17 enhancer -5* and *Rpl* promoter. (D) ChIP analysis for H3K27me3 at (C) the *Il17* promoter and *Il17 enhancer -5* or (D) *Il10* promoter. The experiments were repeated three times with consistent results. Bars show mean \pm SD of fold change relative to DMF-treated Tc17 cells from three (A, C, D) or five (B) combined experiments. (A-D) Statistical analysis was performed using unpaired two-tailed Student's t-test (ns $P>0.05$, * $P<0.05$, ** $P<0.01$, *** $P<0.001$).

Histone deacetylation is catalysed by HDACs, whose activity cannot only be suppressed, but also increased by ROS (Kreuz & Fischle, 2016). To determine the contribution of HDACs during DMF-mediated IL-17 inhibition, Tc17 cells were treated with DMF together with the HDAC inhibitor TSA. Notably, the addition of TSA could partially restore the inhibitory effect of DMF on IL-17 production, indicating that the DMF/ROS axis suppressed acetylation at the *Il17* locus via HDACs (**Fig. 5 B**).

Further, it has been shown that fumarates as well as ROS are able to impact the methylation status of histones (Afanas'ev, 2015; Kreuz & Fischle, 2016; Sullivan et al., 2013). Therefore, we compared permissive methylation levels of H3K4 and methylation of H3K27, which is associated with transcriptional silencing, at the *Il17* locus of Tc17 cells treated with control, DMF alone or together with GSH. We found that DMF also reduced permissive histone trimethylation at H3K4 (**Fig. 5 C**), whereas the repressive trimethylation at H3K27 was not significantly altered (**Fig. 5 D**).

Taken together, these results imply that DMF via ROS upregulation can suppress permissive histone acetylation and methylation at the *Il17* promoter and enhancer, whereas the repressive methylation H3K27me3 was not affected.

5.6 DMF suppresses pathogenicity of Tc17 cells in EAE

5.6.1 Oral DMF treatment diminishes EAE severity

DMF is a commonly prescribed oral drug for RRMS patients. Our aforementioned data show that DMF treatment directly impacts the fate of Tc17 cells *in vitro*, which are known to contribute to inflammatory processes in the CNS (Huber et al., 2013). To examine whether orally administered DMF is able to influence Tc17 cells *in vivo*, we performed EAE experiments in collaboration with Dr. F. Kurschus from University of Mainz.

To analyse the impact of orally given DMF, EAE was induced in WT mice by immunisation with MOG₃₅₋₅₅ peptide and treated with DMF in drinking water during the course of disease (**Fig. 6 A**). In accordance with the literature (Ghoreschi et al., 2011; Linker et al., 2011; Schulze-Topphoff et al., 2016), mice that received oral DMF treatment showed reduced clinical EAE symptoms as compared to the control group (**Fig. 6 B**). The mild disease course

during DMF treatment was accompanied by significantly reduced percentages of IL-17-producing CD8⁺ T cells in the CNS (**Fig. 6 C**) and dLNs (**Fig. 6 D**).

Hence, our data show that beside direct effects on Tc17 cells *in vitro*, the oral administration of DMF suppresses Tc17 cells also *in vivo*, demonstrated by diminished severity of EAE and reduced Tc17 cell infiltration in the CNS and draining lymph nodes (dLN).

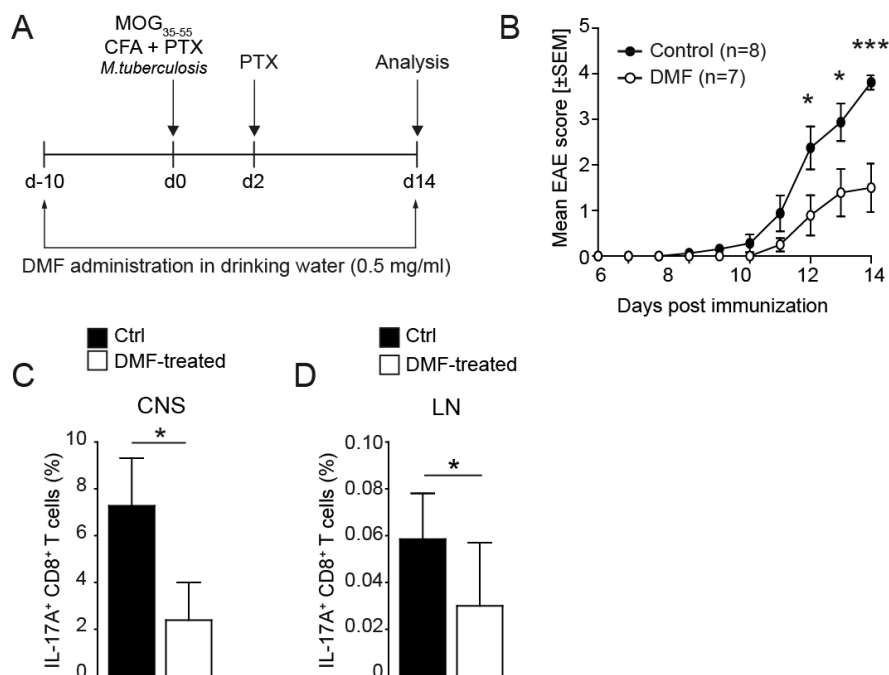


Figure 9: Oral DMF treatment limits EAE severity

(A) Outline of experimental strategy. WT mice were immunised with MOG₃₅₋₅₅, CFA and *M. tuberculosis* for induction of EAE. Pertussis toxin (PTX) was injected i.p. along and on day 2 post immunisation. Mice were treated ± DMF in drinking water starting 10 days before EAE induction and during the course of disease. Analysis was performed on day 14.

(B) Mean clinical scores (± SEM) of MOG₃₅₋₅₅ immunised WT mice (n=8) treated orally with control or DMF for 24 days. *P* values were calculated comparing the scores of WT mice ± DMF. **(C)** Flow cytometric analysis of IL-17A⁺ CD8⁺ T cells from the CNS of WT mice ± DMF. Bars show percentages of IL-17⁺ CD8⁺ T cells in the CNS. **(D)** Flow cytometric analysis of IL-17⁺ CD8⁺ T cells in the LNs of WT mice after EAE induction and oral control- or DMF-treatment as described in A. Bars show percentages of IL-17A⁺ CD8⁺ T cells in the LNs. Experiments were repeated three times with consistent results. Bars show mean ± SD from mice (n = 8) from one representative experiment. Statistical analysis was performed using unpaired two-tailed Student's *t*-test (ns *P*>0.05, * *P*<0.05, ** *P*<0.01, *** *P*<0.001).

5.6.2 DMF limits pathogenicity of Tc17 cells *in vivo*

Our *in vitro* data demonstrate that DMF treatment is able to suppress the Tc17 cell fate, including their ability to produce IL-17. This cytokine contributes to inflammation in the CNS and lesion formation by promoting the generation of pro-inflammatory cytokines and chemokines, which attract neutrophils and macrophages to inflammation sites (Jin & Dong,

2013). Furthermore, it has been shown that Tc17 cells, via their IL-17 production, support Th17 cell-mediated pathogenicity during the onset of EAE (Huber et al., 2013). In addition, we could show that DMF treatment *in vivo* diminished clinical EAE symptoms, but it was not clear whether these effects directly or indirectly impact Tc17 cells.

To analyse the functional impact of DMF-treatment directly on Tc17 cells, we performed T cell adoptive transfer experiments. Therefore, we transferred *in vitro* differentiated congenic control- or DMF-treated Tc17 cells together with low numbers of 2D2 CD4⁺ T cells, which are transgenic for MOG-specific TCR, into EAE-resistant *Irf4*^{-/-} recipient mice (Brüstle et al., 2007; Huber et al., 2013), followed by EAE induction (**Fig. 7 A**). The transfer of low numbers of 2D2 cells alone did not evoke disease outbreak, whereas the combination with control Tc17 cells induced an early onset of disease including acute clinical symptoms, as previously shown (Huber et al., 2013) (**Fig. 7 B**). The severe disease course was characterised by T cell infiltration of both, endogenous and transferred CD8⁺ T cells, into the CNS (**Fig. 7 C, D**). The transferred control Tc17 cells were detectable in dLNs and their IL-17 production was accompanied by higher IL-17- and IFN- γ - production of CD4⁺ T cells within the CNS. In addition, the mice receiving control Tc17 cells were characterised by increased percentages of IL-17-producing CD8⁺ T cells in dLN and elevated percentages of IL-17-producing CD4⁺ and CD8⁺ T cells within the CNS as compared to the control (**Fig. 7 E-I**).

In contrast, recipients of 2D2 cells together with DMF-treated Tc17 cells showed only a mild disease course (**Fig. 7 B**), which was accompanied by significantly elevated T cell numbers in the dLNs and reduced T cell infiltration into CNS (**Fig. 7 C, D**). The transferred DMF-treated Tc17 cells were detectable in dLNs and produced less IL-17 as compared to control Tc17 cells. At the same time, IL-17 and IFN- γ production in CNS-infiltrating CD4⁺ T cells was reduced as compared to the group that received control Tc17 cells (**Fig. 7 E-I**).

In summary, DMF diminishes the co-pathogenic function of Tc17 cells in an *in vivo* mouse model for MS by suppressing their transcriptional program, suggesting a possible mechanism for MS.

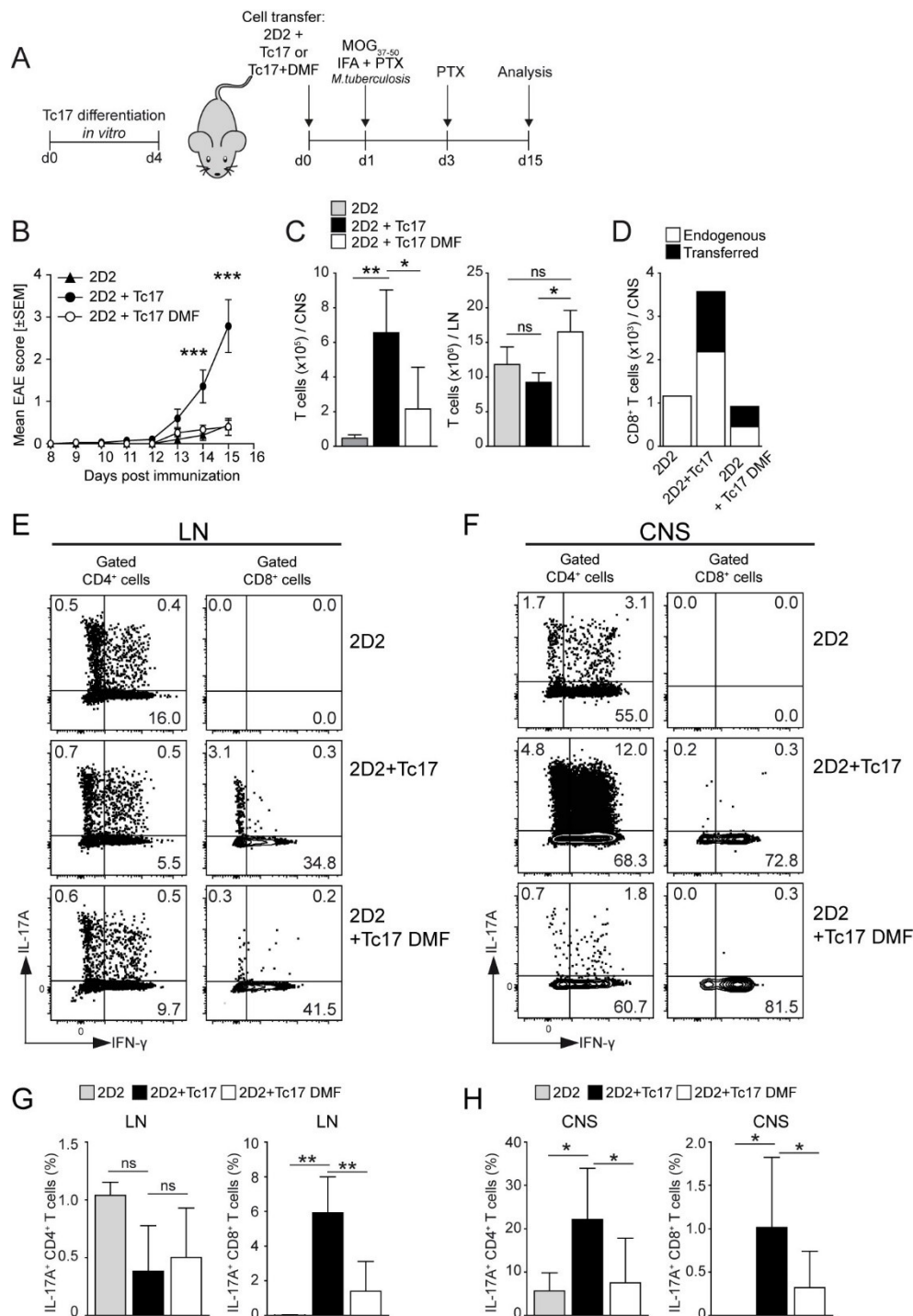


Figure 10: DMF limits CNS autoimmunity by suppressing the co-pathogenic function of Tc17 cells

(A) Outline of experimental strategy. *Irf4*^{-/-} mice receiving cells as described above. EAE was induced on the next day by injection of MOG₃₇₋₅₀, IFA and *M. tuberculosis*. PTX was injected i.p. on day 0 and 2 post immunization. Analysis was performed on day 15. **(B-H)** Analysis of MOG₃₇₋₅₀-immunized *Irf4*^{-/-} mice receiving 1×10^3 CD4⁺ 2D2 cells alone or together with 2.5×10^6 CD8⁺ cells *in vitro* differentiated for four days under type 17 conditions \pm DMF, in the following the cells are termed Tc17 cells. **(B)** Mean clinical scores (\pm SEM) combining two independent experiments of MOG₃₇₋₅₀-immunized *Irf4*^{-/-} ($n = 7$) mice. *P* values were calculated comparing the scores of *Irf4*^{-/-} mice receiving CD4⁺ 2D2 cells together with Tc17 cells \pm DMF. **(C)** Absolute T cell numbers (mean \pm SD of three combined experiments, $n=7$) in the (left) CNS or (right) LN of *Irf4*^{-/-} mice. **(D)** Number of CD8⁺ T cells (mean \pm SD of two combined experiments, $n=5$) in the CNS of *Irf4*^{-/-} mice. **(E, F)** Flow cytometric analysis of IL-17A⁺ and IFN- γ ⁺ gated CD4⁺ and CD8⁺ T

cells in the **(E)** LN or **(F)** CNS of *Irf4*^{-/-} mice. Numbers in plots represent % of gated cells **(G, H)** Percentages of IL-17A⁺ CD4⁺ or CD8⁺ T cells (mean ± SD of three combined experiments, n=7) in **(G)** LN and **(H)** CNS of *Irf4*^{-/-} mice. (A-H) The experiments were repeated three times with consistent results. Dot plots are representative for (E, F) three independent experiments. Statistical analysis was performed using two-way ANOVA and Bonferroni's post-hoc test (B) or unpaired two-tailed Student's t-test (C, D, G, H) (ns $P > 0.05$, * $P < 0.05$, ** $P < 0.01$, *** $P < 0.001$).

5.7 DMF treatment shifts Tc17 cells towards a CTL-like signature

After having validated the modulatory effect by DMF on Tc17 genetic profile and function in the EAE mouse model, we evaluated how DMF shapes the transcriptional signature of Tc17 cells in more detail.

To identify changes on the genome-wide level we further analysed the RNA-Seq data of Tc17 cells treated with DMSO (Ctrl), DMF alone or in combination with GSH. Amongst the 70 most upregulated transcripts we found CTL-associated genes as *Ifng*, *Eomes*, *Gzmb*, *Gzmc* and *Tbx21* (Kaech & Cui, 2012), whose induction was largely dependent on ROS as addition of GSH reversed the effect (**Fig. 8 A**). Furthermore, by applying GSEA we found a significant enrichment of CTL-associated genes in DMF-treated Tc17 cells in a ROS-dependent manner as compared to untreated Tc17 cells. (**Fig. 8 B**). This included CTL marker molecules like perforin, granzyme B and granzyme C (**Fig. 8 C**). The transcription factor T-bet (encoded by *Tbx21*) that regulates effector CTL differentiation (Kallies & Good-Jacobson, 2017) was upregulated on protein level by DMF treatment compared to control (**Fig. 8 D**).

Taken together, these results obtained by RNA-Seq analysis and flow cytometry reveal that DMF-mediated ROS promotes a CTL-like signature and suppressed the Tc17 transcriptional program.

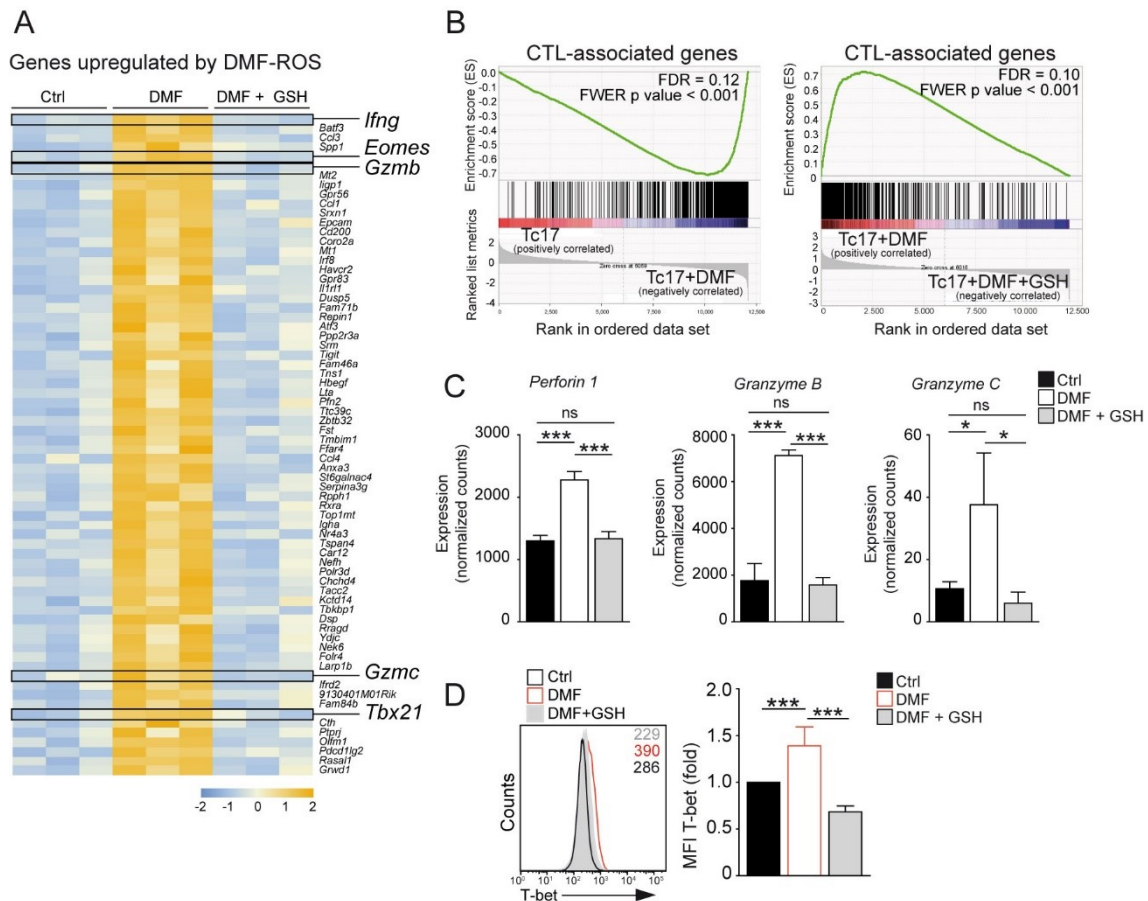


Figure 11: DMF- induced ROS favours a CTL-like gene signature

(A) Heatmap shows color-coded z-scores for the rlog transformed batch-corrected expression values from the dataset described in Figure 4. Displayed are the top 70 core enriched hits of genes upregulated in DMF-treated Tc17 cells. (B) GSEA comparing the relative expression of genes of Tc17 cells treated as indicated, examining the distribution of genes associated with CTL phenotype as defined in GSE110346. (C) Normalized expression counts of selected CTL-associated genes in Tc17 cells with indicated treatment as determined by RNA-Seq. (D) Flow cytometric determination of T-bet levels in CD8⁺ T cells after three days of Tc17 priming with indicated treatment. Numbers in histogram represent MFI. Bars show fold MFI change of T-bet relative to control. Histogram in D is representative for three independent experiments. Bars show mean \pm SD from three (C, C) combined experiments. Statistical analysis was performed using unpaired two-tailed Student's t-test (ns $P > 0.05$, * $P < 0.05$, ** $P < 0.01$, *** $P < 0.001$).

5.8 DMF/ROS axis enhances IL-2 signalling in Tc17 cells

The aforementioned data showed that DMF treatment of Tc17 cells leads to the accumulation of ROS, which is responsible for a shift of the Tc17 profile towards a CTL-like signature, but the underlying signalling remained elusive. In order to elucidate the molecular pathways involved in the suppression of Tc17 cells, the acquired RNA-Seq data was further analysed by GSEA to explore various signalling pathways involved.

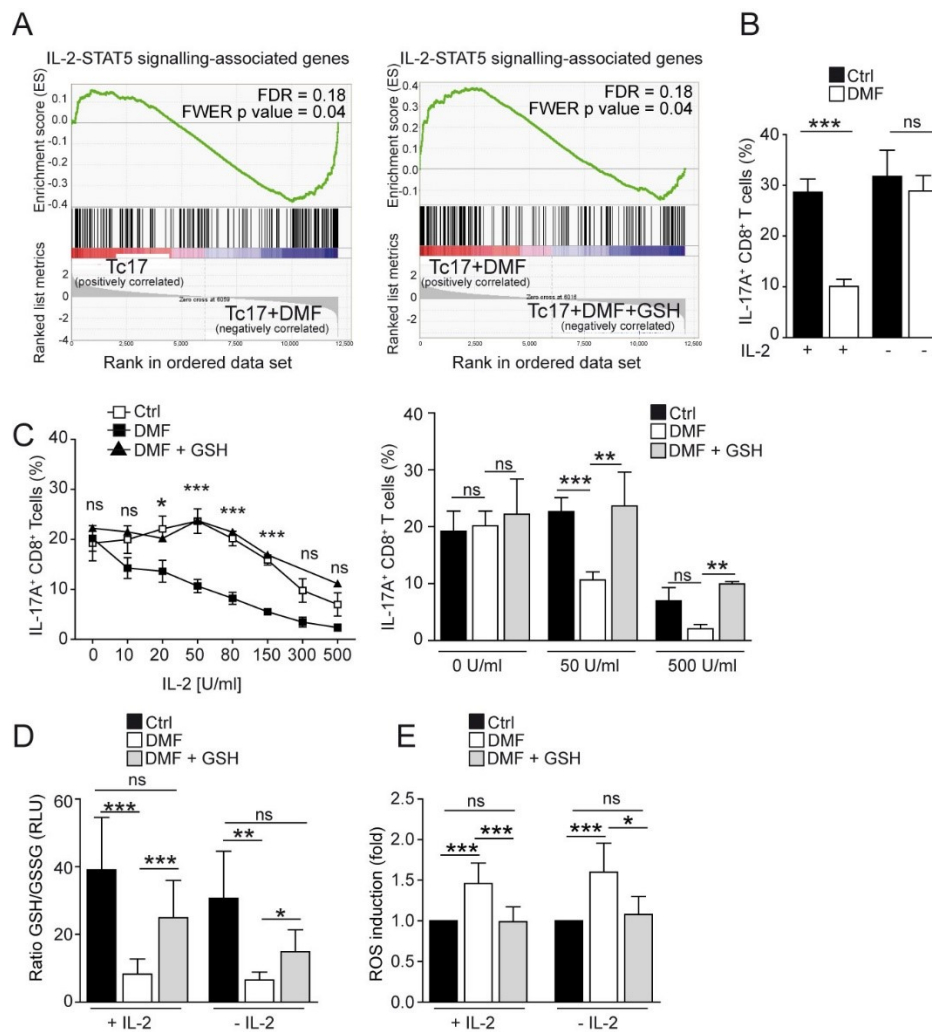


Figure 12: IL-2 signaling is elevated by ROS and required for suppression of IL-17 in Tc17 cells

(A) GSEA comparing the relative expression of genes in Tc17 cells \pm DMF (left) or DMF \pm GSH (right) from the dataset described in Figure 4. Shown is the distribution of genes involved in hallmark IL-2-STAT5-signaling as defined by MSigDB. (B) Flow cytometric analysis of IL-17A⁺ CD8⁺ T cells differentiated for three days under Tc17 conditions with indicated treatment in the presence or absence of 50 U/ml IL-2. (C) Flow cytometric analysis of IL-17A⁺ CD8⁺ T cells differentiated for three days under Tc17 conditions with indicated treatment and increasing IL-2 concentrations. (D) Ratio of reduced to oxidized glutathione levels in CD8⁺ T cells differentiated for 2 h under Tc17 conditions with indicated treatment in the presence or absence of 50 U/ml IL-2. (E) Flow cytometric analysis of ROS levels in CD8⁺ T cells differentiated for 2 h under Tc17 conditions with indicated treatment in the presence or absence of 50 U/ml IL-2 after staining with CM-H₂DCFDA (fold MFI relative to control). Graph in (C) shows \pm SEM from five combined experiments. Bars show mean \pm SD from three (B, D, E) or five (C) combined experiments. Statistical analysis was performed using unpaired two-tailed Student's t-test (ns $P > 0.05$, * $P < 0.05$, ** $P < 0.01$, *** $P < 0.001$).

We found a significant ROS-dependent enrichment of IL-2/STAT5 signalling-associated genes in DMF-treated Tc17 cells, suggesting an involvement of the IL-2 pathway in the suppression of IL-17 production of Tc17 cells (Fig. 9 A), as previously reported for Th17 cells (Laurence et al., 2007). To prove the dependency of DMF on IL-2 signalling, we compared the effect of DMF in

the presence or absence of IL-2 and found that IL-2 signalling was required for the DMF-mediated IL-17 suppression in Tc17 cells, as DMF was not able to limit IL-17 in the absence of IL-2 (**Fig. 9 B**). The effects of IL-2 were dose-dependent, as low IL-2 amounts prevented IL-17 inhibition, whereas high concentrations were already sufficient to suppress IL-17 without addition of DMF (**Fig. 9 C**). As expected, GSH rescued the IL-17 production, demonstrating that the DMF-mediated ROS upregulation led to IL-17 suppression by IL-2 signalling. Finally, to test whether IL-2 signalling and ROS affected each other, we performed GSH-Assay and ROS-staining in the absence or presence of IL-2. Interestingly, we could demonstrate that neither GSH-depletion nor ROS accumulation were dependent on IL-2 (**Fig. 9 D, E**).

Hence, DMF-induced ROS levels impinge on IL-2 signalling pathways, thereby suppressing IL-17 production of Tc17 cells.

5.8.1 DMF limits IL-17 production of Tc17 cells via STAT-5 induction

The aforementioned results revealed that the DMF-mediated ROS accumulation enhances IL-2/STAT5 signalling-associated genes. It is already shown for Th17 cells, that IL-2 via STAT5 inhibits IL-17 production by the competition with STAT3 at *IL17* regulatory elements (Laurence et al., 2007; X. P. Yang et al., 2011). In order to evaluate the contribution of STAT5 to the DMF-mediated IL-17 suppression in Tc17 cells, we performed retroviral overexpression of constitutive active STAT5 and made use of a pharmacological STAT5 inhibitor.

Tc17 cells were differentiated with respective treatment for 2 days *in vitro*, followed by a resting phase overnight and added IL-2 kinetically. Flow cytometric analysis of the cells revealed elevated phosphorylation of STAT5 in DMF-treated Tc17 cells in a ROS-dependent manner (**Fig. 10 A**). To examine whether STAT5 is able to limit the IL-17 production in Tc17 cells, they were overexpressed with a GFP-STAT5-expressing vector (pMIG STAT5) or the corresponding control vector (pMIG empty). To verify that GFP and P-STAT5 expression correlated, staining of P-STAT5 was performed. Indeed, high levels of GFP correlated with enhanced production of P-STAT5 in cells transduced with the pMIG STAT5 vector, but not in cells transduced with pMIG empty as expected. In line, the highest P-STAT5 expression was detected in the highly pMIG STAT5-transduced cells (**Fig. 10 B**). Next, the IL-17 production of Tc17 cells either transduced with pMIG empty or pMIG STAT5 was determined. We found a significant inhibition of IL-17 in P-STAT5 overexpressed Tc17 cells as compared to cells transduced with the control vector (**Fig. 10 C, D**), indicating that P-STAT5 is able to suppress IL-17 production also in Tc17 cells. The inhibitory effect of DMF-ROS-STAT5 pathways was at least partially regulated by competition with STAT3, as the IL-17 suppression by DMF was significantly decreased by overexpression with constitutive active STAT3 (pMIG STAT3) (**Fig. 10**

E). To link the enhanced P-STAT5 production to the DMF-mediated IL-17 suppression, we added a STAT5 inhibitor together with DMF to the cells and analysed the IL-17 production after three days of culture. Of note, the inhibition of STAT5 could only partially restore the IL-17 production of Tc17 cells, suggesting a contribution of further IL-2 dependent pathways to the ROS-mediated suppression of IL-17 in Tc17 cells (**Fig. 10 F**).

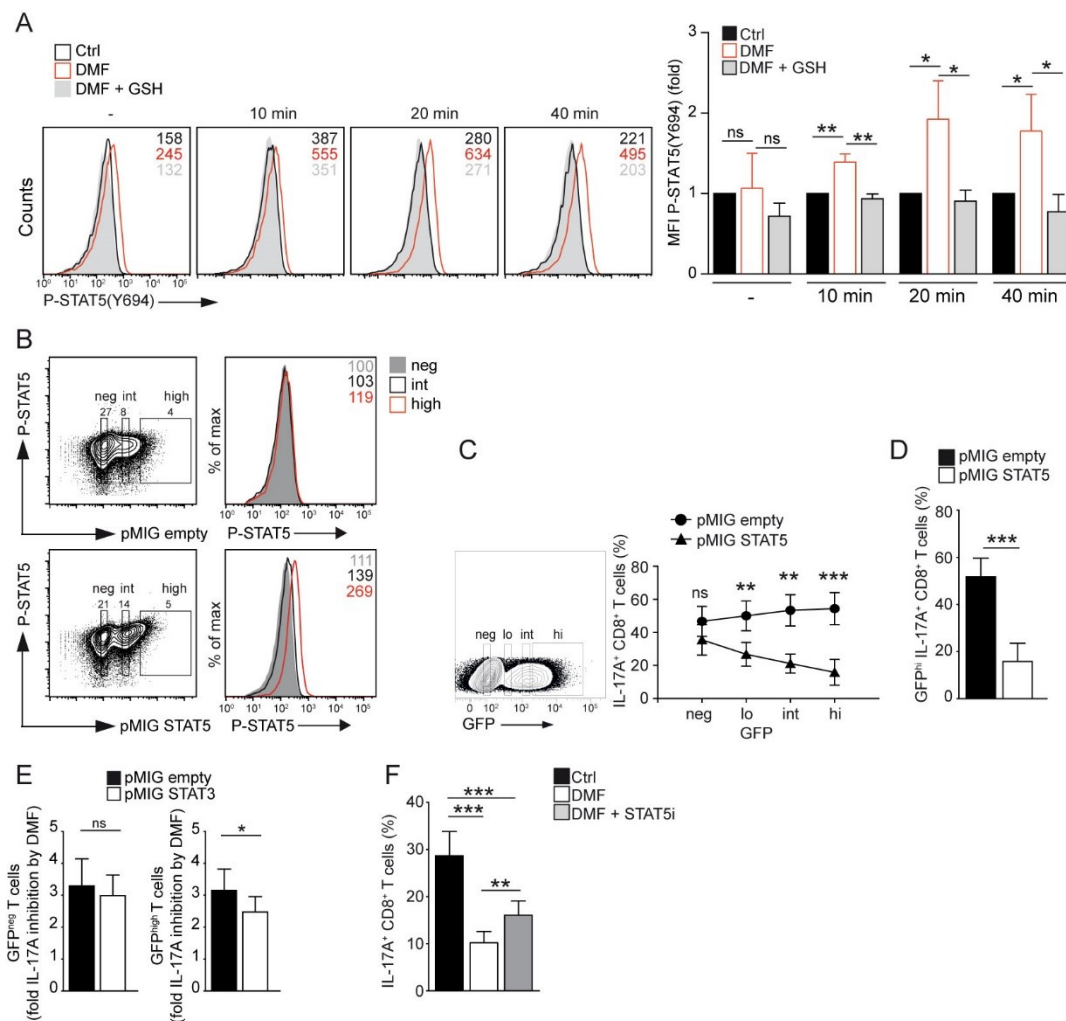


Figure 13: Elevated P-STAT5 contributes to the DMF-mediated IL-17 inhibition of Tc17 cells

(A) Flow cytometric analysis of P-STAT5(Y694) in CD8⁺ T cells differentiated for 2 days under Tc17 conditions with indicated treatment, rested overnight and restimulated with 100 U/ml IL-2 for indicated times under indicated treatment. Numbers in histograms represent MFI. Bars show fold MFI changes relative to control. **(B-E)** CD8⁺ T cells were spin transduced twice with retroviruses expressing either constitutive active P-STAT5 (pMIG STAT5) or constitutive active P-STAT3 (pMIG STAT3) or GFP alone (pMIG empty) as indicated. Then, CD8⁺ T cells were differentiated for 3 days under Tc17 conditions, rested for 3 days and re-cultured under Tc17 conditions for further 3 days. **(B)** Flow cytometric analysis of P-STAT5 (Y694) in CD8⁺ T cells. Dot plots show three subsets, based on the GFP expression intensity (GFP-negative, neg, GFP-intermediate, int, and GFP-high, high) for further analysis of P-STAT5 (Y694) expression in each subset. Numbers in histograms represent MFI. **(C)** Flow cytometric analysis of IL-17A⁺ GFP⁺ CD8⁺ T cells. Contour plot to the left shows four subsets, based on the GFP expression intensity (GFP-negative, neg, GFP-low, lo, GFP-intermediate, int, and GFP-high, hi) for analysis of percentages of IL-17A⁺ CD8⁺ T cells in each subset (graph shown to the right). **(D)** Flow cytometric analysis of GFP^{high} IL-

17A⁺ CD8⁺ T cells. Bars show percentages of GFP^{high} IL-17A⁺ CD8⁺ T cells **(E)** Flow cytometric analysis of IL-17A⁺ GFP⁺ CD8⁺ T cells after transduction with retroviruses expressing either constitutive active P-STAT3 (pMIG STAT3) or GFP alone (pMIG empty). Bars to the left show fold IL-17A inhibition by DMF in GFP^{neg} Tc17 cells. Bars to the right show fold IL-17 inhibition by DMF in GFP^{high} Tc17 cells. **(F)** Flow cytometric analysis of IL-17A⁺ CD8⁺ T cells differentiated for 3 days under Tc17 conditions with indicated treatment (35 μ M STAT5i). Contour-plots and histograms are representative for three (A, B, D) independent experiments. Bars show mean \pm SD from (A, C) three, (F) four or (E) five combined experiments. Statistical analysis was performed using unpaired two-tailed Student's t-test (ns $P > 0.05$, * $P < 0.05$, ** $P < 0.01$, *** $P < 0.001$).

5.8.2 DMF/ROS axis suppresses IL-17 production of Tc17 cells by elevated AKT/FOXO1/T-bet pathway

As the inhibition of STAT5 could only partially restore the IL-17 production in Tc17 cells, we analysed further IL-2 downstream signalling pathways. The CTL fate of CD8⁺ T cells is determined by PI3K-AKT signalling (Macintyre et al., 2014), which is activated by IL-2 (Liao, Lin, & Leonard, 2013). Since we could show that DMF induced a shift towards a CTL-like signature in Tc17 cells on the one side and increased IL-2 signalling on the other, we thought to analyse the impact of DMF on the PI3K-AKT pathways.

DMF increased the phosphorylation of AKT at the mTORC2-dependent S473 as well as on the PDK1-dependent site T308 in a ROS-dependent manner in Tc17 cells (**Fig. 11 A, B**). The lipid phosphatase PTEN limits activation of AKT and mTORC2 by their dephosphorylation, thereby counteracting the activity of PI3K (Ardestani, Lypse, Kido, Leibowitz, & Maedler, 2018). It has been shown that upregulated ROS can inhibit phosphatases by oxidation of their catalytic residues (Kamata et al., 2005). Accordingly, we found hampered *Pten* expression in DMF-treated Tc17 cells (**Fig. 11 C**), suggesting that reduced PTEN levels contributes to the increased phosphorylation of AKT. AKT-mediated phosphorylation of the transcription factor FOXO1 leads to the termination of its transcriptional activity (Finlay & Cantrell, 2011). In line, DMF-treated Tc17 cells showed increased phosphorylation of FOXO1/3a (**Fig. 11 D**) and upregulation of T-bet (**Fig. 8 D**), a transcription factor suppressed by FOXO1 (Michelini, Doedens, Goldrath, & Hedrick, 2013; Rao, Li, Bupp, & Shrikant, 2012). To analyse the contribution of AKT/FOXO1/T-bet pathway to the DMF-mediated IL-17 suppression, we differentiated WT and T-bet-deficient (*Tbx21*^{-/-}) CD8⁺ T cells under Tc17 cell conditions and treated them with DMF and a specific AKT1/2 inhibitor (AKTi). The use of AKTi increased the IL-17 production in control- and to a significantly higher extent in DMF-treated WT, but not in *Tbx21*^{-/-} Tc17 cells (**Fig. 11 E**), thus indicating that T-bet is required for the IL-17 suppression by enhanced AKT signalling. In addition, the DMF-mediated IL-17 inhibition was less pronounced

in *Tbx21*^{-/-} as compared to WT Tc17 cells (Fig. 11 F), demonstrating a contribution of the AKT/FOXO1/T-bet pathway to the DMF-mediated IL-17 limitation in Tc17 cells, in addition to enhanced STAT5 signalling (Fig. 11 G).

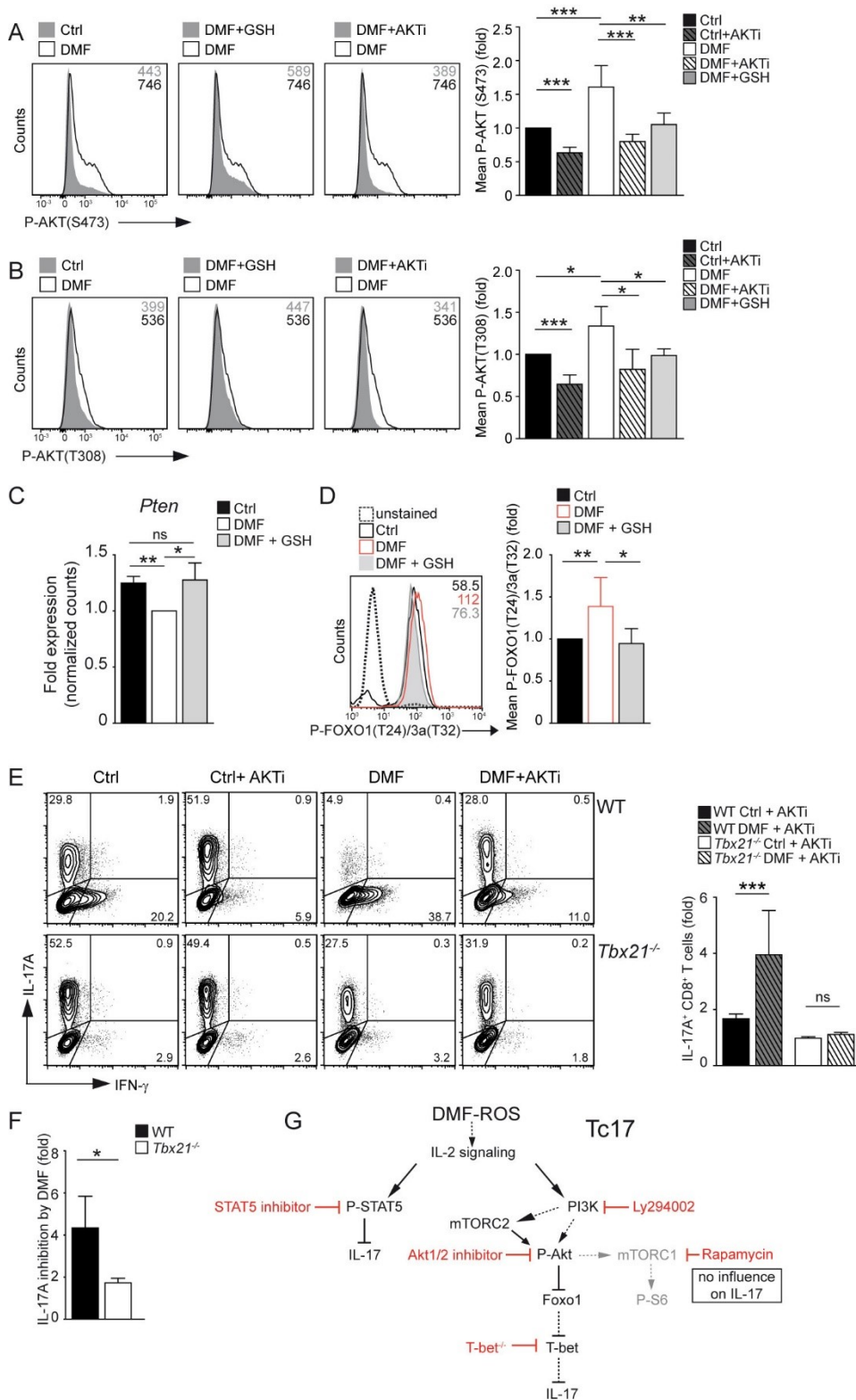


Figure 14: ROS suppress IL-17 production in Tc17 cells via increased AKT/FOXO1/T-bet signalling

(A, B) Flow cytometric analysis of (A) P-AKT(S473) and (B) P-AKT(T308) in CD8⁺ T cells differentiated for 2 days under Tc17 conditions with indicated treatment, rested overnight and restimulated with 100 U/ml IL-2 for 2 h under indicated treatment. Numbers in histograms represent MFI. Bars show fold MFI change relative to control. **(C)** Fold change of normalized expression counts of *Pten* from the dataset described in Figure 4 as determined by RNA-Seq and relative to DMF-treated Tc17 cells. **(D)** Flow cytometric determination of P- FOXO1(T24)/FOXO3a (T32) in CD8⁺ T cells differentiated for 2 days under Tc17 conditions with indicated treatment. Numbers in histograms represent MFI. Bars show fold MFI change relative to control. **(E)** Flow cytometric analysis of IL-17A⁺ and IFN- γ ⁺ WT and *Tbx21*^{-/-} CD8⁺ T cells differentiated for 3 days under Tc17 conditions with indicated treatment. Numbers in plots represent % of gated cells. **(F)** Flow cytometric analysis of IL-17A⁺ CD8⁺ WT and *Tbx21*^{-/-} CD8⁺ T cells differentiated for 3 days under Tc17 conditions with indicated treatment. Bars show fold IL-17A inhibition by DMF. **(G)** Schematic DMF/ROS influence on IL-2 signalling, leading to IL-17 suppression in Tc17 cells. Modified from (Ardestani et al., 2018; Haddadi et al., 2018). Histograms and contour plots are representative for three (A, B), four (E) or five (D) independent experiments. Bars show mean \pm SD from three (A-C), four (E, F) or five (D) combined experiments. (A-F) Statistical analysis was performed using unpaired two-tailed Student's t-test (ns $p > 0.05$, * $p < 0.05$, ** $p < 0.01$, *** $p < 0.001$).

5.9 IL-17 production is differentially regulated in Tc17 and Th17 cells

Besides FOXO1 and T-bet, the PI3K/AKT pathway also induces mTORC1 (Ardestani et al., 2018; Finlay & Cantrell, 2011). In line with the elevated PI3K/AKT pathway, we found an upregulation of mTOR-associated genes after DMF treatment of Tc17 cells (**Fig. 12 A**). In particular, phosphorylation of its downstream target S6 was elevated after DMF treatment (**Fig. 12 B**), demonstrating increased activity of mTORC1. In Th17 cells, mTORC1 is a positive regulator of IL-17 production, as the rapamycin-mediated mTORC1 inhibition limits IL-17 (Shi 2011). However, in contrast to Th17 cells, rapamycin did not limit IL-17 production in Tc17 cells (**Fig. 12 C, D**). Furthermore, the inhibition of AKT failed to influence the production of IL-17 in Th17 cells (**Fig. 12 E**), whereas it was induced in Tc17 cells (**Fig. 11 E**).

Hence, these data indicate that AKT and mTORC1 signalling differentially impact the IL-17 production of Th17 and Tc17 cells (**Fig. 11 G and Fig. 12 F**).

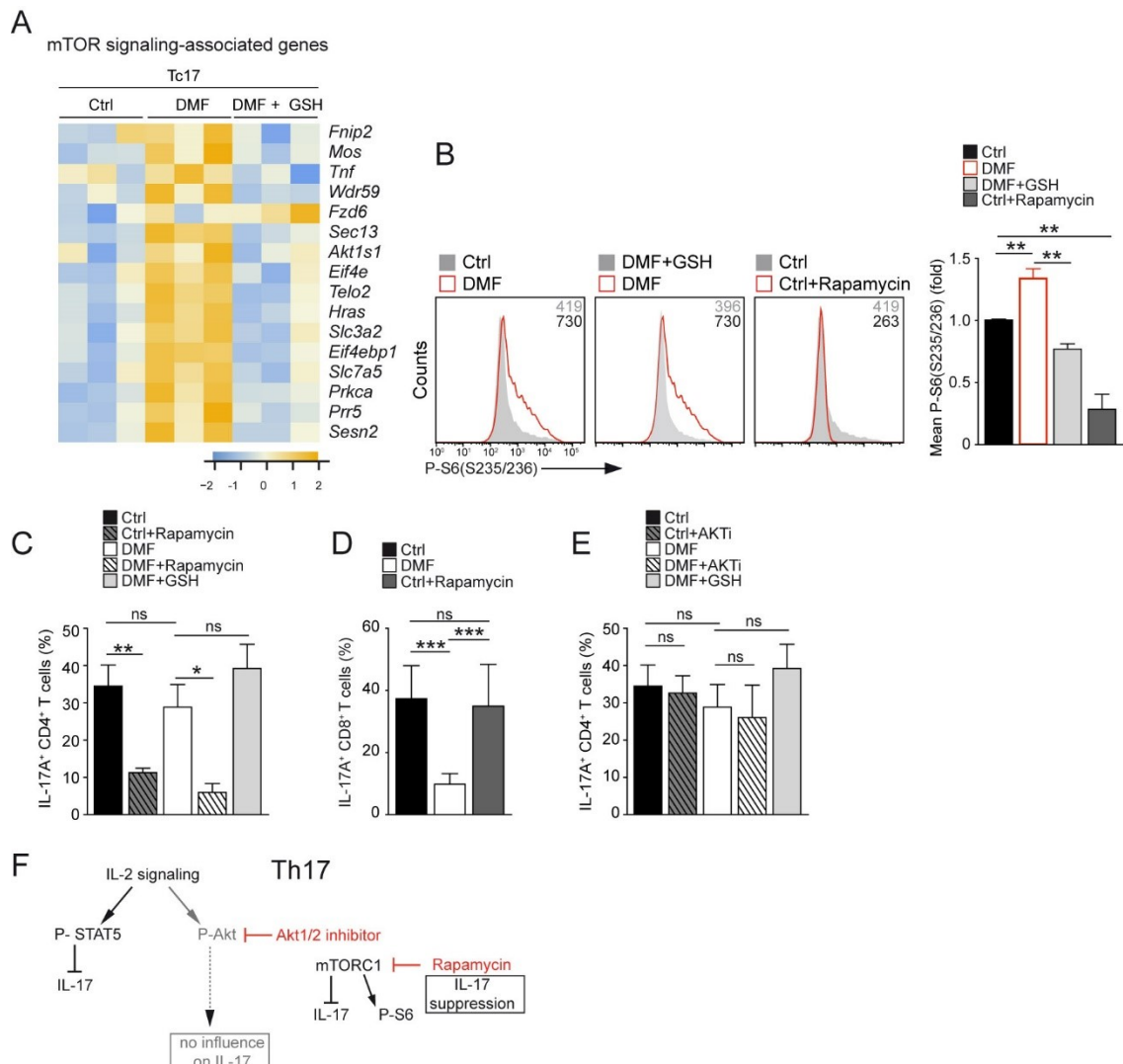


Figure 15: Differential impact of AKT- and mTORC1-signalling on IL-17 production of Tc17 and Th17 cells

(A) Heatmap shows color-coded z-scores for the rlog transformed batch-corrected expression values from the dataset described in Figure 4. Displayed are the 16 most differentially upregulated mTOR signalling-associated genes according to KEGG database in Tc17 cells treated with DMF compared to control. **(B)** Flow cytometric analysis of P-S6(S235/236) in CD8⁺ T cells differentiated for 3 days under Tc17 conditions with indicated treatment. Bars show fold MFI change of P-S6 relative to control. **(C, D, E)** Flow cytometric analysis of IL-17⁺ CD4⁺ or CD8⁺ T cells differentiated for 3 days under type 17 conditions with indicated treatment. **(F)** Schematic influence of IL-2 signalling on Th17 cells. Modified from (Ardestani et al., 2018; Haddadi et al., 2018). Histogram in D is representative for three independent experiments. Bars show mean \pm SD from (B, C, E) three or (D) four combined experiments. Statistical analysis was performed using unpaired two-tailed Student's t-test (ns $P > 0.05$, * $P < 0.05$, ** $P < 0.01$, *** $P < 0.001$).

5.10 DMF suppresses IL-17 production of human Tc17 cells in a ROS-dependent manner

IL-17-producing CD8⁺ T cells have been found in acute active and chronic lesions of MS patients (Tzartos et al., 2008) and Tc17 cells support the pathogenicity of Th17 cells by IL-17 production during the onset of EAE (Huber et al., 2013).

Our data acquired in the murine system demonstrated that DMF via GSH-depletion and ROS induction is able to suppress the Tc17 cell fate, including the production of pro-inflammatory IL-17. To examine whether the findings obtained in mouse Tc17 cells can be translated to the human system, we differentiated human Tc17 cells *in vitro*. These experiments were done in collaboration with Dr. C. Zielinski from Technical University of Munich.

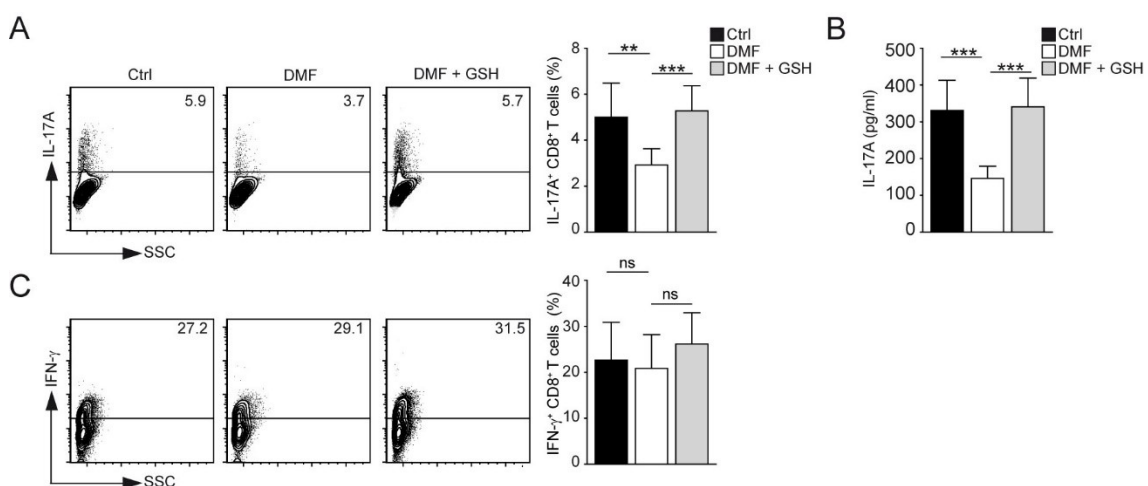


Figure 16: DMF treatment limits IL-17 production in human Tc17 cells

(A-C) CD8⁺CD45RA⁻ T cells were sorted from human peripheral blood of healthy donors and differentiated under Tc17 conditions for 4 days with indicated treatment. (A, C) Flow cytometric analysis of IL-17A⁺ or IFN- γ ⁺ CD8⁺ T cells. Numbers in plots represent % of gated cells. Data are representative of three individual experiments and donors. (B) ELISA analysis of IL-17 in the supernatant from cultures described in A. Bars give mean \pm SD from two combined experiments with different donors. Statistical analysis was performed using unpaired two-tailed Student's t-test (ns $P > 0.05$, * $P < 0.05$, ** $P < 0.01$, *** $P < 0.001$).

Briefly, CD8⁺ CD45RA⁻ T cells of healthy donors were sorted, cultured under Tc17 conditions and treated with control, DMF alone or in combination with GSH as indicated. After four days, IL-17 and IFN- γ levels were analysed by flow cytometry and the measurement of IL-17 concentration in cell culture supernatant was additionally determined by ELISA.

In accordance with the findings in the murine system, DMF significantly suppressed the IL-17 production also in human Tc17 cells in a ROS-dependent manner (Fig. 13 A, B). Surprisingly, IFN- γ levels were not influenced by DMF treatment (Fig. 13 C).

Taken together, DMF-mediated ROS upregulation suppresses IL-17 production in murine and human cells in comparable manner, whereas production of IFN- γ seems to be differentially regulated.

5.11 DMF treatment reduces frequencies of IL-17-producing CD8⁺ T cells in MS patients

CD8⁺ T cells contribute to autoimmune processes in the CNS by production of pro-inflammatory IL-17 (Huber et al., 2013). Our aforementioned data revealed that the RRMS drug DMF suppresses IL-17 production by murine as well as human CD8⁺ T cells *in vitro*. Furthermore, oral DMF application limited T cell infiltration in the CNS and diminished clinical disease symptoms in the mouse model. To examine the impact of DMF treatment on CD8⁺ and CD4⁺ T cells in RRMS patients, we analysed the frequencies of IL-17- and IFN- γ -producing memory CD8⁺ and CD4⁺ T cells before and after the first year of treatment. Biosampling and analysis were performed in collaboration with Dr. B. Tackenberg from the University Hospital Marburg.

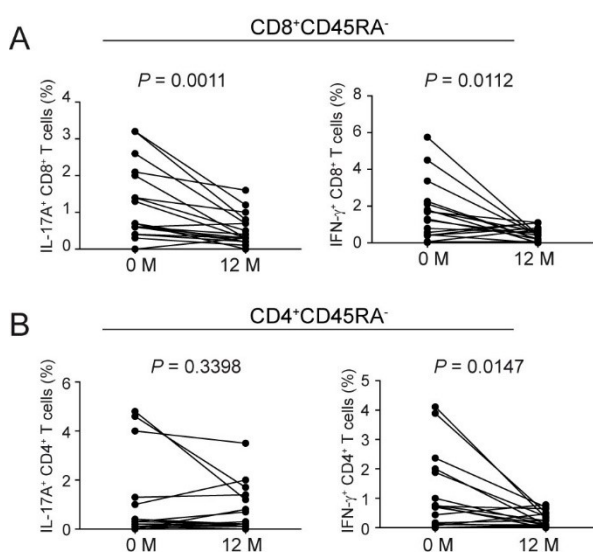


Figure 17: DMF treatment limits IL-17 production of CD8⁺ T cells in MS patients

(A) Flow cytometric analysis of percentages of IL-17A⁺ or IFN- γ ⁺ CD8⁺ CD14⁻ CD45RA⁻ T cells and **(B)** percentages of IL-17A⁺ or IFN- γ ⁺ CD4⁺ CD14⁻ CD45RA⁻ T cells from PB of treatment naïve RRMS patients ($n = 18$) before (0 M) and after 12 months (12 M) of Tecfidera therapy. Statistical analysis was performed using paired two-tailed Student's t-test.

We analysed PB from 18 naïve DMF responders, who were stable in terms of relapses, new/enlarging T2 lesions in magnetic resonance imaging (MRI) and the expanded disability

status scale (EDSS) after the first year of Tecfidera treatment and compared cytokine production with cytokine levels of naïve patients before treatment.

In accordance with the previous data, the frequencies of IL-17-producing memory CD8⁺CD45RA⁻ T cells were significantly reduced, demonstrating a positive response to Tecfidera treatment. In contrast to the *in vitro* data, also the IFN- γ production of memory CD8⁺ T cells was reduced (**Fig. 14 A**). In addition, we analysed the influence of DMF on memory CD4⁺ T cells and found also here a significant reduction of IFN- γ producers, whereas the frequencies of IL-17-producing memory CD4⁺ T cells were not affected, again demonstrating the preferential influence of DMF on IL-17-producing CD8⁺ T cells (**Fig. 14 B**).

Thus, we could show that DMF treatment limits IL-17 production in CD8⁺ T cells also in RRMS patients. In addition to the *in vitro* data, also the IFN- γ production of CD8⁺ and CD4⁺ T cells was diminished, assuming a contribution of further indirect effects *in vivo*.

6. Discussion

Immune modulatory impact of DMF

DMF (marketed as Tecfidera®) is approved for treatment of RRMS since early 2013, but its mode of action has not been fully elucidated (Bomprezzi, 2015). What has become clear so far is that DMF does not only have a single mechanism by which it shows its effect, but rather it exerts a multitude of effects on the immune system. These effects vary from reduced infiltration of immune cells to the CNS (H. Chen et al., 2014), histone hypermethylation of tumour cells (Sullivan et al., 2013), elevated ROS levels by depletion of GSH (Diebold et al., 2017; Ghoreschi et al., 2011) to an induction of antioxidant responses via the NRF2 pathway in neurons and glial cells (Linker & Haghikia, 2016). However, a direct influence of DMF on IL-17-producing CD8⁺ T cells that contribute to the pathogenicity of MS has not been evaluated so far. This thesis provides new insights in DMF's mode of action by revealing its inhibitory impact on murine and human Tc17 cells via ROS accumulation.

6.1 ROS modifies Tc17 cell fate

6.1.1 DMF suppresses IL-17 in Tc17 cells via early GSH-depletion and subsequent ROS accumulation

In several studies it has been shown that DMF binds to intracellular GSH and decreases its antioxidative capacity, thereby leading to elevated ROS levels in various cell types (Ghoreschi et al., 2011; Hoetzenecker et al., 2012; Sullivan et al., 2013; Zheng et al., 2015). Depending on their concentration, on the one hand ROS are able to support CD8⁺ T cell activation (Sena et al., 2013), on the other they can also result in a tremendous impairment of T cell function (Mak et al., 2017). Although a reduction of CD8⁺ T cells was uncovered upon DMF treatment, the functional impact of DMF on CD8⁺ T cells, in particular IL-17-producing CD8⁺ T cells, remained elusive.

Here, we demonstrated that DMF treatment of Tc17 cells *in vitro* resulted in a significant reduction of intracellular GSH levels, followed by ROS upregulation at early time points of differentiation. After 24 h of differentiation a reversed picture with a significant reduction of ROS and an increase of NRF2 target genes emerged, pointing to the induction of antioxidant pathways, already described for DCs, neurons and astrocytes (Ghoreschi et al., 2011; Linker & Haghikia, 2016; Scannevin et al., 2012). Surprisingly, the early accumulation of ROS was sufficient to suppress IL-17 and upregulate IFN- γ production in Tc17 cells, as the

addition of reduced GSH was able to restore cytokine production to a large extent. To evaluate the susceptibility of established Tc17 cells to DMF, we added DMF at later time points. Of note, after at least 17 h upon begin of culture, DMF was not able to limit IL-17 anymore, demonstrating the importance of early DMF presence in order to inhibit IL-17 production of Tc17 cells.

Although we detected elevated ROS levels in Th17 cells as well, we did not observe a significant IL-17 suppression. This is in contrast to previously published data describing a ROS-mediated inhibitory effect on IL-17 production in Th17 cells, the mechanism however remains obscure (Gerriets & Kishton, 2014). These contrary results may be due to differences in the experimental setup of our and their study. Whereas we used DMF to induce ROS upregulation in our experiments, Gerriets et al. made applied dichloroacetate (DCA), an inhibitor of the pyruvate dehydrogenase kinase (PDHK). DCA treatment suppressed glycolysis and increased oxidative metabolism including ROS levels in Th17 cells. Apart from differential ROS induction among the studies, also the levels differed as well. Additionally, while in our experimental setup, DMF only induced moderate ROS increase at early time points, Gerriets et al. showed high ROS accumulation even after three days of differentiation, indicating a more prominent and prolonged ROS upregulation. Taken together, while DMF leads to moderate ROS accumulation early in the differentiation process, DCA induced higher ROS concentrations, probably over a longer time period, which might explain the differential influence on IL-17 production in Th17 cells. Hence, future work must be carried out to assess the impact of differentially created ROS in T cells. Furthermore, it should be examined at which concentrations ROS might have suppressive effects on Th17 cells to ensure safe and effective therapies.

Finally, we demonstrated the stability of IL-17 suppression in Tc17 cells by DMF. Interestingly, IL-17 levels were diminished to a similar extent in cells treated for six days continuously with DMF and cells treated for three days, followed by a three-day resting period without DMF. This indicated a persistent impact of DMF on Tc17 cells with relevance for therapy.

Thus, it can be concluded that the DMF-mediated GSH depletion leads to an early moderate ROS upregulation, causing long-lasting suppressive effects on IL-17 production of Tc17, but not Th17 cells. DMF preferentially inhibits IL-17 production of Tc17 cells when administered at early stages of differentiation. This observation is supported by a study showing that early DMF therapy is highly effective especially in newly-diagnosed cases of MS (Gold G.; Phillips, J. T.; Fox, R. J.; Zhang, A.; Meltzer, L.; Kurukulasuriya, N. C., 2015). Furthermore, continuous

application of DMF might be required in therapy for RRMS patients in order to suppress newly developing pathogenic Tc17 cells.

6.1.2 Involvement of DMF/ROS axis on T cell proliferation and apoptosis

Besides the intensity of TCR signalling, co-stimulation and cytokines, the activation of T cells is influenced by ROS (Franchina et al., 2018). ROS are generated in the mitochondrial electron transport chain (ETC) and their levels are physiologically balanced by antioxidants like GSH (Franchina et al., 2018). Depending on concentration and exposure time, ROS can influence T cell responses in a positive or negative manner (Mak et al., 2017; Sena et al., 2013).

To evaluate whether DMF via ROS accumulation suppressed proliferation of Tc17 cells and thus influenced their cytokine production, we performed CFSE staining and detected only a tendency of reduced proliferative capacity in DMF-treated cells. By comparing the IL-17 suppression in each proliferation cycle, it became clear that DMF limits IL-17 independently of proliferation, as the frequencies of IL-17-producing cells were reduced to a similar extent in each proliferation cycle. Thus, the increased ROS levels induced by DMF do not impair proliferation of Tc17 cells and thereby cytokine production.

The occurrence of lymphopenia or PML in some MS patients under Tecfidera treatment threw a shadow onto the overall positive safety profile of DMF (Linker & Haghikia, 2016). To elucidate if the IL-17 inhibition was a side effect of apoptosis induced by DMF, we performed Annexin V and propidium iodide staining on DMF-treated Tc17 cells compared to controls. It became obvious that DMF at immune modulatory concentrations hardly induced apoptosis in Tc17 cells, whereas higher DMF concentrations were pro-apoptotic, in accordance with previous reports (Diebold et al., 2017). Interestingly, the neutralisation of ROS by GSH reversed the cell death induced by DMF, demonstrating a dose-dependent impact of ROS levels: At moderate levels, ROS exerted immune modulatory effects, whereas high ROS levels had detrimental impact by inducing cell death.

Taken together, DMF executes the Tc17 suppression neither via elevated apoptosis nor reduced proliferation but probably by interfering with further signalling pathways.

6.1.3 ROS shifts the Tc17 profile towards a CTL-like signature

After having demonstrated the influence of elevated ROS levels for limiting IL-17 production in Tc17 cells, we sought to elucidate whether DMF-induced ROS have broader implications on the transcriptome of Tc17 cells. Hence, we performed RNA-Seq to compare gene expression profiles of Tc17 cells treated with control, DMF alone or in combination with GSH. Gene expression profiles clearly showed the global influence of DMF treatment and the reversion by

GSH co-treatment on Tc17 cells. PCA analysis highlighted the impact of the DMF-mediated ROS increase on Tc17 cell transcriptome by pointing out the similar profiles of control and GSH co-treated cells. Functional analysis via GSEA revealed a significant reduction of Tc17-associated genes in DMF-treated samples whereas CTL-associated genes were significantly enriched, including those involved in the induction of cytotoxic molecules as perforin and granzymes. As addition of GSH could reverse these changes, we could clearly show that DMF via ROS accumulation was responsible for the reprogramming towards a CTL-like phenotype. Furthermore, the type 17 TF ROR γ t was reduced on protein level, whereas T-bet, crucial for effector CTL differentiation, was upregulated in DMF-treated samples (Kallies & Good-Jacobson, 2017), suggesting that ROS can act as modulator of T cell plasticity.

Collectively, these data indicate that DMF-induced ROS downregulates Tc17 cells, whereas boosts CTL signatures, indicating their ability to influence CD8⁺ T cell plasticity. Since Tc17 cells contribute to several pathologies including MS, psoriasis and type 1 diabetes (Srenathan et al., 2016), actively regulating ROS levels might represent a potential therapeutic tool for these immunopathologies.

6.1.4 DMF alters histone modifications of Tc17 cells in a ROS-dependent manner

Oxidative stress can exert a strong influence on immunopathologies, including cancer, diabetes and neurodegenerative diseases. There is growing evidence that ROS influences chromatin structure, DNA methylation and histone modifications. The resulting cellular changes including altered gene expression are disease-driving mechanisms of the aforementioned pathologies (Kreuz & Fischle, 2016). Histones especially are extensively affected by ROS, which leads to an altered structure that influences post-translational modifications (Kreuz & Fischle, 2016). Furthermore, it was proved that permissive histone modifications such as H3K27Ac and H3K4me3 are essential for gene expression of the *Il17* locus (Akimzhanov, Yang, & Dong, 2007).

To assess whether ROS influences histone modifications in Tc17 cells, we performed ChIP assays at the promoter and an enhancer of the *Il17* locus in Tc17 cells treated with control, DMF alone or in combination with GSH. We could demonstrate that the DMF-promoted ROS specifically suppressed permissive histone modifications including H4Ac, H3K27Ac and H3K4me3 in Tc17 cells, whereas the repressive methylation H3K27me3 was not influenced. This was quite surprising, as high fumarate concentrations have been shown to inhibit α -ketoglutarate-dependent dioxygenases that are involved in DNA and histone demethylation (Laukka et al., 2016; Xiao et al., 2012). In order to address the question whether DMF also

influences DNA and/or histone methylation genome-wide, which has been reported in previous studies (Xiao et al., 2012), ATAC-Seq or ChIP-Seq analysis would be required.

Besides its direct influence on histones, ROS have been implicated in the induction of HDAC activity, enzymes that catalyse deacetylation and thus gene silencing (Kreuz & Fischle, 2016). Additionally, it was shown previously that ROS can suppress expression of members of cell junction protein as E-cadherin by an HDAC1-dependent decrease of H3Ac, H4Ac as well as H3K4me2 in human hepatoma cells (Lim et al., 2008). Of note, it was shown by Yang et al that IL-2 induced STAT5 is able to reduce permissive histone modifications such as H3Ac at the *IL17* locus by recruitment of a histone deacetylase adaptor protein (X. P. Yang et al., 2011).

To investigate the contribution of HDACs to the ROS-mediated IL-17 suppression, we co-treated Tc17 cells with DMF and the HDAC inhibitor TSA. Our data indicate that the reduction of permissive histone acetylation was in parts mediated by increasing HDAC recruitment or function, as HDAC inhibition by TSA partially restored IL-17 levels.

In summary, DMF-mediated ROS increase can influence histone modifications, leading to reduced permissive acetylation and methylation at the *IL17* locus. This was at least partially mediated by enhancement of HDAC function or recruitment.

6.2 ROS alter Tc17 network by enhancing IL-2 signalling

Our data showed the key role of ROS in Tc17 cell suppression, as neutralisation by GSH or Trolox reversed the effects. In Tc17 cells, besides ROS IL-2 was also absolutely required for the limitation of IL-17 production by DMF. Furthermore, the functional analysis of RNA-Seq data by GSEA revealed an enrichment of IL-2/STAT5-associated genes in DMF-treated Tc17 cells as compared to control. These results show that IL-2 is not only necessary for IL-17 inhibition but is also elevated by DMF/ROS axis, suggesting interdependency between ROS and IL-2 signalling during DMF treatment. However, GSH depletion as well as ROS induction upon DMF addition were not dependent on the presence of IL-2. Therefore, we hypothesised that ROS by enhancing IL-2 signalling caused the suppression of IL-17 in Tc17 cells.

IL-2 has been shown to promote naïve CD4⁺ T cell differentiation into Th1 and Th2 cells, whereas Th17 cell differentiation is suppressed (Liao et al., 2013). Besides its actions on CD4⁺ T cells, IL-2 supports the development of naïve CD8⁺ T cells into effector and memory CTL with induction of IFN- γ , perforin and granzymes (Pipkin et al., 2010). Our data demonstrated a ROS-dependent shift from Tc17 signature towards a CTL-like profile by DMF, resulting in prevention of CNS autoimmunity. It is conceivable that these mechanisms also count for CTLs, in which ROS by enhanced IL2 signalling would drive terminal effector differentiation (Pipkin et al., 2010). The fact that accelerated IL-2 can induce apoptosis in CTLs (Shrikant & Mescher, 2002),

makes this cytokine promising for tumour therapy. In this context, ROS via IL-2 would induce apoptosis in tumour-infiltrating CTLs and thus contribute to tumour progression.

With keeping the importance of IL-2 signalling for DMF-mediated IL-17 suppression in mind, we sought to analyse IL-2 downstream pathways in order to elucidate mechanisms of Tc17 fate suppression more in detail.

6.2.1 Elevated ROS increase STAT5 and PI3K/AKT signalling, thereby limiting IL-17 inhibition

Our results demonstrate that DMF via ROS accumulation enhances IL-2 signalling and elevated phosphorylation of STAT5 in Tc17 cells. In accordance to the published data for Th17 cells (Liao et al., 2013; X. P. Yang et al., 2011), STAT5 can limit IL-17 production also in their CD8⁺ counterparts. It was shown that STAT3 and STAT5 compete for common binding sites at the *Il17* locus and thereby regulate gene transcription by direct opposing actions in Th17 cells (X. P. Yang et al., 2011). By performing STAT3 overexpression we could confirm a comparable mechanism for Tc17 cells, as high STAT3 levels diminished the IL-17 suppression partially. The co-treatment of cells with DMF and a pharmacological STAT5 inhibitor revealed a contributing effect of STAT5 to the DMF/ROS-mediated IL-17 suppression.

Besides STAT5, IL-2 induces also PI3K/AKT pathways and thereby determines CTL fate (Macintyre et al., 2014). This is in line with our finding that DMF via ROS suppress Tc17 cells and equips them with a CTL-like signature, including the transcription factor T-bet. Furthermore, our data demonstrate an ROS-mediated elevated activation of AKT, probably caused by a diminished expression of the phosphatase *Pten*. This is in accordance with previous data, which reported an inhibitory effect of ROS on the activity of phosphatases by oxidation of their catalytic residues (Kamata et al., 2005) and was already described for PTEN in RAW macrophages (Leslie et al., 2003) and the protein-tyrosine phosphatase PTPN2 in hepatocytes (Gurzov et al., 2014). Elevated AKT activity results in the increased phosphorylation of FOXO1, leading to the termination of its transcriptional activity (Finlay & Cantrell, 2011). Accordingly, DMF-treated Tc17 cells showed enhanced P-FOXO1/3a levels and upregulation of T-bet, a TF suppressed by FOXO1 (Michelini et al., 2013; Rao et al., 2012). As DMF could inhibit IL-17 in T-bet-deficient Tc17 cells to a lesser extent, we assumed a T-bet requirement for suppression of IL-17. Furthermore, we demonstrated that the partial IL-17 limitation by AKT signalling was mediated via T-bet, as inhibition of AKT in T-bet-deficient cells had no influence on IL-17 production. Our data is in line with previous literature, showing that T-bet hinders Tc17 cell differentiation (Intlekofer et al., 2008; Xin et al., 2016). In addition,

further work has to be performed to reveal the contribution of further IL-2 downstream pathways, as ERK signalling, to IL-17 suppression by DMF.

In summary, DMF alters Tc17 transcriptional program at least partially via enhanced STAT5 as well as PI3K/AKT/FOXO1/T-bet signalling in a ROS-dependent manner.

6.2.2 Model of differential IL-17 regulation in Th17 and Tc17 cells

We show that DMF treatment preferentially suppresses the IL-17 production of Tc17 cells, whereas Th17 cells remain largely unaffected. This might be due to a different sensitivity towards ROS levels in CD4⁺ and CD8⁺ T cells, as discussed in 6.1.1.

A further possibility for the selective IL-17 suppression in Tc17 cells by DMF might be the differential AKT- and mTORC1-signalling in Tc17 and Th17 cells. Whereas IL-2-induced AKT suppressed the IL-17 production by Tc17 cells, it failed to do so in Th17 cells, pointing to signaling differences between CD4⁺ and CD8⁺ T cells.

Furthermore, our data revealed differences in mTORC1 signalling between Th17 and Tc17 cells. Besides FOXO1 and T-bet, also mTORC1 is induced by the PI3K/AKT pathway (Ardestani et al., 2018; Finlay & Cantrell, 2011). In accordance with the elevated PI3K/AKT signalling, we detected an enhanced mTORC1 activity after DMF treatment in Tc17 cells, indicated by elevated levels of mTOR signalling-associated genes including P-S6. In Th17 cells, mTORC1 is supposed to be a positive regulator of IL-17, as rapamycin suppressed its production (L. Z. Shi et al., 2011). However, in contrast to Th17 cells, the mTORC1 inhibitor rapamycin could not limit IL-17 in Tc17 cells, although suppression of P-S6 revealed its effectiveness.

A possible explanation for this contrast could be given by differential signalling, as already reported for IL-2 signalling in CD4⁺ versus CD8⁺ T cells: whereas CD4⁺ T cells show a biphasic STAT5 phosphorylation, only one P-STAT5 peak is detectable upon IL-2 stimulation in CD8⁺ T cells (G. A. Smith et al., 2017). Therefore, additional functional differences in IL-2 downstream-signalling cascades in both T cell classes are conceivable. However, further work has to be carried out to investigate the exact differences between Tc17 and Th17 cells concerning their responsiveness to DMF treatment.

Taken together, the preferential IL-17 suppression in Tc17 cells as compared to Th17 cells could be explained by several convergent effects. Besides a different ROS sensitivity in CD4⁺ and CD8⁺ T cells, also variances in mTORC1 and AKT signalling might contribute to a differential response to DMF treatment.

6.3 Impact of DMF treatment on EAE pathogenesis

6.3.1 The course of EAE is attenuated by oral DMF application

Multiple sclerosis is a heterogeneous, T cell-mediated disease characterized by demyelination and multifocal inflammation. Besides T cells, inflammatory lesions are additionally infiltrated by B cells, monocytes, macrophages and plasma cells, indicating a multicellular pathophysiological process leading to axonal damage (Comabella & Khoury, 2012; Dendrou et al., 2015; Nylander & Hafler, 2012). Several *in vivo* and *in vitro* studies point to the beneficial impact of DMF treatment during MS and the animal model EAE (Ghoreschi et al., 2011; Gold G.; Phillips, J. T.; Fox, R. J.; Zhang, A.; Meltzer, L.; Kurukulasuriya, N. C., 2015). It has been reported that DMF attenuates the progression of disease by various mechanism, including limitation of immune cell infiltration into the CNS via HCA₂ receptor (H. Chen et al., 2014), modulation of DCs and B cells towards an anti-inflammatory phenotype (Ghoreschi et al., 2011; Li et al., 2017) and induction of anti-oxidative response in neurons and glial cells (Linker & Haghikia, 2016). Additionally, our aforementioned data show that DMF treatment directly impacts the *in vitro* differentiation of Tc17 cells that contribute to autoimmune processes in the CNS (Huber et al., 2013).

Here we show that oral administration of DMF can limit severity of clinical symptoms during EAE as well as reduce the infiltration of IL-17-producing CD8⁺ T cells into dLN and CNS as compared to control group. This demonstrates that oral DMF application is able to attenuate EAE severity, as already described in the literature (Ghoreschi et al., 2011; Linker et al., 2011; Schulze-Topphoff et al., 2016).

Taken together, the improved disease outcome after oral DMF treatment is probably the result of a multitude of mechanisms, whereby the effect on IL-17-producing CD8⁺ T cells represents one. Therefore, besides its suppressive effect on Tc17 cell differentiation *in vitro*, oral DMF treatment can limit Tc17 cells also *in vivo*, demonstrated by reduced percentages of IL-17-producing CD8⁺ T cells in dLN and CNS compared to the control. However, based on this data it is not possible to distinguish between direct and indirect DMF effects on Tc17 cells.

6.3.2 DMF treatment limits co-pathogenic function of Tc17 cells in EAE

A series of studies have highlighted the pathogenic role of IL-17 in the development of MS by using EAE (Langrish et al., 2005). IL-17 augments inflammatory processes in the CNS by promoting the generation of further pro-inflammatory cytokines and chemokines, which attract neutrophils and macrophages to inflammation sites (Jin & Dong, 2013). In addition, IL-17 production has been associated with active disease and was detected in brain lesions of

MS patients (Fletcher, Lalor, Sweeney, Tubridy, & Mills, 2010). Although, MS has been considered as being driven by CD4⁺ T cells, recent studies revealed the contribution of other immune cells, including CD8⁺ T cells (Friese & Fugger, 2009; Salou, Nicol, Garcia, & Laplaud, 2015). The fact that CD8⁺ T cells outnumber CD4⁺ T cells 3- to 10-fold in chronically inflamed MS plaques gives further evidence for an important role of CD8⁺ T cells in MS (Babbe et al., 2000; Booss et al., 1983). Furthermore, previous data from our group revealed a co-pathogenic function of Tc17 cells during the onset of EAE by enhancing the pathogenicity of Th17 cells via their IL-17 production (Huber et al., 2013).

After having demonstrated the beneficial impact of orally administered DMF in EAE on the one hand and the stable IL-17 suppression by Tc17 cells *in vitro* on the other, we sought to elucidate a direct functional effect by DMF on Tc17 cells *in vivo*. This is why we chose an adoptive transfer EAE model to assess the impact of DMF treatment on Tc17 cells resulting in low IL-17 production *in vivo*.

In this model, Tc17 cells were differentiated *in vitro*, treated with control or DMF and adoptively transferred into recipient *Irf4*^{-/-} mice that are resistant to EAE (Brüstle et al., 2007; Huber et al., 2013). Simultaneously, MOG-specific TCR-transgenic CD4⁺ 2D2 T cells were transferred into the mice to induce EAE. Of note, transferred DMF-treated Tc17 cells evoked significantly less severe EAE symptoms characterised by significantly diminished T cell infiltration in the CNS and elevated T cell numbers in dLNs, demonstrating that DMF treatment reduced pathogenicity of Tc17 cells. More importantly, the high IL-17 production of control-treated Tc17 cells in dLNs correlated with a significant higher IL-17 production by Th17 cells in the CNS as compared to the animals that received DMF-treated Tc17 cells.

In summary, these data reveal that DMF treatment limits the co-pathogenic function of Tc17 cells by suppressing their IL-17 production. The reduced IL-17 levels of Tc17 cells are accompanied by a diminished pathogenic IL-17 production in Th17 cells, resulting in lower migration of both, IL-17-producing CD4⁺ and CD8⁺ T cells into the CNS. Furthermore, these experiments demonstrate the complex interaction between T cell subsets and underline the key role of IL-17 production by CD8⁺ T cells in EAE.

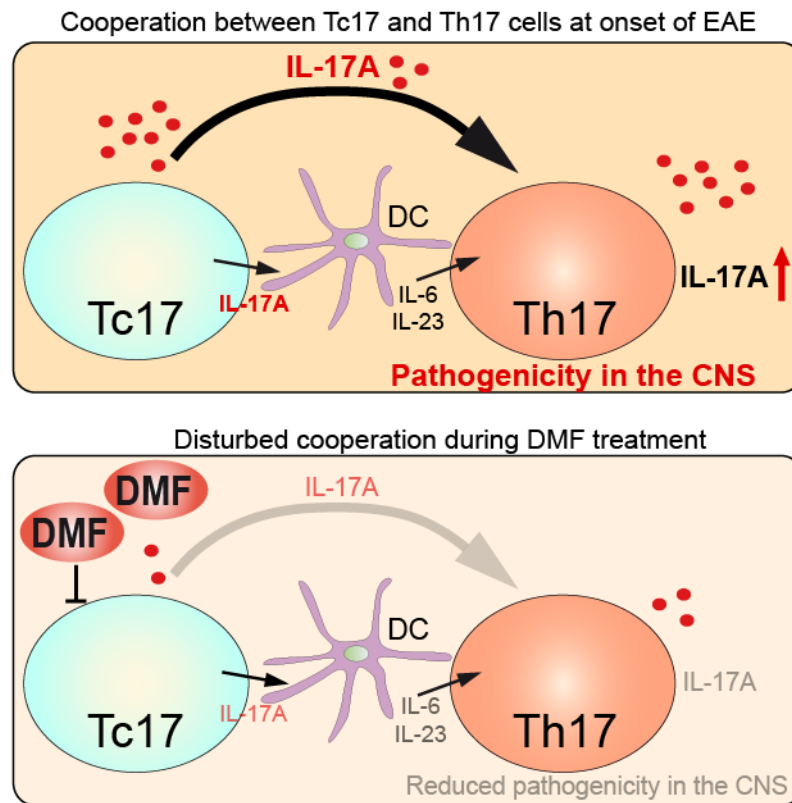


Figure 18: DMF disturbs the cooperation between Tc17 and Th17 cells during the onset of EAE

Schematic display of the cooperation between Tc17 and Th17 cells during the onset of EAE (above) and the disturbed cooperation while DMF treatment (below). By their IL-17A production, Tc17 cells provide reverse help to Th17 cells and thereby increase their pathogenicity, including high IL-17A production. In the presence of DMF however, the IL-17 production of Tc17 cells is suppressed, resulting in a diminished pathogenicity of Th17 cells. Modified from (Huber & Lohoff, 2015)

6.4 DMF treatment suppresses human IL-17-producing CD8⁺ T cells

In accordance with the data obtained from murine Tc17 cells, we showed that DMF also suppresses the IL-17 production of human Tc17 cells *in vitro*. Similar to the murine system, the DMF-mediated inhibition of human cells was ROS-dependent, suggesting similar mechanisms. In contrast, IFN- γ production was not elevated upon DMF treatment, indicating differences in IFN- γ regulation between murine and human Tc17 cells.

Along with the results *in vitro*, we demonstrated that a stable response to DMF therapy in RRMS patients was associated with a significant reduction of IL-17-producing CD8⁺ T cells. In accordance, *in vitro* data from murine Th17 cells, IL-17-producing CD4⁺ T cells were hardly affected. Therefore, the extent of IL-17 production in CD8⁺ T cells of RRMS patients with DMF treatment could be a reliable marker for determination of therapy success. In contrast to the murine system, the IFN- γ production of CD8⁺ T cells of patients was reduced by DMF treatment, indicating again differential regulation of IFN- γ production in human and murine Tc17 cells.

Hence, DMF treatment suppresses the IL-17 production of murine as well as human CD8⁺ T cells, whereas IFN- γ seems to be regulated differently.

6.5 Potential implications of DMF/ROS-mediated Tc17 suppression

In the course of this study, moderate ROS accumulation, promoted by the MS drug DMF has been identified as a suppressor of human and murine Tc17 cells. Besides their pathogenic function in autoimmune processes of the CNS, these cells contribute to protective immune responses against bacterial, viral and fungal infections (Hamada et al., 2009; Naik et al., 2015; Nanjappa et al., 2017; Yeh et al., 2010). Therefore, the limitation of IL-17-producing CD8⁺ T cells during DMF therapy might also result in disturbed clearance of pathogens and should be part of future work.

Furthermore, the role of pro-inflammatory IL-17 in tumour immunity has been highly discussed and is controversial (Qian et al., 2017). However, the majority of studies reported an inflammation-associated support of cancer development (Murugaiyan & Saha, 2009; Qian et al., 2017). In our study we revealed that DMF leads to a shift from IL-17-producing Tc17 cells towards cells with CTL signature in a ROS-dependant manner. Several points support a positive contribution of CTLs to anti-tumour responses by their production of IFN- γ and cytolytic molecules (Maher & Davies, 2004). IFN- γ , which is induced by DMF/ROS axis, has been shown to have direct and indirect anti-tumour properties (Qin et al., 2003). Additionally, the expression of cytotoxic molecules as perforin and granzymes in DMF-treated Tc17 cells was evaluated on mRNA level. However, the acquirement of cytotoxic functionality has to be proved by cytotoxicity assays and *in vivo* experiments of LCMV infection or tumour models.

Finally, Tc17 cells contribute to the pathogenesis of psoriasis as they are present in psoriatic skin lesions and correlate with severity of psoriatic arthritis (Srenathan et al., 2016). Considering that fumarate has been successfully applied for treatment of psoriasis since the 1990s (Reich et al., 2009), it is conceivable that the described suppression of Tc17 phenotype by DMF also applies for psoriasis, suggesting a common DMF-ROS-driven protective mechanism in Tc17-associated immune pathologies.

In summary, the ability of DMF to suppress Tc17 cells and IL-17 production could influence other immune responses, especially during infections and cancer therapy. As DMF mediates its major effects via ROS, understanding the impact of oxidative stress on CD8⁺ T cell fate decisions should be analysed more in detail.

6.6 Final discussion and outlook

The results reported in this study demonstrate that DMF, an approved treatment for RRMS, limits the pro-inflammatory IL-17 production in human and murine Tc17 cells ROS-dependently. In detail, cell-permeable DMF binds to the ROS scavenger GSH and causes an accumulation of ROS at early time points. This early ROS increase is sufficient to induce a shift towards a CTL-like signature while suppressing Tc17 fate, leading to their reduced co-pathogenic function during EAE. Thus, ROS was identified as an essential regulator of T cell fate and plasticity in Tc17 cells. The modification of Tc17 cells is accompanied by altered histone modifications: DMF via ROS suppresses permissive methylation and acetylation at the *IL17* locus, partially by interfering with HDACs. However, future work must be carried out to evaluate how DMF impacts epigenetic modifications in detail. Furthermore, we could demonstrate that IL-2 is required for the IL-17 inhibition by DMF and that the IL-2 downstream pathways PI3K/AKT/FOXO1 as well as STAT5 are upregulated by ROS and partially contributed to the IL-17 inhibition. Remarkably, the PI3K/AKT/FOXO1 pathway restricts IL-17 production only in Tc17 but not in Th17 cells, providing an explanation for the preferential suppression of CD8⁺ T cells. Thus, further work has to be performed to analyse the exact differences in IL-17 signalling between Tc17 and Th17 cells. Accordingly, DMF-treated RRMS patients show a reduction of IL-17-producing CD8⁺ memory T cells whereas IL-17 production in CD4⁺ T cells remains unaffected. Consequently, the analysis of IL-17 production of CD8⁺ T cells in MS patients under DMF treatment could represent a novel and reliable marker of therapeutical success.

Collectively, we show that DMF via ROS suppresses Tc17 cells fate, including its co-pathogenic role during EAE and MS. Hence, ROS is a potential regulator of CD8⁺ T cell plasticity and the use of pro-and antioxidants might represent a promising tool in preventing Tc17-mediated pathologies like MS, psoriasis or IL-17-driven tumorigenesis including pancreatic or colorectal cancer.

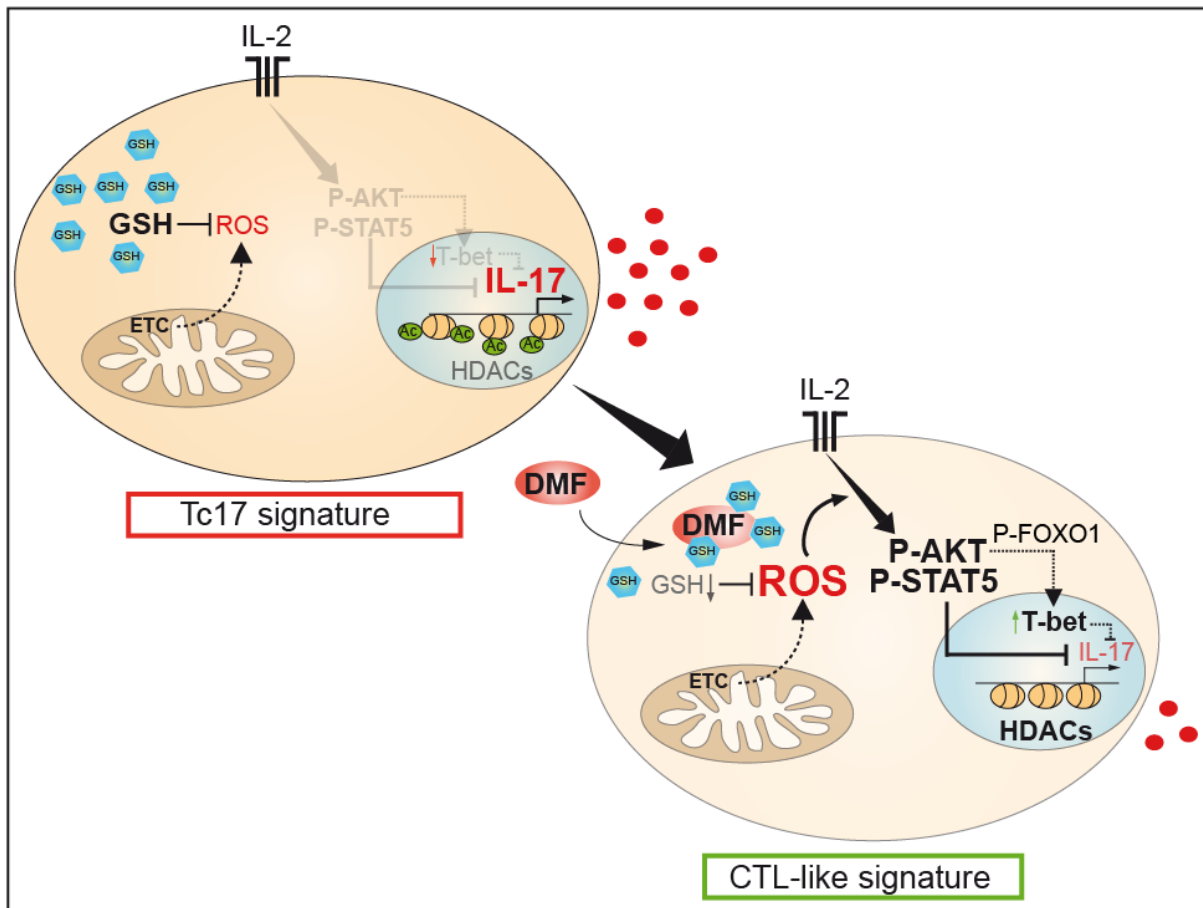


Figure 19: Influence of DMF on Tc17 cells

Schematic display of the signalling in Tc17 cells in the absence (above) or presence of DMF (below). Cytoplasmic GSH levels neutralise basal ROS contents that are produced in the electron transport chain (ETC). In the presence of DMF, GSH is depleted and results in elevated ROS levels. Accumulated ROS enhances the IL-2 pathway, leading to upregulation of P-AKT and P-STAT5 signalling. P-STAT5 probably directly reduced *IL17* transcription, whereas P-AKT via P-FOXO1 and T-bet suppresses *IL17* expression.

7. References

- 't Hart, B. A., Gran, B., & Weissert, R. (2011). EAE: Imperfect but useful models of multiple sclerosis. *Trends in Molecular Medicine*.
- Abromson-Leeman, S., Bronson, R. T., & Dorf, M. E. (2009). Encephalitogenic T cells that stably express both T-bet and ROR γ t consistently produce IFN γ but have a spectrum of IL-17 profiles. *Journal of Neuroimmunology*, 215(1–2), 10–24.
- Afanas'ev, I. (2015). Mechanisms of Superoxide Signaling in Epigenetic Processes: Relation to Aging and Cancer. *Aging and Disease*, 6(3), 216.
- Akimzhanov, A. M., Yang, X. O., & Dong, C. (2007). Chromatin remodeling of interleukin-17 (IL-17)-IL-17F cytokine gene locus during inflammatory helper T cell differentiation. *The Journal of Biological Chemistry*, 282(9), 5969–5972.
- Allfrey, V., Faulkner, R., & Mirsky, A. (1964). Acetylation and methylation of histones and their possible role in the regulation of RNA synthesis. ... *of Sciences of the United States ...*, 315(1938), 786–794.
- Araki, K., Turner, A. P., Shaffer, V. O., Gangappa, S., Keller, S. A., Bachmann, M. F., ... Ahmed, R. (2009). mTOR regulates memory CD8 T-cell differentiation. *Nature*, 460(7251), 108–112.
- Ardestani, A., Lupse, B., Kido, Y., Leibowitz, G., & Maedler, K. (2018). mTORC1 Signaling: A Double-Edged Sword in Diabetic β Cells. *Cell Metabolism*, 27, 314–331.
- Arra, A., Lingel, H., Kuroпка, B., Pick, J., Schnoeder, T., Fischer, T., ... Brunner-Weinzierl, M. C. (2017). The differentiation and plasticity of Tc17 cells are regulated by CTLA-4-mediated effects on STATs. *OncImmunology*, 6(2).
- Babbe, H., Roers, A., Waisman, A., Lassmann, H., Goebels, N., Hohlfeld, R., ... Rajewsky, K. (2000). Clonal Expansions of Cd8⁺ T Cells Dominate the T Cell Infiltrate in Active Multiple Sclerosis Lesions as Shown by Micromanipulation and Single Cell Polymerase Chain Reaction. *The Journal of Experimental Medicine*, 192(3), 393–404.
- Bachmann, M. F., & Oxenius, A. (2007). Interleukin 2: From immunostimulation to immunoregulation and back again. *EMBO Reports*.
- Belikov, A. V., Schraven, B., & Simeoni, L. (2015). T cells and reactive oxygen species. *Journal of Biomedical Science*.
- Blanco, P., Viallard, J.-F., Pellegrin, J.-L., & Moreau, J.-F. (2005). Cytotoxic T lymphocytes and autoimmunity. *Current Opinion in Rheumatology*, 17(6), 731–734.
- Blatnik, M., Thorpe, S. R., & Baynes, J. W. (2008). Succination of Proteins by Fumarate. *Annals of the New York Academy of Sciences*, 1126(1), 272–275.
- Bomprezzi, R. (2015). Dimethyl fumarate in the treatment of relapsing-remitting multiple sclerosis: an overview. *Therapeutic Advances in Neurological Disorders*, 8(1), 20–30.
- Booss, J., Esiri, M. M., Tourtellotte, W. W., & Mason, D. Y. (1983). Immunohistological analysis of T lymphocyte subsets in the central nervous system in chronic progressive multiple sclerosis. *Journal of the Neurological Sciences*, 62(1–3), 219–232.

- Boyman, O., & Sprent, J. (2012). The role of interleukin-2 during homeostasis and activation of the immune system. *Nature Reviews Immunology*.
- Brucklacher-Waldert, V., Stuermer, K., Kolster, M., Wolthausen, J., & Tolosa, E. (2009). Phenotypical and functional characterization of T helper 17 cells in multiple sclerosis. *Brain*, *132*(12), 3329–3341.
- Brüstle, A., Heink, S., Huber, M., Rosenplänter, C., Stadelmann, C., Yu, P., ... Lohoff, M. (2007). The development of inflammatory TH-17 cells requires interferon-regulatory factor 4. *Nature Immunology*.
- Cannarile, M. A., Lind, N. A., Rivera, R., Sheridan, A. D., Camfield, K. A., Wu, B. B., ... Goldrath, A. W. (2006). Transcriptional regulator Id2 mediates CD8+ T cell immunity. *Nature Immunology*, *7*(12), 1317–1325.
- Carrascosa, L. C., Klein, M., Kitagawa, Y., Lückel, C., Marini, F., König, A., ... Huber, M. (2017). Reciprocal regulation of the IL9 locus by counteracting activities of transcription factors IRF1 and IRF4. *Nature Communications*.
- Chang, H.-C., Sehra, S., Goswami, R., Yao, W., Yu, Q., Stritesky, G. L., ... Kaplan, M. H. (2010). The transcription factor PU.1 is required for the development of IL-9-producing T cells and allergic inflammation. *Nature Immunology*, *11*(6), 527–534.
- Chatterjee, R., & Vinson, C. (2012). CpG methylation recruits sequence specific transcription factors essential for tissue specific gene expression. *Biochimica et Biophysica Acta*, *1819*(7), 763–770.
- Chaudhary, B., & Elkord, E. (2016). Regulatory T Cells in the Tumor Microenvironment and Cancer Progression: Role and Therapeutic Targeting. *Vaccines*, *4*(3), 28.
- Chen, H., Assmann, J. C., Krenz, A., Rahman, M., Grimm, M., Karsten, C. M., ... Schwaninger, M. (2014). Hydroxycarboxylic acid receptor 2 mediates dimethyl fumarate's protective effect in EAE. *Journal of Clinical Investigation*, *124*(5), 2188–2192.
- Chen, X., Song, M., Zhang, B., & Zhang, Y. (2016). Reactive Oxygen Species Regulate T Cell Immune Response in the Tumor Microenvironment. *Oxidative Medicine and Cellular Longevity*, *2016*, 11–16.
- Cheng, G., Yu, A., Dee, M. J., & Malek, T. R. (2013). IL-2R signaling is essential for functional maturation of regulatory T cells during thymic development. *Journal of Immunology (Baltimore, Md. : 1950)*, *190*(4), 1567–1575.
- Cho, B. A., Sim, J. H., Park, J. A., Kim, H. W., Yoo, W. H., Lee, S. H., ... Kim, H. R. (2012). Characterization of effector memory CD8+ T cells in the synovial fluid of rheumatoid arthritis. *J Clin Immunol*, *32*(4), 709–720.
- Ciric, B., El-behi, M., Cabrera, R., Zhang, G.-X., & Rostami, A. (2009). IL-23 Drives Pathogenic IL-17-Producing CD8+ T Cells. *The Journal of Immunology*, *182*(9), 5296–5305.
- Comabella, M., & Khoury, S. J. (2012). Immunopathogenesis of multiple sclerosis. *Clinical Immunology (Orlando, Fla.)*, *142*(1), 2–8.
- Comi, G., Radaelli, M., & Soelberg Sørensen, P. (2017). Evolving concepts in the treatment of relapsing multiple sclerosis. *The Lancet*.
- Compston, A., & Coles, A. (2008). Multiple sclerosis. *The Lancet*.

- Cote-Sierra, J., Foucras, G., Guo, L., Chiodetti, L., Young, H. A., Hu-Li, J., ... Paul, W. E. (2004). Interleukin 2 plays a central role in Th2 differentiation. *Proceedings of the National Academy of Sciences*, *101*(11), 3880–3885.
- Cretney, E., Xin, A., Shi, W., Minnich, M., Masson, F., Miasari, M., ... Kallies, A. (2011). The transcription factors Blimp-1 and IRF4 jointly control the differentiation and function of effector regulatory T cells. *Nature Immunology*.
- Damsker, J. M., Hansen, A. M., & Caspi, R. R. (2010). Th1 and Th17 cells. *Ann N.Y. Acad Sci*, *1183*, 211–221.
- Dendrou, C. A., Fugger, L., & Friese, M. A. (2015). Immunopathology of multiple sclerosis. *Nature Reviews Immunology*.
- Deng, W., & Blobel, G. A. (2010). Do chromatin loops provide epigenetic gene expression states? *Current Opinion in Genetics and Development*.
- Denic, A., Wootla, B., & Rodriguez, M. (2013). CD8 + T Cells in Multiple Sclerosis. *Expert Opin Ther Targets*, *17*(9), 1053–1066.
- Devadas, S., Zaritskaya, L., Rhee, S. G., Oberley, L., & Williams, M. S. (2002). Discrete generation of superoxide and hydrogen peroxide by T cell receptor stimulation: selective regulation of mitogen-activated protein kinase activation and fas ligand expression. *The Journal of Experimental Medicine*, *195*(1), 59–70.
- Diebold, M., Sievers, C., Bantug, G., Sanderson, N., Kappos, L., Kuhle, J., ... Derfuss, T. (2017). Dimethyl fumarate influences innate and adaptive immunity in multiple sclerosis. *Journal of Autoimmunity*.
- Dimitrova, E., Turberfield, A. H., & Klose, R. J. (2015). Histone demethylases in chromatin biology and beyond. *EMBO Reports*, *16*(12), 1620–1639.
- Dinesh, R. K., Skaggs, B. J., La Cava, A., Hahn, B. H., & Singh, R. P. (2010). CD8+ Tregs in lupus, autoimmunity, and beyond. *Autoimmunity Reviews*, *9*(8), 560–568.
- Dupont, C., Armant, D. R., & Brenner, C. A. (2009). Epigenetics: Definition, mechanisms and clinical perspective. *Seminars in Reproductive Medicine*.
- Ermis, U., Weis, J., & Schulz, J. B. (2013). PML in a Patient Treated with Fumaric Acid. *New England Journal of Medicine*, *368*(17), 1657–1658.
- Feau, S., Arens, R., Togher, S., & Schoenberger, S. P. (2011). Autocrine IL-2 is required for secondary population expansion of CD8 + memory T cells. *Nature Immunology*, *12*(9), 908–913.
- Finlay, D., & Cantrell, D. A. (2011). Metabolism, migration and memory in cytotoxic T cells. *Nature Reviews Immunology*.
- Fleischer, V., Friedrich, M., Rezk, A., Bühler, U., Witsch, E., Uphaus, T., ... Luessi, F. (2017). Treatment response to dimethyl fumarate is characterized by disproportionate CD8+ T cell reduction in MS. *Multiple Sclerosis Journal*.
- Fletcher, J. M., Lalor, S. J., Sweeney, C. M., Tubridy, N., & Mills, K. H. G. (2010). T cells in multiple sclerosis and experimental autoimmune encephalomyelitis. *Clinical and Experimental Immunology*.
- Fox, R. J., Miller, D. H., Phillips, J. T., Hutchinson, M., Havrdova, E., Kita, M., ... Dawson, K. T. (2012).

- Placebo-controlled phase 3 study of oral BG-12 or glatiramer in multiple sclerosis. *The New England Journal of Medicine*, 367(12), 1087–1097.
- Franchina, D. G., Dostert, C., & Brenner, D. (2018). Reactive Oxygen Species: Involvement in T Cell Signaling and Metabolism. *Trends in Immunology*, 0(0), 1–14.
- Friese, M. A., & Fugger, L. (2009). Pathogenic CD8 + T cells in multiple sclerosis. *Annals of Neurology*.
- Gandhi, R., Laroni, A., & Weiner, H. L. (2010). Role of the innate immune system in the pathogenesis of multiple sclerosis. *Journal of Neuroimmunology*.
- Geginat, J., Lanzavecchia, A., & Sallusto, F. (2003). Proliferation and differentiation potential of human CD8+ memory T-cell subsets in response to antigen or homeostatic cytokines. *Blood*, 101(11), 4260–4266.
- Gelderman, K. A., Hultqvist, M., Holmberg, J., Olofsson, P., & Holmdahl, R. (2006). T cell surface redox levels determine T cell reactivity and arthritis susceptibility. *Proceedings of the National Academy of Sciences*, 103(34), 12831–12836.
- Gerriets, V., & Kishton, R. (2014). Metabolic programming and PDHK1 control CD4+ T cell subsets and inflammation. *The Journal of Clinical Investigation*, 125(15), 1–14.
- Ghoreschi, K., Brück, J., Kellerer, C., Deng, C., Peng, H., Rothfuss, O., ... Röcken, M. (2011). Fumarates improve psoriasis and multiple sclerosis by inducing type II dendritic cells. *The Journal of Experimental Medicine*, 208(11), 2291–2303.
- Gilmour, K. C., Pine, R., & Reich, N. C. (1995). Interleukin 2 activates STAT5 transcription factor (mammary gland factor) and specific gene expression in T lymphocytes. *Proceedings of the National Academy of Sciences of the United States of America*, 92(23), 10772–10776.
- Gold G.; Phillips, J. T.; Fox, R. J.; Zhang, A.; Meltzer, L.; Kurukulasuriya, N. C., R. . G. (2015). Efficacy and safety of delayed-release dimethyl fumarate in patients newly diagnosed with relapsing-remitting multiple sclerosis (RRMS). *Mult Scler*, 21(1), 57–66.
- Gold, R., Kappos, L., Arnold, D. L., Bar-Or, A., Giovannoni, G., Selmaj, K., ... Dawson, K. T. (2012). Placebo-Controlled Phase 3 Study of Oral BG-12 for Relapsing Multiple Sclerosis. *The New England Journal of Medicine*, 367(12), 1098–1107.
- Goldenberg, M. M. (2012). Multiple sclerosis review. *P & T: A Peer-Reviewed Journal for Formulary Management*, 37(3), 175–184.
- Gurzov, E. N., Tran, M., Fernandez-Rojo, M. A., Merry, T. L., Zhang, X., Xu, Y., ... Tiganis, T. (2014). Hepatic oxidative stress promotes insulin-STAT-5 signaling and obesity by inactivating protein tyrosine phosphatase N2. *Cell Metabolism*, 20(1), 85–102.
- Haak, S., Croxford, A. L., Kreyborg, K., Heppner, F. L., Pouly, S., Becher, B., & Waisman, A. (2009). IL-17A and IL-17F do not contribute vitally to autoimmune neuro-inflammation in mice. *Journal of Clinical Investigation*, 119(1), 61–69.
- Haas, J., Hug, A., Viehöver, A., Fritzsching, B., Falk, C. S., Filser, A., ... Wildemann, B. (2005). Reduced suppressive effect of CD4+CD25high regulatory T cells on the T cell immune response against myelin oligodendrocyte glycoprotein in patients with multiple sclerosis. *European Journal of Immunology*, 35(11), 3343–3352.

- Haddadi, N., Lin, Y., Travis, G., Simpson, A. M., McGowan, E. M., & Nassif, N. T. (2018). PTEN/PTENP1: “Regulating the regulator of RTK-dependent PI3K/Akt signalling”, new targets for cancer therapy. *Molecular Cancer*.
- Hamada, H., Garcia-Hernandez, M. d. I. L., Reome, J. B., Misra, S. K., Strutt, T. M., McKinstry, K. K., ... Dutton, R. W. (2009). Tc17, a Unique Subset of CD8 T Cells That Can Protect against Lethal Influenza Challenge. *The Journal of Immunology*.
- Hartley, S. W., & Mullikin, J. C. (2015). QoRTs: A comprehensive toolset for quality control and data processing of RNA-Seq experiments. *BMC Bioinformatics*, 16(1).
- Hauser, S. L., Waubant, E., Arnold, D. L., Vollmer, T., Antel, J., Fox, R. J., ... Smith, C. H. (2008). B-cell Depletion with Rituximab in Relapsing-Remitting Multiple Sclerosis. *N Engl J Med*, 358(7), 676–688.
- Hemmer, B., Cepok, S., Nessler, S., & Sommer, N. (2002). Pathogenesis of multiple sclerosis: An update on immunology. *Current Opinion in Neurology*.
- Hinrichs, C. S., Kaiser, A., Paulos, C. M., Cassard, L., Sanchez-Perez, L., Heemskerk, B., ... Restifo, N. P. (2009). Type 17 CD8+ T cells display enhanced antitumor immunity. *Blood*, 114(3), 596–599.
- Hoetzenecker, W., Echtenacher, B., Guenova, E., Hoetzenecker, K., Woelbing, F., Brück, J., ... Röcken, M. (2012). ROS-induced ATF3 causes susceptibility to secondary infections during sepsis-associated immunosuppression. *Nature Medicine*, 18(1), 128–134.
- Holmøy, T., & Hestvik, A. L. K. (2008). Multiple sclerosis: Immunopathogenesis and controversies in defining the cause. *Current Opinion in Infectious Diseases*.
- Hu, X., & Ivashkiv, L. B. (2009). Cross-regulation of Signaling Pathways by Interferon- γ : Implications for Immune Responses and Autoimmune Diseases. *Immunity*.
- Huber, M., Heink, S., Grothe, H., Guralnik, A., Reinhard, K., Elflein, K., ... Lohoff, M. (2009). Th17-like developmental process leads to CD8+ Tc17 cells with reduced cytotoxic activity. *European Journal of Immunology*.
- Huber, M., Heink, S., Pagenstecher, A., Reinhard, K., Ritter, J., Visekruna, A., ... Lohoff, M. (2013). IL-17A secretion by CD8+ T cells supports Th17-mediated autoimmune encephalomyelitis. *Journal of Clinical Investigation*.
- Huber, M., & Lohoff, M. (2015). Change of paradigm: CD8+ T cells as important helper for CD4+ T cells during asthma and autoimmune encephalomyelitis. *Allergo Journal International*.
- Hwang, E. S., Szabo, S. J., Schwartzberg, P. L., & Glimcher, L. H. (2005). T helper cell fate specified by kinase-mediated interaction of T-bet with GATA-3. *Science*, 307(5708), 430–433.
- Intlekofer, A. M., Banerjee, A., Takemoto, N., Gordon, S. M., DeJong, C. S., Shin, H., ... Reiner, S. L. (2008). Anomalous type 17 response to viral infection by CD8+ T cells lacking T-bet and eomesodermin. *Science*, 321(5887), 408–411.
- Ivanov, I. I., McKenzie, B. S., Zhou, L., Tadokoro, C. E., Lepelley, A., Lafaille, J. J., ... Littman, D. R. (2006). The Orphan Nuclear Receptor ROR γ t Directs the Differentiation Program of Proinflammatory IL-17+ T Helper Cells. *Cell*, 126(6), 1121–1133.
- Ivanov, I. I., Zhou, L., & Littman, D. R. (2007). Transcriptional regulation of Th17 cell differentiation.

Seminars in Immunology.

- Jackson, S. H., Devadas, S., Kwon, J., Pinto, L. A., & Williams, M. S. (2004). T cells express a phagocyte-type NADPH oxidase that is activated after T cell receptor stimulation. *Nature Immunology*, 5(8), 818–827.
- Jadidi-Niaragh, F., & Mirshafiey, A. (2011). Th17 Cell, the new player of neuroinflammatory process in multiple sclerosis. *Scandinavian Journal of Immunology.*
- Jin, W., & Dong, C. (2013). IL-17 cytokines in immunity and inflammation. *Emerging Microbes and Infections.*
- Joshi, N. S., Cui, W., Chandele, A., Lee, H. K., Urso, D. R., Hagman, J., ... Kaech, S. M. (2007). Inflammation Directs Memory Precursor and Short-Lived Effector CD8+ T Cell Fates via the Graded Expression of T-bet Transcription Factor. *Immunity*, 27(2), 281–295.
- Kaech, S. M., & Cui, W. (2012). Transcriptional control of effector and memory CD8+ T cell differentiation. *Nature Reviews Immunology.*
- Kalia, V., Sarkar, S., Subramaniam, S., Haining, W. N., Smith, K. A., & Ahmed, R. (2010). Prolonged Interleukin-2 α Expression on Virus-Specific CD8+ T Cells Favors Terminal-Effector Differentiation In Vivo. *Immunity*, 32(1), 91–103.
- Kallies, A., & Good-Jacobson, K. L. (2017). Transcription Factor T-bet Orchestrates Lineage Development and Function in the Immune System. *Trends in Immunology.*
- Kallies, A., Hawkins, E. D., Belz, G. T., Metcalf, D., Hommel, M., Corcoran, L. M., ... Nutt, S. L. (2006). Transcriptional repressor Blimp-1 is essential for T cell homeostasis and self-tolerance. *Nature Immunology.*
- Kallies, A., & Nutt, S. L. (2007). Terminal differentiation of lymphocytes depends on Blimp-1. *Current Opinion in Immunology.*
- Kallies, A., Xin, A., Belz, G. T., & Nutt, S. L. (2009). Blimp-1 Transcription Factor Is Required for the Differentiation of Effector CD8+ T Cells and Memory Responses. *Immunity.*
- Kamata, H., Honda, S. I., Maeda, S., Chang, L., Hirata, H., & Karin, M. (2005). Reactive oxygen species promote TNF α -induced death and sustained JNK activation by inhibiting MAP kinase phosphatases. *Cell*, 120(5), 649–661.
- Kanno, Y., Vahedi, G., Hirahara, K., Singleton, K., & O’Shea, J. J. (2012). Transcriptional and Epigenetic Control of T Helper Cell Specification: Molecular Mechanisms Underlying Commitment and Plasticity. *Annual Review of Immunology*, 30(1), 707–731.
- Kaplan, M. H., Hufford, M. M., & Olson, M. R. (2015). The development and in vivo function of T helper 9 cells. *Nature Reviews Immunology.*
- Kappos, L., Gold, R., Miller, D. H., Macmanus, D. G., Havrdova, E., Limmroth, V., ... O’Neill, G. N. (2008). Efficacy and safety of oral fumarate in patients with relapsing-remitting multiple sclerosis: a multicentre, randomised, double-blind, placebo-controlled phase IIb study. *Lancet*, 372(9648), 1463–1472.
- Kastrati, I., Siklos, M. I., Calderon-Gierszal, E. L., El-Shennawy, L., Georgieva, G., Thayer, E. N., ... Frasor, J. (2016). Dimethyl Fumarate Inhibits the Nuclear Factor κ B Pathway in Breast Cancer Cells by

- Covalent Modification of p65 Protein. *The Journal of Biological Chemistry*, 291(7), 3639–3647.
- Kebir, H., Kreymborg, K., Ifergan, I., Dodelet-Devillers, A., Cayrol, R., Bernard, M., ... Prat, A. (2007). Human TH17 lymphocytes promote blood-brain barrier disruption and central nervous system inflammation. *Nature Medicine*, 13(10), 1173–1175.
- Kim, G. H., Ryan, J. J., & Archer, S. L. (2013). The Role of Redox Signaling in Epigenetics and Cardiovascular Disease. *Antioxidants & Redox Signaling*, 18(15), 1920–1936.
- Kishimoto, T., Taga, T., & Akira, S. (1994). Cytokine signal transduction. *Cell*.
- Klenerman, P., & Hill, A. (2005). T cells and viral persistence: Lessons from diverse infections. *Nature Immunology*.
- Komiyama, Y., Nakae, S., Matsuki, T., Nambu, A., Ishigame, H., Kakuta, S., ... Iwakura, Y. (2006). IL-17 Plays an Important Role in the Development of Experimental Autoimmune Encephalomyelitis. *The Journal of Immunology*, 177(1), 566–573.
- Kondo, T., Takata, H., Matsuki, F., & Takiguchi, M. (2009). Cutting Edge: Phenotypic Characterization and Differentiation of Human CD8+ T Cells Producing IL-17. *The Journal of Immunology*.
- Korn, T., Bettelli, E., Gao, W., Awasthi, A., Jäger, A., Strom, T. B., ... Kuchroo, V. K. (2007). IL-21 initiates an alternative pathway to induce proinflammatory TH17 cells. *Nature*, 448(7152), 484–487.
- Kouzarides, T. (2002). Histone methylation in transcriptional control. *Current Opinion in Genetics & Development*, 12(2), 198–209.
- Kraaij, M. (2010). Induction of regulatory T cells by macrophages is dependent on production of reactive oxygen species. *Proceedings of the ...*
- Kreuz, S., & Fischle, W. (2016). Oxidative stress signaling to chromatin in health and disease. *Epigenomics*, 8(6), 843–862.
- Kryczek, I., Bruce, A. T., Gudjonsson, J. E., Johnston, A., Aphale, A., Vatan, L., ... Zou, W. (2008). Induction of IL-17+ T Cell Trafficking and Development by IFN- : Mechanism and Pathological Relevance in Psoriasis. *The Journal of Immunology*, 181(7), 4733–4741.
- Kuang, D.-M., Peng, C., Zhao, Q., Wu, Y., Zhu, L.-Y., Wang, J., ... Zheng, L. (2010). Tumor-Activated Monocytes Promote Expansion of IL-17-Producing CD8+ T Cells in Hepatocellular Carcinoma Patients. *The Journal of Immunology*, 185(3), 1544–1549.
- Langrish, C. L., Chen, Y., Blumenschein, W. M., Mattson, J., Basham, B., Sedgwick, J. D., ... Cua, D. J. (2005). IL-23 drives a pathogenic T cell population that induces autoimmune inflammation. *The Journal of Experimental Medicine*, 201(2), 233–240.
- Lassmann, H. (2017). Targets of therapy in progressive MS. *Multiple Sclerosis Journal*, 23(12), 1593–1599.
- Laukka, T., Mariani, C. J., Ihanola, T., Cao, J. Z., Hokkanen, J., Kaelin, W. G., ... Koivunen, P. (2016). Fumarate and succinate regulate expression of hypoxia-inducible genes via TET enzymes. *Journal of Biological Chemistry*, 291(8), 4256–4265.
- Laurence, A., Tato, C. M., Davidson, T. S., Kanno, Y., Chen, Z., Yao, Z., ... O’Shea, J. J. J. (2007). Interleukin-2 Signaling via STAT5 Constrains T Helper 17 Cell Generation. *Immunity*, 26(3), 371–381.
- Leslie, N. R., Bennett, D., Lindsay, Y. E., Stewart, H., Gray, A., & Downes, C. P. (2003). Redox regulation of

- PI 3-kinase signalling via inactivation of PTEN. *EMBO Journal*, 22(20), 5501–5510.
- Li, R., Rezk, A., Ghadiri, M., Luessi, F., Zipp, F., Li, H., ... Bar-Or, A. (2017). Dimethyl Fumarate Treatment Mediates an Anti-Inflammatory Shift in B Cell Subsets of Patients with Multiple Sclerosis. *The Journal of Immunology*, 198(2), 691–698.
- Liao, W., Lin, J. X., & Leonard, W. J. (2013). Interleukin-2 at the Crossroads of Effector Responses, Tolerance, and Immunotherapy. *Immunity*.
- Lim, S. O., Gu, J. M., Kim, M. S., Kim, H. S., Park, Y. N., Park, C. K., ... Jung, G. (2008). Epigenetic Changes Induced by Reactive Oxygen Species in Hepatocellular Carcinoma: Methylation of the E-cadherin Promoter. *Gastroenterology*, 135(6).
- Lin, J. X., Li, P., Liu, D., Jin, H. T., He, J., Rasheed, M. A. U., ... Leonard, W. J. (2012). Critical Role of STAT5 Transcription Factor Tetramerization for Cytokine Responses and Normal Immune Function. *Immunity*, 36(4), 586–599.
- Linker, R. A., & Haghikia, A. (2016). Dimethyl fumarate in multiple sclerosis: latest developments, evidence and place in therapy. *Therapeutic Advances in Chronic Disease*.
- Linker, R. A., Lee, D. H., Ryan, S., Van Dam, A. M., Conrad, R., Bista, P., ... Gold, R. (2011). Fumaric acid esters exert neuroprotective effects in neuroinflammation via activation of the Nrf2 antioxidant pathway. *Brain*, 134(3), 678–692.
- Loma. (2011). Multiple sclerosis: Pathogenesis and treatment. *Current Neuropharmacology*, 9(3), 409–416.
- Longbrake, E. E., & Cross, A. H. (2015). Dimethyl fumarate associated lymphopenia in clinical practice. *Multiple Sclerosis*.
- Loser, K., Vogl, T., Voskort, M., Lueken, A., Kupas, V., Nacken, W., ... Beissert, S. (2010). The toll-like receptor 4 ligands Mrp8 and Mrp14 are crucial in the development of autoreactive CD8⁺T cells. *Nature Medicine*, 16(6), 713–717.
- Lu, S. C. (2013). Glutathione synthesis. *Biochimica et Biophysica Acta (BBA) - General Subjects*, 1830(5), 3143–3153.
- Lu, Y., Hong, B., Li, H., Zheng, Y., Zhang, M., Wang, S., ... Yi, Q. (2014). Tumor-specific IL-9-producing CD8⁺ Tc9 cells are superior effector than type-I cytotoxic Tc1 cells for adoptive immunotherapy of cancers. *Proceedings of the National Academy of Sciences*, 111(6), 2265–2270.
- Macintyre, A. N., Gerriets, V. A., Nichols, A. G., Michalek, R. D., Rudolph, M. C., Deoliveira, D., ... Rathmell, J. C. (2014). The glucose transporter Glut1 is selectively essential for CD4 T cell activation and effector function. *Cell Metabolism*, 20(1), 61–72.
- Maher, J., & Davies, E. T. (2004). Targeting cytotoxic T lymphocytes for cancer immunotherapy. *British Journal of Cancer*.
- Mak, T. W., Grusdat, M., Duncan, G. S., Dostert, C., Nonnenmacher, Y., Cox, M., ... Brenner, D. (2017). Glutathione Primes T Cell Metabolism for Inflammation. *Immunity*, 46(4), 675–689.
- Malek, T. R., & Castro, I. (2010). Interleukin-2 Receptor Signaling: At the Interface between Tolerance and Immunity. *Immunity*.
- Man, K., Miasari, M., Shi, W., Xin, A., Henstridge, D. C., Preston, S., ... Kallies, A. (2013). The transcription

- factor IRF4 is essential for TCR affinity-mediated metabolic programming and clonal expansion of T cells. *Nature Immunology*, *14*(11), 1155–1165.
- Matuszewicz, D., Kivisäkk, P., He, B., Kostulas, N., Özenci, V., Fredrikson, S., & Link, H. (1999). Interleukin-17 mRNA expression in blood and CSF mononuclear cells is augmented in multiple sclerosis. *Multiple Sclerosis Journal*, *5*(2), 101–104.
- McFarland, H. F., & Martin, R. (2007). Multiple sclerosis: A complicated picture of autoimmunity. *Nature Immunology*.
- McGuire, V. A., Ruiz-Zorrilla Diez, T., Emmerich, C. H., Strickson, S., Ritorto, M. S., Sutavani, R. V., ... Arthur, J. S. C. (2016). Dimethyl fumarate blocks pro-inflammatory cytokine production via inhibition of TLR induced M1 and K63 ubiquitin chain formation. *Scientific Reports*, *6*.
- Meister, A. (1983). Selective modification of glutathione metabolism. *Science*, *220*(4596), 472–477.
- Michel, L., Touil, H., Pikor, N. B., Gomerman, J. L., Prat, A., & Bar-Or, A. (2015). B cells in the multiple sclerosis central nervous system: Trafficking and contribution to CNS-compartmentalized inflammation. *Frontiers in Immunology*, *6*(DEC), 1–12.
- Michelini, R. H., Doedens, A. L., Goldrath, A. W., & Hedrick, S. M. (2013). Differentiation of CD8 memory T cells depends on Foxo1. *The Journal of Experimental Medicine*.
- Mishra, M. K., & Yong, V. W. (2016). Myeloid cells — targets of medication in multiple sclerosis. *Nature Reviews Neurology*, *12*(9), 539–551.
- Mittrücker, H.-W., Visekruna, A., & Huber, M. (2014). Heterogeneity in the Differentiation and Function of CD8+ T Cells. *Archivum Immunologiae et Therapiae Experimentalis*, *62*(6), 449–458.
- Mosmann, T. R., Cherwinski, H., Bond, M. W., Giedlin, M. A., & Coffman, R. L. (1986). Two types of murine helper T cell clone. I. Definition according to profiles of lymphokine activities and secreted proteins. *Journal of Immunology (Baltimore, Md. : 1950)*, *136*(7), 2348–2357.
- Mullen, A. C., High, F. A., Hutchins, A. S., Lee, H. W., Villarino, A. V., Livingston, D. M., ... Reiner, S. L. (2001). Role of T-bet in commitment of TH1 cells before IL-12-dependent selection. *Science*, *292*(5523), 1907–1910.
- Murphy, K., & Weaver, C. (2017). *JANEWAY. Janeway's Immunobiology*.
- Murugaiyan, G., & Saha, B. (2009). Protumor vs Antitumor Functions of IL-17. *The Journal of Immunology*, *183*(7), 4169–4175.
- Naik, S., Bouladoux, N., Linehan, J. L., Han, S. J., Harrison, O. J., Wilhelm, C., ... Belkaid, Y. (2015). Commensal-dendritic-cell interaction specifies a unique protective skin immune signature. *Nature*, *520*(7545), 104–108.
- Nanjappa, S. G., McDermott, A. J., Fites, J. S., Galles, K., Wüthrich, M., Deepe, G. S., & Klein, B. S. (2017). Antifungal Tc17 cells are durable and stable, persisting as long-lasting vaccine memory without plasticity towards IFN γ cells. *PLoS Pathogens*.
- Nurieva, R., Yang, X. O., Martinez, G., Zhang, Y., Panopoulos, A. D., Ma, L., ... Dong, C. (2007). Essential autocrine regulation by IL-21 in the generation of inflammatory T cells. *Nature*, *448*(7152), 480–483.
- Nylander, A., & Hafler, D. a. (2012). Multiple sclerosis. *J Clin Invest*, *122*(4), 1180–1188.

- Peters, A., Fowler, K. D., Chalmin, F., Merkler, D., Kuchroo, V. K., & Pot, C. (2015). IL-27 Induces Th17 Differentiation in the Absence of STAT1 Signaling. *The Journal of Immunology*, *195*(9), 4144–4153.
- Pipkin, M. E., Sacks, J. A., Cruz-Guilloty, F., Lichtenheld, M. G., Bevan, M. J., & Rao, A. (2010). Interleukin-2 and Inflammation Induce Distinct Transcriptional Programs that Promote the Differentiation of Effector Cytolytic T Cells. *Immunity*, *32*(1), 79–90.
- Pröbstel, A. K., Sanderson, N. S. R., & Derfuss, T. (2015). B cells and autoantibodies in multiple sclerosis. *International Journal of Molecular Sciences*.
- Qian, X., Chen, H., Wu, X., Hu, L., Huang, Q., & Jin, Y. (2017). Interleukin-17 acts as double-edged sword in anti-tumor immunity and tumorigenesis. *Cytokine*.
- Qin, Z., Schwartzkopff, J., Pradera, F., Kammertoens, T., Seliger, B., Pircher, H., & Blankenstein, T. (2003). A critical requirement of interferon gamma-mediated angiostasis for tumor rejection by CD8+ T cells. *Cancer Research*, *63*, 4095–4100.
- Raczkowski, F., Ritter, J., Heesch, K., Schumacher, V., Guralnik, A., Hocker, L., ... Huber, M. (2013). The transcription factor Interferon Regulatory Factor 4 is required for the generation of protective effector CD8+ T cells. *Proceedings of the National Academy of Sciences*.
- Rao, R. R., Li, Q., Bupp, M. R. G., & Shrikant, P. A. (2012). Transcription Factor Foxo1 Represses T-bet-Mediated Effector Functions and Promotes Memory CD8 + T Cell Differentiation. *Immunity*, *36*(3), 374–387.
- Reboldi, A., Coisne, C., Baumjohann, D., Benvenuto, F., Bottinelli, D., Lira, S., ... Sallusto, F. (2009). C-C chemokine receptor 6-regulated entry of TH-17 cells into the CNS through the choroid plexus is required for the initiation of EAE. *Nature Immunology*, *10*(5), 514–523.
- Reich, K., Thaci, D., Mrowietz, U., Kamps, A., Neureither, M., & Luger, T. (2009). Wirksamkeit und Sicherheit von Fumarsäureestern in der Langzeittherapie der Psoriasis - Eine Retrospektive Studie (FUTURE). *JDDG - Journal of the German Society of Dermatology*, *7*(7), 603–611.
- Res, P. C. M., Piskin, G., de Boer, O. J., van der Loos, C. M., Teeling, P., Bos, J. D., & Teunissen, M. B. M. (2010). Overrepresentation of IL-17A and IL-22 Producing CD8 T Cells in Lesional Skin Suggests Their Involvement in the pathogenesis of psoriasis. *PLoS ONE*, *5*(11).
- Ringnér, M., & Ringner, M. (2008). What is principal component analysis? *Nat Biotechnol*, *26*(3), 303–304.
- Rivers, T. M. (1933). Observations on Attempts To Produce Acute Disseminated Encephalomyelitis in Monkeys. *Journal of Experimental Medicine*, *58*(1), 39–53.
- Rosenkranz, T., Novas, M., & Terborg, C. (2015). PML in a Patient with Lymphocytopenia Treated with Dimethyl Fumarate. *New England Journal of Medicine*, *372*(15), 1476–1478.
- Rutishauser, R. L., Martins, G. A., Kalachikov, S., Chandele, A., Parish, I. A., Meffre, E., ... Kaech, S. M. (2009). Transcriptional Repressor Blimp-1 Promotes CD8+ T Cell Terminal Differentiation and Represses the Acquisition of Central Memory T Cell Properties. *Immunity*, *31*(2), 296–308.
- Salou, M., Nicol, B., Garcia, A., & Laplaud, D.-A. (2015). Involvement of CD8+ T Cells in Multiple Sclerosis. *Frontiers in Immunology*, *6*.
- Scannevin, R. H., Chollate, S., Jung, M. -y., Shackett, M., Patel, H., Bista, P., ... Rhodes, K. J. (2012).

- Fumarates Promote Cytoprotection of Central Nervous System Cells against Oxidative Stress via the Nuclear Factor (Erythroid-Derived 2)-Like 2 Pathway. *Journal of Pharmacology and Experimental Therapeutics*, 341(1), 274–284.
- Schilling, S., Goelz, S., Linker, R., Luehder, F., & Gold, R. (2006). Fumaric acid esters are effective in chronic experimental autoimmune encephalomyelitis and suppress macrophage infiltration. *Clin Exp Immunol*, 145(1), 101–107.
- Schulze-Topphoff, U., Varrin-Doyer, M., Pekarek, K., Spencer, C. M., Shetty, A., Sagan, S. A., ... Zamvil, S. S. (2016). Dimethyl fumarate treatment induces adaptive and innate immune modulation independent of Nrf2. *Proceedings of the National Academy of Sciences*, 113(17), 4777–4782.
- Seidel, P., Merfort, I., Hughes, J. M., Oliver, B. G. G., Tamm, M., & Roth, M. (2009). Dimethylfumarate inhibits NF- κ B function at multiple levels to limit airway smooth muscle cell cytokine secretion. *American Journal of Physiology. Lung Cellular and Molecular Physiology*, 297(2), L326–L339.
- Sena, L. A., & Chandel, N. S. (2012). Physiological roles of mitochondrial reactive oxygen species. *Molecular Cell*.
- Sena, L. A., Li, S., Jairaman, A., Prakriya, M., Ezponda, T., Hildeman, D. A., ... Chandel, N. S. (2013). Mitochondria Are Required for Antigen-Specific T Cell Activation through Reactive Oxygen Species Signaling. *Immunity*, 38(2), 225–236.
- Shevach, E. M., DiPaolo, R. a, Andersson, J., Zhao, D.-M., Stephens, G. L., & Thornton, A. M. (2006). The lifestyle of naturally occurring CD4+ CD25+ Foxp3+ regulatory T cells. *Immunological Reviews*, 212, 60–73.
- Shi, G., Cox, C. A., Vistica, B. P., Tan, C., Wawrousek, E. F., & Gery, I. (2008). Phenotype Switching by Inflammation-Inducing Polarized Th17 Cells, but Not by Th1 Cells. *The Journal of Immunology*, 181(10), 7205–7213.
- Shi, L. Z., Wang, R., Huang, G., Vogel, P., Neale, G., Green, D. R., & Chi, H. (2011). HIF1 α -dependent glycolytic pathway orchestrates a metabolic checkpoint for the differentiation of T_H 17 and T_{reg} cells. *The Journal of Experimental Medicine*, 208(7), 1367–1376.
- Shrikant, P., & Mescher, M. (2002). Opposing effects of IL-2 in tumor immunotherapy: promoting CD8 T cell growth and inducing apoptosis. *Journal of Immunology (Baltimore, Md : 1950)*, 169(4), 1753–1759.
- Smith, G. A., Taunton, J., & Weiss, A. (2017). IL-2R abundance differentially tunes IL-2 signaling dynamics in CD4+and CD8+T cells. *Science Signaling*, 10(510).
- Smith, M. D., Martin, K. A., Calabresi, P. A., & Bhargava, P. (2017). Dimethyl fumarate alters B-cell memory and cytokine production in MS patients. *Annals of Clinical and Translational Neurology*, 4(5), 351–355.
- Spencer, C. M., Crabtree-Hartman, E. C., Lehmann-Horn, K., Cree, B. A. C., & Zamvil, S. S. (2015). Reduction of CD8⁺ T lymphocytes in multiple sclerosis patients treated with dimethyl fumarate. *Neurology - Neuroimmunology Neuroinflammation*, 2(3), e76.
- Srenathan, U., Steel, K., & Taams, L. S. (2016). IL-17+ CD8+ T cells: Differentiation, phenotype and role in

- inflammatory disease. *Immunology Letters*.
- Staudt, V., Bothur, E., Klein, M., Lingnau, K., Reuter, S., Grebe, N., ... Bopp, T. (2010). Interferon-Regulatory Factor 4 Is Essential for the Developmental Program of T Helper 9 Cells. *Immunity*, *33*(2), 192–202.
- Stumhofer, J. S., Laurence, A., Wilson, E. H., Huang, E., Tato, C. M., Johnson, L. M., ... Hunter, C. A. (2006). Interleukin 27 negatively regulates the development of interleukin 17-producing T helper cells during chronic inflammation of the central nervous system. *Nature Immunology*, *7*(9), 937–945.
- Su, Y.-C., Lee, C.-C., & Kung, J. T. (2010). Effector function-deficient memory CD8⁺ T cells clonally expand in the liver and give rise to peripheral memory CD8⁺ T cells. *Journal of Immunology (Baltimore, Md. : 1950)*, *185*(12), 7498–7506.
- Subramanian, A., Tamayo, P., Mootha, V. K., Mukherjee, S., Ebert, B. L., Gillette, M. A., ... Mesirov, J. P. (2005). Gene set enrichment analysis: A knowledge-based approach for interpreting genome-wide expression profiles. *Proceedings of the National Academy of Sciences*, *102*(43), 15545–15550.
- Sui, P., Wiesner, D. L., Xu, J., Zhang, Y., Lee, J., Van Dyken, S., ... Sun, X. (2018). Dimethyl fumarate targets GAPDH and aerobic glycolysis to modulate immunity. *Science*, pp. 1–16.
- Sukumar, M., Liu, J., Ji, Y., Subramanian, M., Crompton, J. G., Yu, Z., ... Gattinoni, L. (2013). Inhibiting glycolytic metabolism enhances CD8⁺T cell memory and antitumor function. *Journal of Clinical Investigation*, *123*(10), 4479–4488.
- Sullivan, L. B., Martinez-Garcia, E., Nguyen, H., Mullen, A. R., Dufour, E., Sudarshan, S., ... Chandel, N. S. (2013). The Proto-oncometabolite Fumarate Binds Glutathione to Amplify ROS-dependent signaling. *Molecular Cell*, *51*(2), 236–248.
- Szabo, S. J., Kim, S. T., Costa, G. L., Zhang, X., Fathman, C. G., & Glimcher, L. H. (2000). A Novel Transcription Factor, T-bet, Directs Th1 Lineage Commitment. *Cell*, *100*(6), 655–669.
- Tabarkiewicz, J., Pogoda, K., Karczmarczyk, A., Pozarowski, P., & Giannopoulos, K. (2015). The Role of IL-17 and Th17 Lymphocytes in Autoimmune Diseases. *Archivum Immunologiae et Therapiae Experimentalis*.
- Tahiliani, M., Koh, K. P., Shen, Y., Pastor, W. A., Bandukwala, H., Brudno, Y., ... Rao, A. (2009). Conversion of 5-methylcytosine to 5-hydroxymethylcytosine in mammalian DNA by MLL partner TET1. *Science*, *324*(5929), 930–935.
- Tajima, M., Wakita, D., Noguchi, D., Chamoto, K., Yue, Z., Fugo, K., ... Nishimura, T. (2008). IL-6-dependent spontaneous proliferation is required for the induction of colitogenic IL-17-producing CD8⁺ T cells. *The Journal of Experimental Medicine*, *205*(5), 1019–1027.
- Tang, Y., Guan, S. P., Chua, B. Y. L., Zhou, Q., Ho, A. W. S., Wong, K. H. S., ... Kemeny, D. M. (2012). Antigen-specific effector CD8⁺ T cells regulate allergic responses via IFN- γ and dendritic cell function. *Journal of Allergy and Clinical Immunology*, *129*(6), 1611–1620.
- Tannahill, G. M., Curtis, A. M., Adamik, J., Palsson-Mcdermott, E. M., McGettrick, A. F., Goel, G., ... O'Neill, L. A. J. (2013). Succinate is an inflammatory signal that induces IL-1 β through HIF-1 α . *Nature*, *496*(7444), 238–242.

- Tse, H. M., Thayer, T. C., Steele, C., Cuda, C. M., Morel, L., Piganelli, J. D., & Mathews, C. E. (2010). NADPH Oxidase Deficiency Regulates Th Lineage Commitment and Modulates Autoimmunity. *The Journal of Immunology*, *185*(9), 5247–5258.
- Tzartos, J. S., Friese, M. A., Craner, M. J., Palace, J., Newcombe, J., Esiri, M. M., & Fugger, L. (2008). Interleukin-17 production in central nervous system-infiltrating T cells and glial cells is associated with active disease in multiple sclerosis. *American Journal of Pathology*.
- Visekruna, A., Ritter, J., Scholz, T., Campos, L., Guralnik, A., Poncette, L., ... Huber, M. (2013). Tc9 cells, a new subset of CD8+ T cells, support Th2-mediated airway inflammation. *European Journal of Immunology*, *43*(3), 606–618.
- Wang, R., Dillon, C. P., Shi, L. Z., Milasta, S., Carter, R., Finkelstein, D., ... Green, D. R. (2011). The Transcription Factor Myc Controls Metabolic Reprogramming upon T Lymphocyte Activation. *Immunity*, *35*(6), 871–882.
- Williams, M. A., Tyznik, A. J., & Bevan, M. J. (2006). Interleukin-2 signals during priming are required for secondary expansion of CD8+memory T cells. *Nature*, *441*(7095), 890–893.
- Xiao, M., Yang, H., Xu, W., Ma, S., Lin, H., Zhu, H., ... Guan, K. L. (2012). Inhibition of α -KG-dependent histone and DNA demethylases by fumarate and succinate that are accumulated in mutations of FH and SDH tumor suppressors. *Genes and Development*, *26*(12), 1326–1338.
- Xin, A., Masson, F., Liao, Y., Preston, S., Guan, T., Gloury, R., ... Kallies, A. (2016). A molecular threshold for effector CD8+ T cell differentiation controlled by transcription factors Blimp-1 and T-bet. *Nature Immunology*, *17*(4), 422–432.
- Yang, X. O., Pappu, B., Nurieva, R., Akimzhanov, A., Kang, H. S., Chung, Y., ... Dong, C. (2008). TH17 lineage differentiation is programmed by orphan nuclear receptors ROR α and ROR γ . *Immunity*, *28*(1), 29–39.
- Yang, X. P., Ghoreschi, K., Steward-Tharp, S. M., Rodriguez-Canales, J., Zhu, J., Grainger, J. R., ... Laurence, A. (2011). Opposing regulation of the locus encoding IL-17 through direct, reciprocal actions of STAT3 and STAT5. *Nature Immunology*, *12*(3), 247–254.
- Yao, S., Buzo, B. F., Pham, D., Jiang, L., Taparowsky, E. J., Kaplan, M. H., & Sun, J. (2013). Interferon regulatory factor 4 sustains CD8+ T cell expansion and effector differentiation. *Immunity*, *39*(5), 833–845.
- Yeh, N., Glosson, N. L., Wang, N., Guindon, L., McKinley, C., Hamada, H., ... Kaplan, M. H. (2010). Tc17 Cells Are Capable of Mediating Immunity to Vaccinia Virus by Acquisition of a Cytotoxic Phenotype. *The Journal of Immunology*.
- Yen, H., Harris, T. J., Wada, S., Grosso, J. F., Getnet, D., Goldberg, M. V., ... Drake, C. G. (2009). Tc17 CD8 T cells: functional plasticity and subset diversity. *Journal of Immunology (Baltimore, Md. : 1950)*, *183*(11), 7161–7168.
- Yu, A., Zhu, L., Altman, N. H., & Malek, T. R. (2009). A Low Interleukin-2 Receptor Signaling Threshold Supports the Development and Homeostasis of T Regulatory Cells. *Immunity*, *30*(2), 204–217.
- Zentner, G. E., & Henikoff, S. (2013). Regulation of nucleosome dynamics by histone modifications. *Nature Structural and Molecular Biology*.

- Zhang, S., Ke, X., Zeng, S., Wu, M., Lou, J., Wu, L., ... Pan, S. (2015). Analysis of CD8+ Treg cells in patients with ovarian cancer: a possible mechanism for immune impairment. *Cell Mol Immunol*, *12*(5), 580–591.
- Zhao, G., Liu, Y., Fang, J., Chen, Y., Li, H., & Gao, K. (2014). Dimethyl fumarate inhibits the expression and function of hypoxia-inducible factor-1 α (HIF-1 α). *Biochemical and Biophysical Research Communications*, *448*(3), 303–307.
- Zheng, L., Cardaci, S., Jerby, L., Mackenzie, E. D., Sciacovelli, M., Johnson, T. I., ... Gottlieb, E. (2015). Fumarate induces redox-dependent senescence by modifying glutathione metabolism. *Nature Communications*, *6*.
- Zhou, L., Chong, M. M. W., & Littman, D. R. (2009). Plasticity of CD4+ T Cell Lineage Differentiation. *Immunity*.
- Zhou, L., Ivanov, I. I., Spolski, R., Min, R., Shenderov, K., Egawa, T., ... Littman, D. R. (2007). IL-6 programs TH-17 cell differentiation by promoting sequential engagement of the IL-21 and IL-23 pathways. *Nature Immunology*, *8*(9), 967–974.
- Zhu, J., & Paul, W. E. (2008). CD4 T cells: Fates, functions, and faults. *Blood*, *112*(5), 1557–1569.
- Zhu, J., Yamane, H., Cote-Sierra, J., Guo, L., & Paul, W. E. (2006). GATA-3 promotes Th2 responses through three different mechanisms: Induction of Th2 cytokine production, selective growth of Th2 cells and inhibition of Th1 cell-specific factors. *Cell Research*.
- Zhu, J., Yamane, H., & Paul, W. (2010). Differentiation of effector CD4 T cell populations. *Annu Rev Immunol.*, *28*(1), 445–489.

8. Appendix

8.1 List of academic teachers

Following ladies and gentlemen were teachers during my studies at the University of Marburg (2009-2018):

Bauer, Baumeister, Beck, Bölker, Brandis-Heep, Brandl, Brändle, Bremer, Buttgereit, Exner, Feuser, Galland, Garten, Grollig, Hassel, Heider, Homberg, Huber, Kaufmann, Kost, Kostron, Lingelbach, Linklater, Lohoff, Maier, Maisner, Mösch, Önel, Przyborski, Renkawitz-Pohl, Rexer, Schachtner, Steinhoff, Višekruna, Weber, Yu, Zauner

8.2 Danksagung

Zu guter Letzt möchte ich die Gelegenheit nutzen und mich bei den vielen Menschen bedanken, die mich während meiner Promotion begleitet und unterstützt haben.

Mein ganz besonderer Dank gilt Prof. Magdalena Huber für die Betreuung meiner Dissertation, die wissenschaftlichen Diskussionen sowie die Ermöglichung einige Monate in Australien verbringen zu dürfen. Herzlichen Dank für deine Unterstützung und deine ansteckende Begeisterung für die Wissenschaft!

Zudem möchte ich mich bei Prof. Michael Lohoff für die Möglichkeit bedanken am Institut für Medizinische Mikrobiologie meine Dissertation anfertigen zu können. Vielen Dank für die kritischen Diskussionen und deine Hilfsbereitschaft!

Ein herzliches Dankeschön auch an alle Kooperationspartner, die zum Gelingen dieser Arbeit beigetragen haben, besonders Prof. Axel Kallies und seine Gruppe in Melbourne sowie Matthias Klein und Federico Marini aus Mainz.

Vielen Dank auch an Prof. Ulrich Steinhoff und PD Dr. Alexander Višekruna für eure wissenschaftliche Hilfe und Unterstützung!

Besonders möchte ich mich besonders bei allen Mitgliedern der AG Huber Anna, Hartmann, Dennis, Felix, Niklas, Doro und Eva für die fachliche, emotionale und kulinarische Unterstützung bedanken. Vielen Dank für die tolle Teamarbeit!

Des Weiteren möchte ich vor allem Lu, Agnes und Niyati danken, die während dieser Zeit nicht nur „Leidensgenossen“ waren, sondern zu guten Freunden geworden sind. Ein riesengroßes Dankeschön für eure Unterstützung und die unvergessliche Zeit!

Bei allen jetzigen und ehemaligen Mitarbeitern des Labors, besonders Addi, Anne, Alekhya, Bärbel, Claudia, Conny, Daniel, DG, Elena, Flo, Kang, Maik, Meike, Melli, Olaf, Petra, Rossana, Sabrina und Safa möchte ich mich herzlich für die Hilfsbereitschaft, das gute Arbeitsklima sowie die oft benötigte „Nervennahrung“ bedanken.

Vielen Dank für die schöne und unvergessliche Zeit in- und außerhalb des Labors!

Ganz besonders möchte ich mich bei meinen Eltern und Geschwistern für ihre immerwährende Unterstützung, ihr Verständnis sowie ihren Glauben an mich bedanken.

Vielen Dank!